UNIVERSITÀ DEGLI STUDI DI PADOVA

Dipartimento di Ingegneria Industriale
Corso di Laurea in Ingegneria Energetica

TESI DI LAUREA MAGISTRALE

PERFORMANCE ANALYSIS OF ORGANIC RANKINE CYCLES USING MULTI-COMPONENT WORKING FLUIDS TAILORED FOR SOLAR APPLICATIONS

Relatore: Prof.ssa Anna Stoppato
Correlatore: Prof. Fredrik Haglind

Laureando: Enrico Baldasso

Anno Accademico 2014 - 2015

Abstract

The increasing awareness on the environmental problems related to the use of the traditional fossil fuel based power plants forces us to investigate and exploit more sustainable sources of energy. Among the different renewable sources of energy, solar power could play a primary role in the development of a new and more sustainable electricity generation system.

While large scale concentrated solar power plants based on the steam Rankine cycle have already been proved to be cost effective, research is still under progress for small scale low temperature solar-driven power plants. The steam Rankine cycle is suitable for high temperature applications, but its efficiency drastically decreases as the heat source temperature drops, in these cases a much more promising configuration is the so-called organic Rankine cycle.

The purpose of this thesis is to optimize a low temperature organic Rankine cycle tailored for solar applications. The optimization parameters are the working fluid and the turbine inlet temperature and pressure. Both pure fluids and binary mixtures are considered as possible working fluids and thus one of the primary aims of the study is to evaluate whether the use of multi-component working fluids might lead to increased solar to electricity efficiencies.

The considered configuration includes a solar field made of parabolic collectors and a recuperative organic Rankine cycle. Pressurized water is selected as heat transfer fluid and its maximum temperature is fixed to 150^oC. The solar source is modelled considering the solar irradiation of Sevilla (Spain) and the target power output is 100 kW_{el}. A part load analysis is carried out in order to define the most suitable control strategy and both the overall annual production and the average solar to electrical efficiency are estimated with an annual simulation.

The results suggest that the use of binary working fluids in an overall solar power system leads to lower performance improvements than in the waste heat recovery case (which was also investigated). When the part load control strategy considers a constant value for the turbine inlet temperature the mixture behaves similarly to the pure fluid configuration in off-design conditions, but is able to operate with lower values of the solar collected energy. Anyway this cannot be considered true for every possible control strategy.

Preface

This thesis represents my final project for my Master Degree in Energy Engineering at the University of Padova and it has been carried out at the Technical University of Denmark (DTU), Department of Mechanical Engineering, Thermal Energy Systems section, during a 5 months period (September 2014 - January 2015).

I would like to thank my supervisors Fredrik Haglind and Anna Stoppato for giving me the possibility to develop my final project in such an interesting field and for the continuous guidance they provided me.

My special thanks also to Ph.D. students Anish Modi and Jesper Graa Andreasen for their endless patience and essential help, without your suggestions and constructive criticism this thesis would not be as it is now.

I am grateful also to researcher Leonardo Pierobon who provided me some valuable help in the development of the part load model.

Finally, I would like to thank all my family for their endless support and encouragements during all these months, and my office mates, Kristóf and Marc: you made all the long working hours much more enjoyable.

Contents

Abstract **i**

Preface **iii**

1 Introduction **5**
1.1 Computational tools 5
1.2 Structure of the work 6

2 Thermodynamic Cycles Overview **7**
2.1 Rankine Cycle 9
2.2 Organic Rankine Cycle 9
2.2.1 Fluid selection 10
2.2.2 Pure working fluids 14
2.3 Supercritical Cycles 16
2.4 Cycles using zeotropic mixtures 17

3 Power Cycle Analysis **19**
3.1 Design Model description 19
3.2 Model adjustment 22
3.3 Genetic Algorithm 24
3.4 Low temperature heat source 25
3.4.1 Low temperature fluids 25
3.4.2 Pure fluids results 26
3.4.3 Mixtures results 29
3.5 Moderate temperature heat source 33
3.5.1 Moderate temperature fluids 33
3.5.2 Pure fluids results 34
3.5.3 Mixtures results 39
3.6 Discussion 41

4 Concentrated solar power technology **45**
4.1 Technology overview 45
4.1.1 Solar power towers 46
4.1.2 Parabolic dish systems 47
4.1.3 Parabolic trough collectors 47
4.1.4 Linear Fresnel reflectors 48
4.2 Calculation of collected solar energy 49

4.3 Solar field model 52
4.4 Solar model validation 57
4.5 Solar field regression model 58

5 Overall System Analysis **61**
5.1 Pure fluids results 64
5.2 Mixtures results 69
5.3 Pure Cyclohexane and Cyclohexane/Cyclopentane comparison . . . 72
5.3.1 Economical considerations 72
5.3.2 Sensitivity Analysis 74
5.4 Discussion 76

6 Annual Analysis **79**
6.1 Part Load model 79
6.1.1 Heat Exchangers 80
6.1.2 Turbine 80
6.1.3 Pump 81
6.1.4 Electric generator 81
6.1.5 Condenser 81
6.1.6 Solar Field 81
6.2 Control Strategies 82
6.3 Part Load results 82
6.3.1 Influence of Ambient temperature 85
6.3.2 Influence of Wind speed 85
6.3.3 Minimum acceptable load 89
6.4 Regression model 89
6.5 Annual Simulation 90
6.5.1 Influence of Design DNI 95
6.6 Discussion 96

7 Conclusions **99**
7.1 Recommendations for further work 101

Nomenclature

Abbreviations

DNI	Direct normal irradiation
GWP	Global warming potential
HCE	Heat collector element
$HFOs$	Hydrofluoroolefins
IAM	Incident angle modifier
ODP	Ozone depleting potential
ORC	Organic Rankine cycle
TIT	Turbine inlet temperature

Symbols

α	Absorptance
Δ	Difference
δ	Declination angle
$\dot{m}$	Mass flow rate
$\dot{q}$	Specific heat flux
η	Efficiency
ϕ	Latitude
ρ	Reflectance/density
τ	Transmittance
θ	Incidence angle
θ_z	Zenit angle
A_p	Collector aperture area
c_p	Specific heat

D	Diameter
f	Friction factor
G	Specific mass flow rate
h	Specific enthalpy
L_{loc}	Longitude of the location
L_{st}	Standard meridian for the local timezone
n	Day of the year
p	Pressure
Q	Heat
Re	Reynolds number
S	Surface
T	Temperature
V	Speed
W	Power
x	quality

Subscripts

abs	Absorber
amb	Ambient
ap	Approach point
c	Critical/cold
$cond$	Condenser
des	Design
el	Electrical
$evap$	Evaporator
gen	Generator
gl	Glazing
h	Hot
htf	Heat transfer fluid
in	Inlet

is	Iscntropic
ml	Mean logarithm
opt	Optical
out	Outlet
p	Pump
pp	Pinch point
rec	Recuperator
$spec$	Specific
t	Turbine
wf	Working fluid

Chapter 1

Introduction

Organic Rankine cycles have already been proved to be suitable candidates for the exploitation of low and moderate temperature heat sources. A more recent field of interest is the analysis of zeotropic mixtures as possible working fluids for these power cycles. As already shown by several studies the introduction of binary working fluids leads to performance improvement thanks to a better matching between the power cycle and the hot and cold sources. However very few analysis have taken into account an overall solar-driven organic Rankine cycle using multicomponent working fluids.

The purpose of this thesis is therefore to investigate the use of zeotropic mixtures both in low (150^oC) and moderate (310^oC) temperature solar power plants. The first objective is to evaluate whether the use of mixtures leads to better cycle efficiencies compared to the use of pure fluids and to find out in which temperature range their use is more promising. Once defined this temperature level the thesis will investigate off-design performance of a system composed of a solar field and a power cycle in order to assess the performance differences between pure fluids and zeotropic mixtures on annual basis.

Many studies have been carried out in this field (especially concerning low temperature power cycles) but most of them focus only on design condition performance of the power cycle. Through this thesis it will be possible to understand how the use of mixtures relates with off-design condition and in particular with a heat source that is highly variable (the sun).

1.1 Computational tools

Most of the work of this thesis has been carried out using the Matlab environment. The organic Rankine cycle design model was provided by Jesper Graa Andreasen, while all the others models have been built as a part of the project. All the optimizations have been carried out using the genetic algorithm available in the Matlab optimization toolbox and the fluid thermodynamic properties have been calculated using Refprop 9.1. The heat transfer model for the solar field has been developed in EES and was then implemented in the Matlab code as a regression curve.

1.2 Structure of the work

This overall thesis is structured as follows:

- Chapter 2 describes the state of art of the organic Rankine cycle and in particular enlightens the most desirable properties of the working fluids;
- In Chapter 3 a primary screening is performed in order to find out in which temperature level the use of zeotropic mixtures seems more profitable. The considered temperature levels for the heat source are 150 and 310^oC;
- Chapter 4 gives a general overview on the Concentrated solar power technologies and describes the heat transfer model for the parabolic trough system;
- In Chapter 5 an overall solar system is optimized and analysed in order to understand the advantages and the drawbacks deriving from the use of binary working fluids;
- In Chapter 6 the part load model is introduced and the results of the annual simulation are commented;
- Chapter 7 summarises the obtained results and gives some advices on how to further develop this analysis.

Chapter 2

Thermodynamic Cycles Overview

The efficient conversion of heat into power is one of the greatest challenge of modern engineering. As stated by the second law of thermodynamics it is not possible to perform a complete conversion of heat into power, nor to to obtain mechanical work by cooling any portion of matter below the temperature of the coldest of the surrounding objects. Since the conversion of heat into power is always characterised by some losses, the aim of modern power plants is to reduce them as much as possible in order to increase the net power production or to minimize the heat required to produce a defined amount of power.

The upper limit for the efficiency of a process that converts a certain amount of thermal energy into mechanical work is given by the Carnot cycle (Figure 2.1) and it is equal to:

$$\eta = \frac{W}{Q_{hot}} = 1 - \frac{T_1}{T_2} \tag{2.1}$$

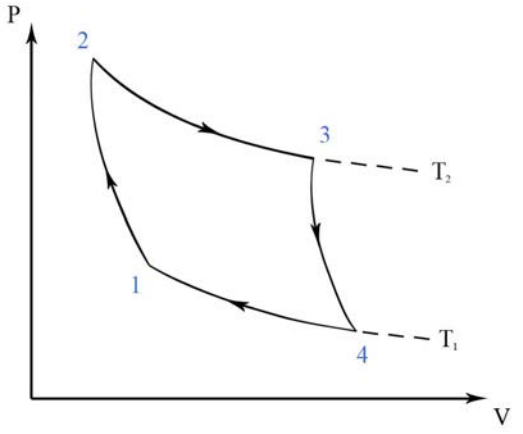

Figure 2.1: The Carnot cycle

The Carnot cycle is a theoretical thermodynamic reversible cycle working between two isothermal heat sources but it is not technically feasible.

During the past many thermodynamic cycle configurations have been proposed as ways to effectively convert heat into power, but only a few of them showed interesting performance. In the field of power production the most widely used cycle is the so-called Steam Rankine cycle (Figure 2.2) which is ideally composed by two isothermal and two adiabatic processes.

The Bryton-Joule cycle is the key technology behind gas turbines and even though its efficiency is lower, it is characterised by great compactness and lower installation costs [1]. Since gas turbine exhaust gases are still characterised by high temperatures (550-600 ^{o}C) it is possible to use them as the heating source in a bottoming cycle (usually a Rankine cycle) in order to obtain combined cycles with efficiencies up to 60%.

In the automotive field the common choices are internal combustion engines based upon the Diesel or Otto cycles. Internal combustion engines are widely used also in the field of power production, but the energy source has to be available as a fuel and so they are not suitable for solar applications. External combustion engines based on the Stirling cycle have also been investigated but they are not a mature technology yet.

Many other configurations are under development (Kalina cycle, Gas injected steam turbine, Integrated gasification combined cycle) and all of them aim to reach higher conversion efficiencies. The development of high efficiency cycles has to be pursued in order to achieve both environmental advantages and economical gains. When talking about fossil fuels or bio-fuels based power plants higher efficiencies allow to produce the same amount of net power output while decreasing the amount of pollution released to the environment and the costs for the fuel. In the case of solar and waste heat recovery applications greater efficiencies enable to decrease the land surface required by the solar field or to produce more energy from the given heat source and thus lead to economical benefits.

In the field of solar energy different kind of power plants have been proposed. Central receivers can be coupled either with a Kalina cycle or a Rankine cycle [2]. The use of micro gas turbines and Stirling engines have been investigated for the parabolic dish technology [3]. In the case of line focusing devices the most common technologies are the Rankine cycle and the Organic Rankine cycle. In more recent years the hybridisation of solar energy with fossil fuels based power plants has been an interesting field of research: the hybridisation process ensures higher conversion efficiencies and a more constant power production. Both solar aided coal-fired [4] and solar gas-turbine [5] power plants have been proposed.

This thesis will investigate the use of solar energy for low and moderate temperature applications and so only Rankine and Organic Rankine cycles will be considered.

2.1 Rankine Cycle

The Rankine cycle is based on the concepts of the Carnot cycle, but some adjustment are made in order to make it technically feasible. In its most simple configuration it is composed by two isobaric and two adiabatic transformations (see Figure 2.2): this means that the absorption of the heat is no longer performed at constant temperature and so the efficiency will be lower.

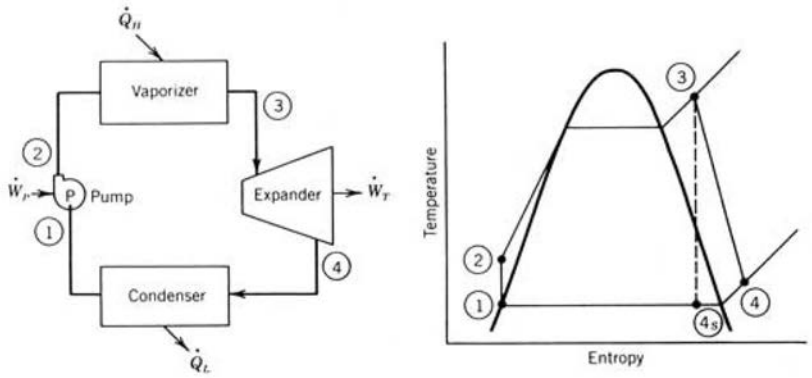

Figure 2.2: The Rankine cycle

The ideal cycle efficiency for a Rankine cycle can be written as:

$$\eta_{th} = \frac{Q^+ + Q^-}{Q^+} = 1 - \frac{T_1}{\overline{T_{23}}} \tag{2.2}$$

Where:

$$\overline{T_{23}} = \frac{\int_2^3 T ds}{s_3 - s_2} \tag{2.3}$$

From equation 2.3 it is clear that in order to improve the overall performance of this thermodynamic cycle it is necessary to increase the temperature level at which the heat is absorbed. This is usually achieved by adding new components to the basic structure: super-heaters allow to increase the maximum temperature level of the working fluids, re-heaters to increase the amount of heat absorbed at high temperature, and regenerative heat exchangers to increase the temperature of the working fluid at the boiler inlet. Nowadays performances are limited by technological issues (maximum allowable temperatures and pressures) and economical evaluations (a complicated and thus expensive configuration is not always the best choice, especially when dealing with small-size power plants).

2.2 Organic Rankine Cycle

The conventional Steam Rankine cycle is widely used for traditional power plants but its effectiveness decreases as the temperature of the heat source drops below 370^{o}C [6]. Even though the use of steam as a working fluid is related to several advantages [7]:

- It has very good thermal/chemical stability (no risk of decomposition);
- It has very low viscosity (low pumping work is required);
- It is good energy carrier (high latent and specific heat);
- It is non-toxic, non-flammable and it is not a threat to the environment (zero ODP, zero GWP);
- It is cheap and abundant;

Many problems related to the properties of the working fluid itself appear for low and moderate temperature applications [8]:

- It is necessary to super heat the fluid in order to prevent condensation during expansion;
- The risk of erosion of turbine blades might appear;
- The pressure of the evaporator can be excessive;
- The required turbines can be complex and expensive;

A possible solution to avoid those problems is the introduction of the organic Rankine cycle, which is characterised by the same structure of the Rankine cycle, but uses a different working fluid: usually an organic compound characterised by higher molecular mass and lower ebullition/critical temperature than water.

Since the size of this kind of plants is generally small, their configuration is usually kept as simple as possible. The only mandatory components are: a heat exchanger, a turbine, a condenser and a pump. The heat exchanger usually has the role of economiser and evaporator (a super-heating zone is sometimes present), the turbine is often single stage in order to reduce the investment cost and the recuperator is introduced only when it leads to significant performance improvements.

Some of the most important advantages of using an organic compound as the working fluid are the following [7]: the evaporation takes place at a lower pressure and requires less heat, when using dry or isentropic fluids the expansion ends in the vapour region and therefore there is no need of superheating nor the risk of blade erosion. Moreover, since the pressure ratio is smaller single stage turbine can be used.

2.2.1 Fluid selection

The choice of a proper working fluid is an essential step in the development of an efficient and cost-effective ORC. The selected organic compound has a huge impact on some of the most important characteristics of the power plant: efficiency, size of the various components, design of the expander machine, system stability, safety and environmental concerns [9].

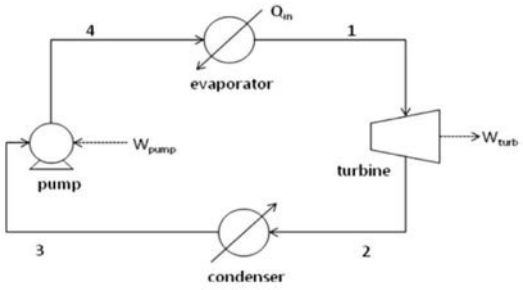

(a) without recuperator

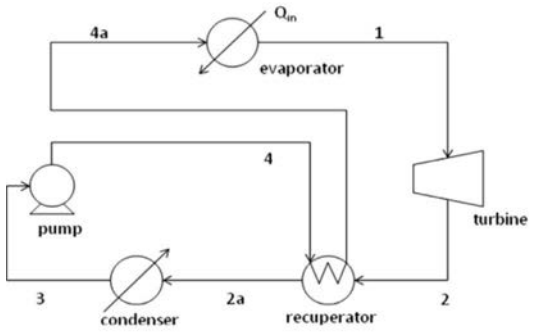

(b) with recuperator

Figure 2.3: Configuration of an ORC (a) without recuperator (b) with recuperator [10]

Given the importance of the working fluid selection, a very wide literature is available on the subject. The choice of an appropriate organic compound is affected by many factors: the characteristics of the available heat source, the size of the plant, the current legislation, and therefore every new plant has to be analysed on its own. It is anyway possible to draw some conclusions about desirable properties of the organic fluids [9]:

Working fluids' category

One of the most crucial characteristics of the working fluids is the slope of their saturation curve. From this point of view the different fluids can be divided into three categories: dry, wet and isentropic (Figure 2.4). Wet fluids (like water) are characterised by a negative slope of the saturation curve in the T-s diagram and therefore they need to enter in the expander in a super-heated state in order not to have too low values of vapour quality at the turbine outlet. Isentropic fluids are defined by a nearly infinite slope of the saturation curve and therefore plants using them as working fluids don't require the presence of the super-heating section. The slope of the saturation curve is instead positive for dry fluids: in this case the fluid might still be highly super-heated at the turbine outlet and as a consequence it might be necessary to add a recuperator in order not to waste too much valuable heat. The addition of the recuperator increases not only the cycle efficiency, but also the investment costs and therefore some authors believe that isentropic fluids are the most suitable for low temperature waste-heat recovery systems [11].

Vaporisation latent heat

When the working fluid is characterised by an high value of the vaporisation latent heat most of the heat energy is absorbed during the vaporisation process ad therefore is it not necessary to regulate superheating and expansion with rigenerative feed heating in order to achieve higher values of efficiency [12]. On the other side fluids with low vaporisation latent heat seem to be more suitable for waste heat recovery systems: in this case the heat source is characterised by a variable temperature and so the heat extraction in the evaporator leads to great irreversibility. If instead the heat is absorbed mainly in the preheating and superheating process a better coupling between the source and the working fluid can be achieved [13] (Figure 2.5).

Density

Fluids' density greatly affects the costs of the system: low density leads to higher volume flow rates and as a consequence to an increase of both heat exchanger losses and turbine size [14, 18].

Specific Heat

Fluids with low values of liquid specific heat should be preferable since they require less pumping work and this indirectly increases the net power output [14]. Anyway the calculation results from Borsukiewicz-Godzur [15] show that there is not a direct relationship between this two factors.

Vapour density

A proper value of the vapour density is a primary factor for the fluid selection. Having a high value for this parameter is particularly important for fluids that have a low condensing pressure: a higher value of the vapour density leads to lower volume flow rate and thus both to a decrement of the pressure losses in the heat exchangers and to a smaller size of the expander [14, 16, 18].

Critical Temperature

The critical temperature of a working fluid is defined as the temperature of the peak point of its saturation curve in the T-s diagram and plays a primary role in the definition of the temperature range in which the fluid can be used effectively. High values of the critical temperature usually lead to higher cycle efficiencies, but also to lower condensing pressure which are not always desirable [17]. Moreover, high critical temperature also leads to operating conditions characterised by lower specific density and thus to oversized components [18]. On the other hand a high condensing pressure often leads to a poor thermodynamic configuration.

Boiling temperature

Mago et al. [19] analysed the influence of boiling point temperature of different working fluids (R113, R123, R245ca and isobutane) on the thermal efficiency of the power cycle and found out that the best efficiency is achieved by the fluid with the

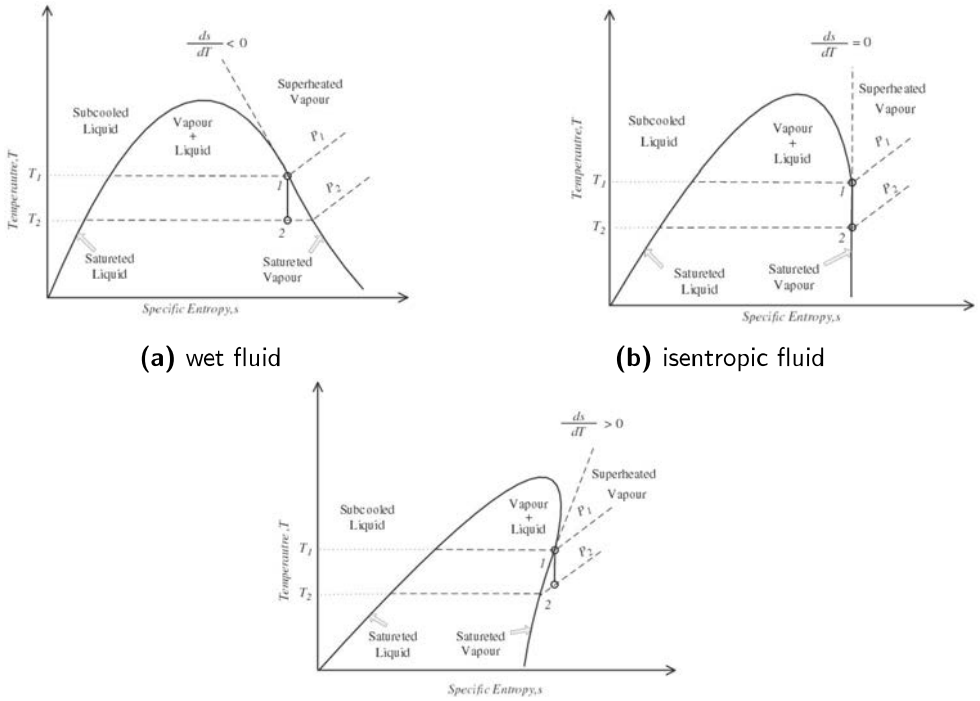

(a) wet fluid

(b) isentropic fluid

(c) dry fluid

Figure 2.4: T-s diagram for different fluids: (a) wet, (b) isentropic, (c) dry [9]

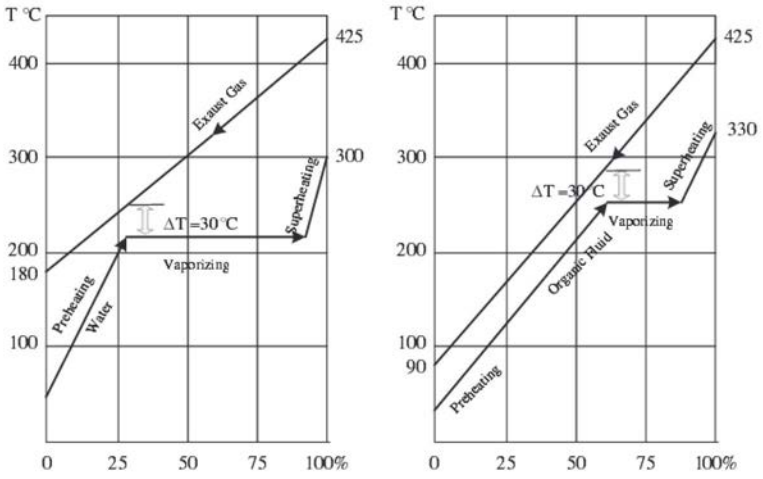

Figure 2.5: Effect of vaporisation latent heat on the heat transfer process [13]

highest boiling point. Anyway their analysis is restricted to a limited number of fluids and therefore the results are questionable. From further analysis it emerges that the highest thermal efficiency can be obtained with the fluid characterised by the highest boiling point among the same family [20], but that this is not true when dealing with fluids of different families [21].

Freezing point

In order to avoind freezing issues the freezing point of the fluid has to be lower than the lowest operating temperature of the power cycle.

Molecular weight

Turbines for heavy fluids usually have low peripheral speed, a small number of stages and higher efficiencies. On the other hand higher heat exchangers area is required by fluids with high critical pressure and molecular weight [22].

Viscosity

The viscosity of the fluid both in the liquid and in the vapour phase is directly related to the friction losses in heat exchangers and pipes. Fluids with low values of viscosity are preferable.

Conductivity

Fluid conductivity positively affects the heating exchange coefficients. Fluid with higher conductivity will assure good heat exchange properties and thus decrease the size ad the costs of the heat exchangers.

Environmental, Safety and Stability properties

Environmental, safety and stability issues can not be neglected when designing an organic Rakine cycle. One of the main concerns regarding the use of organic fluid is that some of them are ozone-depleting or green house effect substances. According to the Montreal Protocol, which regulates the use of ODP substances, some fluids have already been phased out (R11, R12, R113, R114, R115), while others (R21, R22, R123, R124, R141b, R142b) will be phased out in 2020 or 2030. Some restriction concerning the use of green house effect fluids have also been encouraged with the Kyoto Protocol.

Other desirable properties of working fluids are: non-toxicity, non-flammability, non-corrosiveness and thermal stability (especially for moderate temperature heat sources).

2.2.2 Pure working fluids

As it is clear from the previous section, it is not possible to define the perfect working fluid for organic Rankine applications. A screening of the performances of

the various fluids has to be carried out for every different case. From a structural point of view the different candidates can be divided into the following groups:

1. **Hydrocarbons** (linear, branched and aromatic): they have desirable thermodynamic properties but flammability issues;
2. **Perfluorocarbons**: stable and inert, but thermodynamically undesirable;
3. **Siloxanes**: they have low toxicity and flammability level, high molecular mass and can be used as a high temperature heat carrier. They are often available as mixtures and therefore isobaric evaporation doesn't occur at constant temperature;
4. **Ethers and Fluorinated Ethers**: they are usually not considered due to flammability issues and poor thermodynamic properties;
5. **Partially flouro-substituted straight chain hydrocarbons**: some of them are zero ODP fluids and thus of potential interest;
6. **Alcohols**: not really attractive since they are soluble in water, have poor thermodynamic properties and flammability issues;
7. **Inorganic**: they are inexpensive and have small environmental impact, but their use is connected to some operational problems.

2.3 Supercritical Cycles

The use of organic Rankine cycles for the exploitation of low and moderate temperature heat sources leads to efficiency improvements compared to the steam Rankine cycle but still there are some limitations related to the fact that the isothermal boiling process creates a bad thermal match between the heat source and the working fluid. The temperature difference through which the heat exchange process occurs in the evaporator tends to increase and thus leads to large irreversabilities [23].

The use of mixtures or supercritical cycles can reduce this problem and therefore lead to overall better performances (Figure 2.8).

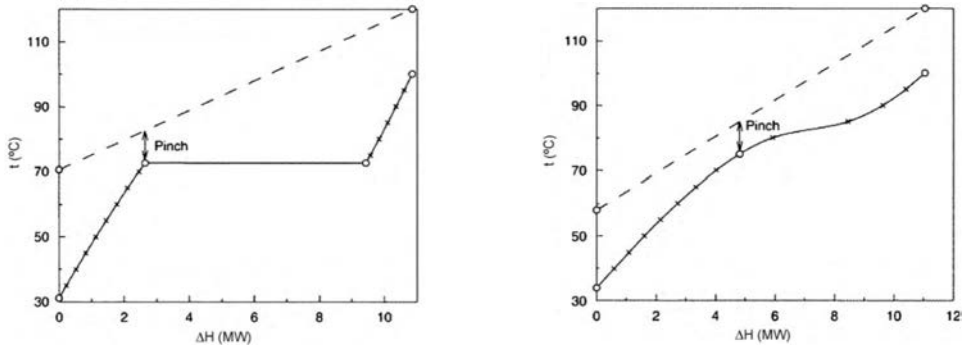

(a) organic Rankine cycle **(b)** supercritical Rankine cycle

Figure 2.6: Representation of the heat transfer process between the low temperature heat source and the working fluid in the main heat exchanger [14]

The main difference between the traditional rankine cycle and the supercritical configuration lies in the heat exchangers: while in the traditional plants the working fluid is first pre-heated, then evaporated and finally super-heated, in the supercritical power plants the working fluid is pumped directly to a supercritical pressure and therefore the heating process does not pass through the two-phase region. Even though supercritical cycles may lead to better performances they usually require higher working pressures and therefore difficulties in the plant operation and safety concerns might appear [14].

2.4 Cycles using zeotropic mixtures

The use of zeotropic mixtures of as working fluids for organic Rankine cycles is a new concept under investigation that might allow to take advantage of a non isothermal boiling process (like in the supercritical cycles) and at the same time avoid the problems related to high operating pressures. In this case the non-isothermal phase shift comes from the unequal concentration of the liquid and vapour phase during the evaporation process [24]: this lead to a temperature glide that is function of the mixture composition (Figure 2.7).

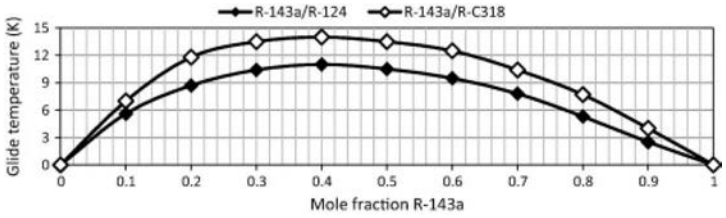

Figure 2.7: Temperature glide as a function of mixture composition

The unequal concentration of vapour and liquid phase occurs even in the condensing process and thus even additional gains could be achieved due to a better coupling between the cooling medium and the working fluid in the condenser [23] (Figure 2.8). Furthermore zeotropic mixture can be used also in a supercritical configuration, according to Chen et al. [23] this leads to a much lower exergy distruction both in the condenser and in the boiler and thus to higher efficiencies. Many studies have been carried out considering a geothermal heat source. Herberle et al [29] showed that the second law efficiency of the best mixture of isobutane and isopentane is 8% higher than the one for pure isobutane. Andreasen et al [26] proposed a generic methodology for organic Rankine cycle optimization: the result indicated that the introduction of binary working fluids can lead to higher power productions and to lower pressure levels. Moreover the results of an experimental study of a low-temperature solar Rankine cycle system conducted by Wang et al [27] showed that zeotropic mixtures have the potential to increase the overall efficiency.

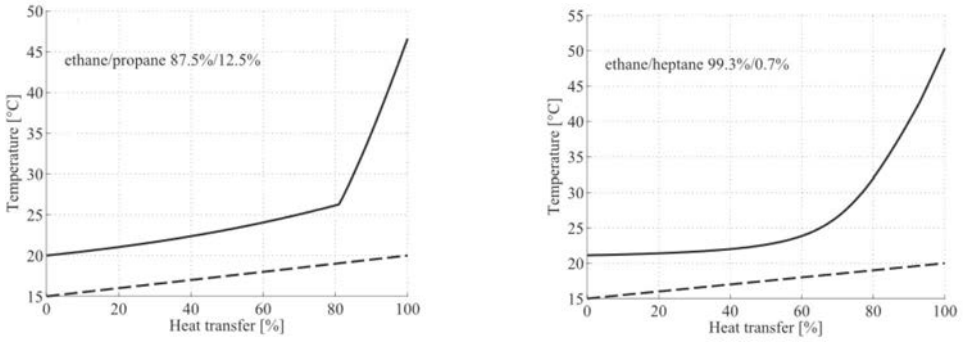

(a) ethane/propane **(b)** ethane/heptane

Figure 2.8: Representation of the condensing process using different zeotropic mixtures: (a) ethane/propane (b) ethane/heptane [25]

Chapter 3

Power Cycle Analysis

The purpose of this thesis is to investigate the use of zeotropic mixtures in solar applications and therefore a primary objective is to understand whether the use of these substances leads to better performance in design conditions.

As a first analysis the power cycle performance has been investigated with the aim of maximizing the net power production: the only fixed parameters are the heat source inlet temperature and mass flow rate. No limit has been set for the heat source outlet temperature and therefore the results will show if the use of mixtures allows to better exploit a heat source of a given temperature.

Two different temperature levels have been considered: a low grade (150^{o}C) and a moderate grade (310 ^{o}C) heat source. Many studies have already been carried out for low temperature heat sources [23, 25, 27, 28, 29, 30, 31, 32], while very little literature is available for higher temperatures [28, 35, 36]. As the level of the heat source increases problems related to working fluid thermal stability appear and therefore a heat source temperature of 310 ^{o}C was chosen in order to guarantee the stability of all the selected fluids.

The available studies focus mainly on geothermal sources and thus only design conditions are considered. The aim of this work instead is to analyse the performance of a solar-tailored power plant and so, once defined the most promising thermal level and suitable mixture, an off-design simulation will be performed in order to evaluate the effectiveness of zeotropic mixtures with respect to an highly variable heat source like the sun.

3.1 Design Model description

The design model, except for the presence of the recuperator, is the same used in [25] and was provided by J.G. Andreasen. All the thermodynamic properties are calculated using Refprop 9.1 database. Heat losses from the system to the environment and pressure losses (both in the heat exchangers and in the pipelines) have been neglected. Additional assumption are: steady state condition and homogeneous flow in therms of thermodynamic properties. As shown in Figure 3.1 the only

considered components are the following:

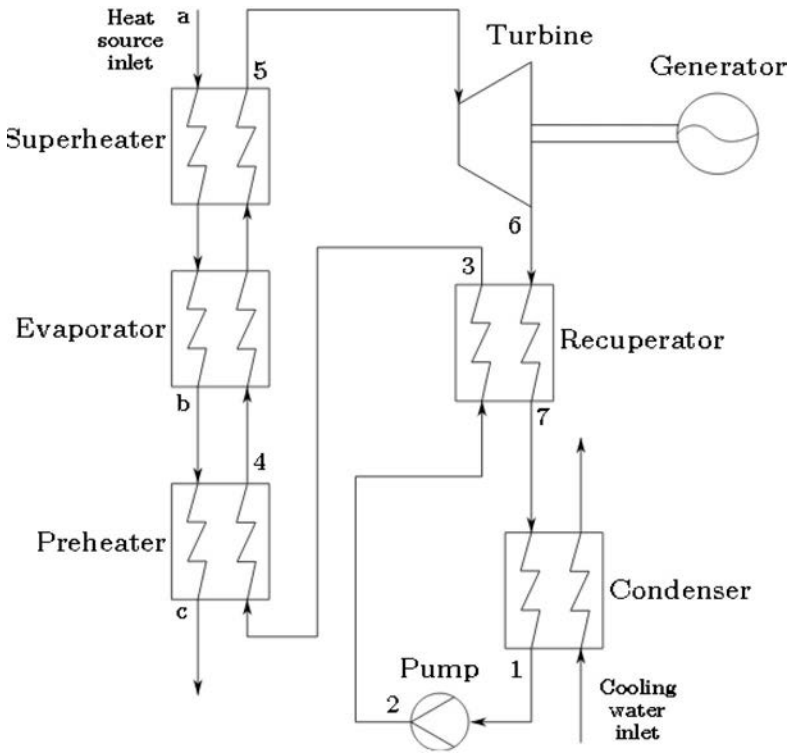

Figure 3.1: Power cycle sketch [26]

Boiler

In the boiler the heating of the working fluid is performed. During the optimisation process both sub-critical and supercritical configurations are investigated. In sub-critical conditions the boiler is divided into three separate zones: a pre-heating zone, an evaporation zone and a super-heating zone (optional), while in supercritical conditions a single heat exchanger performs the overall heat release from the heat carrier to the working fluid. Since energy losses to the environment are neglected, the energy balance of the boiler is calculated as follows:

$$\dot{m}_{htf}(h_a - h_c) = \dot{m}_{wf}(h_5 - h_3) \tag{3.1}$$

The performance parameters considered are the pinch point temperature difference (ΔT_{pp}) and the approach point temperature difference (ΔT_{ap}). The former defines the minimum temperature difference allowed in the process and is estimated upon thermodynamic and economical considerations: a lower value of this parameter increases the system performance by decreasing the irreversibility connected to the heat exchange process but at the same time increases the surface area required to perform the heat transfer and thus leads to higher costs. The latter is defined as the temperature difference between the heat source and the fluid temperature at the outlet of the boiler:

$$\Delta T_{ap} = T_a - T_5 \tag{3.2}$$

The ΔT_{ap} fixes the maximum allowed temperature of the working fluid and its value is usually higher than the ΔT_{pp} [1] in the super-heating process the heating curves of the heat source and of the working fluid have a similar slope and therefore a lower values of the ΔT_{ap} results in a greater area of the heat exchanger characterised by lower values of the temperature difference and so to a higher increment of the investment costs.

Turbine

The turbine is the key element where the gross power output is produced. The pressure ratio of the turbine is defined by the cycle high pressure and the condensing pressure. If the expansion occurs in the two-phase region the expander efficiency decreases and the risk of blade erosion appears: as a consequence a minimum value of 0.86 for the vapour outlet quality is usually required for steam power plants. In this work, in order to consider a constant value for turbine efficiency, only dry expansion is considered ($x_6 \geq 1$). The irreversibilities of the expansion process are taken into account by means of an isentropic efficiency coefficient defined as:

$$\eta_{is,t} = \frac{h_5 - h_6}{h_5 - h_{6,is}} \tag{3.3}$$

The turbine power output is therefore calculated with the following equation:

$$W_t = \dot{m}_{wf} \left(h_5 - h_{6,is}\right) \eta_{is,t} \tag{3.4}$$

Recuperator

Certain configurations are characterised by highly super-heated vapour at the turbine outlet and so it is preferable to introduce this element in order to increase the temperature level of the working fluid at the inlet of the boiler and at the same time decrease the heating flow that has to be dissipated in the condenser. The recuperator in included only for those plant configurations that fulfil the following condition:

$$\Delta T_{rec} = T_6 - T_2 > \Delta T_{pp,rec} \tag{3.5}$$

The energy balance of the recuperator is:

$$h_3 - h_2 = h_6 - h_7 \tag{3.6}$$

A pinch point temperature is defined also for the recuperator ($\Delta T_{pp,rec}$) and the possibility to recover heat in the two-phase region is included (if the selected working fluid is a zeotropic mixture it is sometimes possible to recover some heat even from the first stages of the condenser).

Condenser

The model includes a water condenser: the vapour quality at the condenser outlet is fixed and equal to 0. The only fixed parameters in this component are the cooling water inlet temperature, the cooling water temperature difference (ΔT_{cond}) and the pinch point temperature difference ($\Delta T_{pp,cond}$). The condensing pressure is therefore free to vary and function of the fluid/mixture properties. For certain plant configurations the calculated condensing pressure is not in the feasibility range and therefore the possibility to define the condensing pressure have been included (see 3.2).

The energy balance of the condenser can be written as follows:

$$\dot{m}_{wf}(h_7 - h_1) = \dot{m}_{water}(h_{out} - h_{in}) \tag{3.7}$$

Pump

The final element of the cycle is a pump that has the function to pump the fluid back to the high pressure after the condenser. As the pressure losses are neglected the pump operates with same pressure ratio of the turbine. An isentropic efficiency coefficient is defined even for this component:

$$\eta_{is.p} = \frac{h_1 - h_{2,is}}{h_1 - h_2} \tag{3.8}$$

The power absorbed by the pump is thus calculated in the following way:

$$W_p = \dot{m}_{wf}(h_2 - h_1) \tag{3.9}$$

The output value of the model is the net electrical output, which is equal to:

$$W_{el} = W_t \, \eta_{gen} - W_p \tag{3.10}$$

3.2 Model adjustment

In order to better suit the power cycle to solar applications and to increase the range of the output parameters to be analysed in the discussion section, some adjustment have been made. The more important are:

Heat transfer fluid

For the moderate temperature case the heat carrier, initially pressurised water, has been changed to Therminol VP-1, a thermal oil widely used for solar applications, whose property data is available in the producer website. The use of this heat carrier makes the plant easier to operate and allows to decrease the pressure of the solar system. As the price of the thermal oil has a big impact on the plant investment costs, water is still considered as the heat carrier in the low temperature case.

New boiler model

The thermal oil heat capacity is strongly dependent on the temperature (see figure 3.2) and therefore the provided boiler model, which was based on the assumption of a linear profile of the heat source temperature, showed low accuracy in estimation of the pinch point location. In order to avoid undesired inaccuracies in the calculations a new boiler model was built. In the new model the energy balance between the hot and the cold fluid is performed for every discretization step and this ensures a greater accuracy in the results (see Table 3.1).

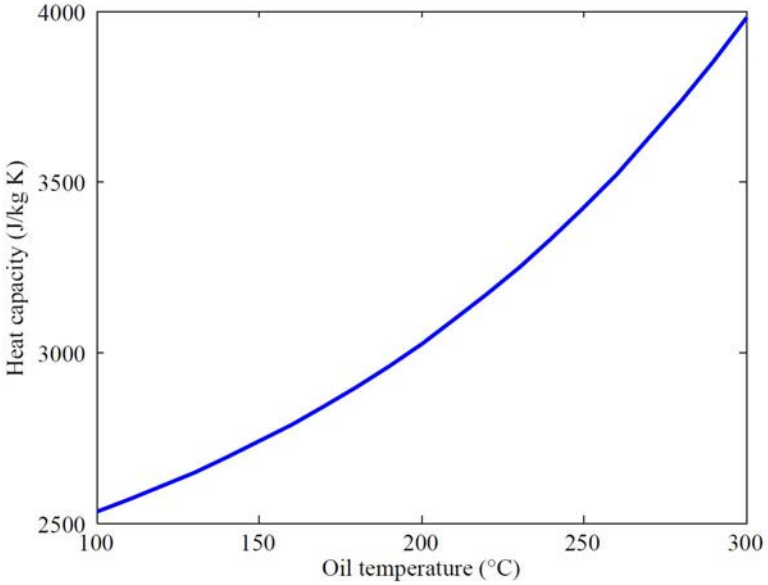

Figure 3.2: heat capacity dependence on temperature

Table 3.1: Pinch point calculation with different boiler models

	ΔT_{pp} [^oC]		
	Target	Old model	New model
optimized cyclohexane	8	5.799	7.998
optimised md3m	8	6.795	8
optimised mxylene	8	8.005	8.005

Electrical efficiency

In order to compare the performance of the different working fluids the calculation of the electrical efficiency has been introduced. The electrical efficiency of the power cycle has been defined as follows:

$$\eta_{el} = \frac{W_{el}}{Q_{in}} = \frac{W_{el}}{\dot{m}_{htf}\ (h_a - h_c)} \tag{3.11}$$

Condensing pressure

Since the condensing pressure was a free parameter, only related to the cooling water inlet temperature and to the condenser pinch point, the resulting values were sometimes outside the feasibility range (0.03 - 0.05 bar [38]). In order to investigate the performance of feasible power plants a fixed value of the condensing pressure was introduced for those fluids whose condensing pressure was not acceptable. In these cases the cooling water inlet temperature is calculated in order to suit the pinch point and temperature increment requirements.

3.3 Genetic Algorithm

The described Organic Rankine cycle design model is used in order to investigate the effectiveness of the different pure fluids and mixtures. The parameters that are left free to vary during the optimization process are the mixture composition, the cycle maximum pressure and the turbine inlet temperature.

The other cycle performance parameters (i.e. pinch point temperatures, isentropic efficiencies, cooling water inlet temperature and temperature increase) are instead kept constant.

Most of the optimizations in this thesis have been performed with a genetic algorithm. This optimization technique is based on the principle of natural selection: given a starting generation every individual is evaluated by mean of a fitness function (or objective function) and then a new generation of individuals is created. The analogy with the evolutionary process lies in the fact that every new generation is created by mating elements of the previous one, and that the best individuals of every generation are the ones with the biggest chances to transmit their genes (set of guess values) to the following one.

The genetic algorithm is particularly suited to optimize a thermodynamic problem where local minima and discontinuities are most likely to occur. In fact, thanks to the processes of crossover (creation of a new individual mixing the characteristics of two previous individuals) and mutation (creation of a new individual by introducing a random variation to a single individual of the previous generation) the algorithm is usually able to escape from local minima and to find the overall best solution.

In this primary analysis the selected objective function is the power plant electricity production: the aim is therefore to understand whether the use of binary working fluids leads to a better exploitation of a low or moderate temperature heat source.

Another approach might be to consider the electrical efficiency as the optimisation parameter, but this leads to solutions where the exploitation of the heat source is really poor (the efficiency of the power cycle takes into account the heat that is absorbed by the power cycle, not the heat that is theoretically available).

The optimised configurations resulting from this analysis won't probably have the same characteristics of a power plant optimised considering a complete solar power system composed by the solar field and the power cycle, but still the results will allow to draw a comparison between the different working fluids and to estimate in which temperature level the use of mixture leads to better performance increments.

3.4 Low temperature heat source

As the first study case of this analysis a 150^oC heat source is considered. The pressurized water mass flow rate is kept constant and equal to 10 kg/s. All the other assumptions considered are listed in table 3.2 and are based on similar studies found in literature.

Table 3.2: Low temperature assumptions

Property	Value	Unit
Pressurized water flow rate	10	kg/s
Pressurized water inlet temperature	150	^oC
Cooling water inlet temperature	20	^oC
ΔT_{ap}	10	^oC
$\Delta T_{pp,evap}$	8	^oC
$\Delta T_{pp,rec}$	8	^oC
$\Delta T_{cooling-water}$	5	^oC
$\Delta T_{pp,cond}$	8	^oC
$\eta_{is,p}$	0,70	
$\eta_{is,t}$	0,70	

3.4.1 Low temperature fluids

As there is a wide literature regarding the use of mixtures in low temperature applications this study will focus only on mixtures whose efficiency has already been proved [23, 25, 27, 28, 29, 30, 31, 32]. The pure fluids considered and their properties are shown in table 3.3. It has been decided not to include Hydro-fluorocarbons (HFCs) in this analysis: these fluids haven't been banished from the Montreal protocol but their phase out have already been proposed [34].On the other hand 4th generation refrigerants like R1234ze and R1234yf have been included in the list of possible candidates: these fluids belong to the category of Hydrofluoroolefins (HFOs) and are characterised by lower global warming potential than HFCs.

Table 3.3: Low temperature pure fluids

Fluid	Category	T_c $[^oC]$	P_c $[bar]$	ODP	GWP	Source
n-butane	natural ref.	151,97	37,96	0,12	725	[40, 41]
Cyclohexane	Cyclo alkanes	280	40,7	n.a	n.a.	[9, 41]
Cyclopentane	Cyclo alkanes	238,55	45,1	0	<25	[45]
n-hexane	Alkanes	236	30,6	0	0	[9, 43, 54]
iso-hexane	Cyclo alkanes	225	30,4	n.a.	n.a.	[9]
iso-pentane	Alkanes	187	33,7	0	0	[9, 44]
iso-butane	Hydrocarbons	135	36,4	0	20	[9]
n-Pentane	Alkanes	196,5	33,6	0	20	[44]
R1234yf	HFO	94,7	33,82	0	4	[55]
R1234ze	HFO	109,4	36,36	0	6	[55]

3.4.2 Pure fluids results

The optimization parameters considered in order to find out the best configuration for each working fluid are the turbine inlet temperature and the cycle high pressure. These variables are the input values defined by the genetic algorithm and are left free to vary in the ranges enlightened in table 3.4. For the cycle maximum pressure a maximum limit of 40 bar has been defined: according to L. Barbazza [33] this is the maximum allowed pressure for brazed plate heat exchangers.

Table 3.4: Selected boundaries for the optimization process

Parameter	Lower Bound	Upper bound
Cycle high pressure	1 $[bar]$	40 $[bar]$
Turbine inlet temperature	60 $[^oC]$	140 $[^oC]$

As it is possible to understand from the computed results (see table 3.5) all the most effective fluids are HFOs. The most promising hydrocarbon is iso-butane, but its power production is almost 15 % lower than R1234ze (the most promising working fluid). All the calculated condensing pressures are within the feasibility range and in particular all the most promising fluids have condensing pressures suitable to the use of atmospheric condensers ($P_{cond} > 1$ bar) and thus it would be possible to install a simple and not expensive condenser.

As depicted in Figures 3.3 and 3.4 (every point represents a different fluid in its optimised configuration), primary factors in the definition of the effectiveness of the different fluids are the turbine inlet temperature and the outlet temperature of the pressurized water (T_c): a higher value of the working fluid maximum temperature results in lower irreversibility in the heating process, while a lower value of the

heat source outlet temperature is a signal of a better exploitation of the heat source.

Table 3.5: Low temperature pure fluids results

Fluid	High pressure [bar]	TIT ^oC	P cond [bar]	η_{th}	T_c [^oC]	W_{el} [kW]	ΔW [%]
R1234ze	37,36	112,83	6,31	8,74	51,06	365,20	0,00
R1234yf	40,00	113,39	8,40	8,52	51,42	354,68	-2,88
isobutane	18,60	96,49	4,37	9,45	72,06	311,86	-14,61
butane	12,96	91,78	3,08	9,39	74,59	299,92	-17,88
ipentane	5,79	90,06	1,20	9,69	78,48	293,74	-19,57
ihexane	2,61	93,32	0,39	10,38	84,50	288,51	-21,00
hexane	1,77	87,71	0,28	9,62	79,41	287,97	-21,15
pentane	5,61	97,64	0,91	10,74	87,30	285,73	-21,76
cyclohexane	1,36	91,33	0,18	10,11	84,90	279,17	-23,56
cyclopentane	3,10	87,92	0,57	9,52	80,96	278,66	-23,70

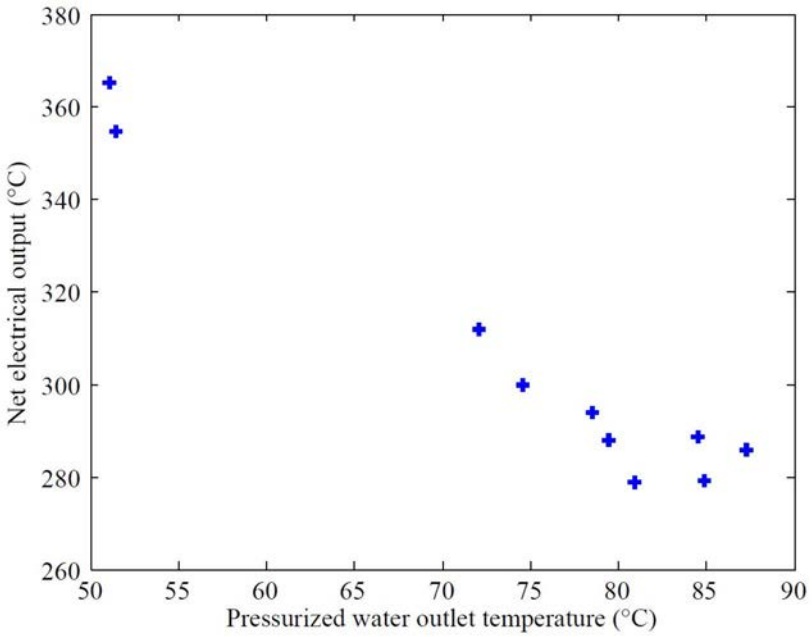

Figure 3.3: Influence of the heat source outlet temperature on the net electrical output

Looking at the pressure levels it can be notice that the HFOs reach the best performances with high values of cycle maximum pressure and that their optimised configurations are supercritical. As explained in section 2.3 this configuration is characterised by the absence of the isothermal phase shift zone and therefore enables to increase the effectiveness of the heat exchange process (Figure 3.5). In particular the configuration that considers R1234yf as working fluid reaches the best electrical output with the maximum allowed pressure level and therefore it

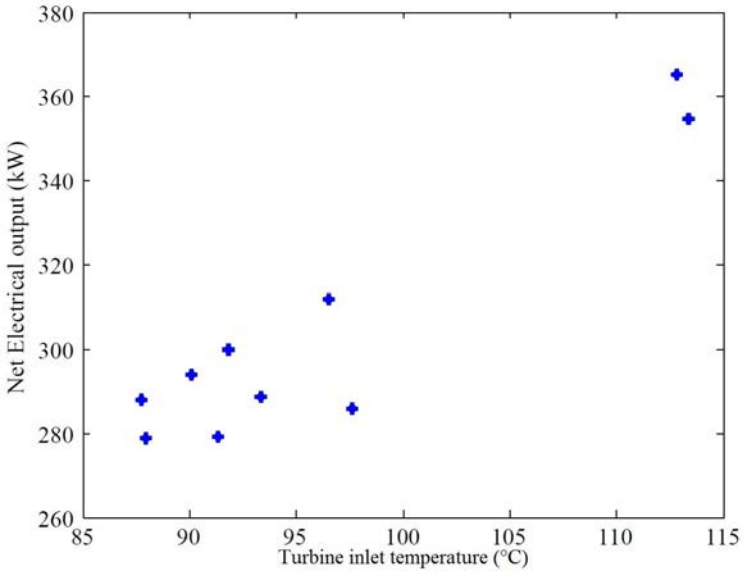

Figure 3.4: Influence of the turbine inlet temperature on the net electrical output

might be possible to achieve even more performing configurations by increasing the maximum allowed pressure.

The supercritical configuration is not possible for the other working fluids since the maximum allowed cycle temperature (140^cC) is lower than their critical temperature. In these cases the optimisation process leads to a saturated cycle (see Figure 3.6): at the outlet of the boiler the working fluid is saturated vapour or slightly superheated (the maximum super-heating occurs with cyclohexane and it is around 0.55 ^oC). The saturated configuration is characterised by two advantages: firstly the cycle maximum pressure is lower and this enables to decrease the investment costs (especially for the heat exchangers) and secondly the lack of the super-heating allows to have a simpler boiler configuration. Nonetheless in real power plants it is usually preferable to consider a super-heating of 5-10 ^oC in order to be sure not to have any droplet of fluid during the expansion in the turbine.

The results show no straight relationship between cycle efficiency and net power output: this is related to the fact that the heat absorbed by the working fluid is not a fixed parameter (the water exit temperature is function of cycle pressure, maximum temperature and working fluid characteristics) and thus configurations with lower efficiency but high utilisation factor may perform better than solutions where the efficiency is high but the source is poorly exploited.

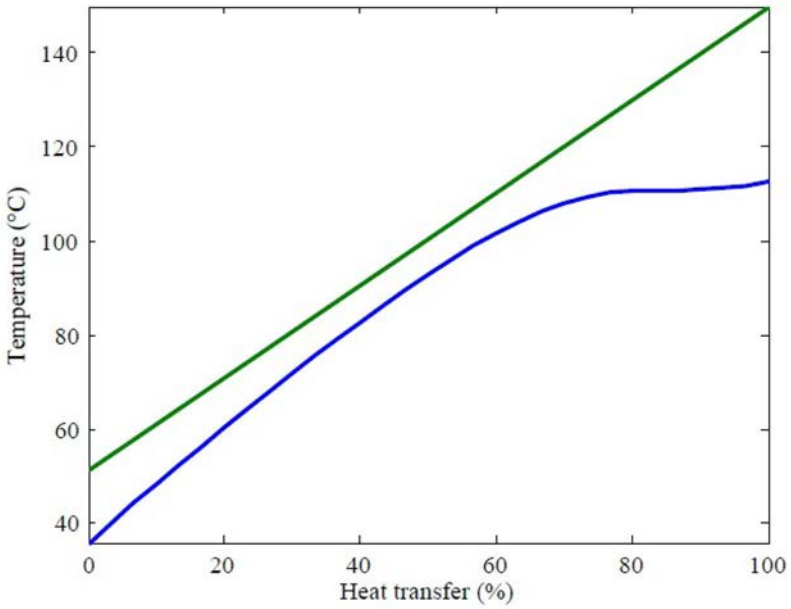

Figure 3.5: Supercritical configuration: boiler temperature profile for the R1234ze optimised configuration

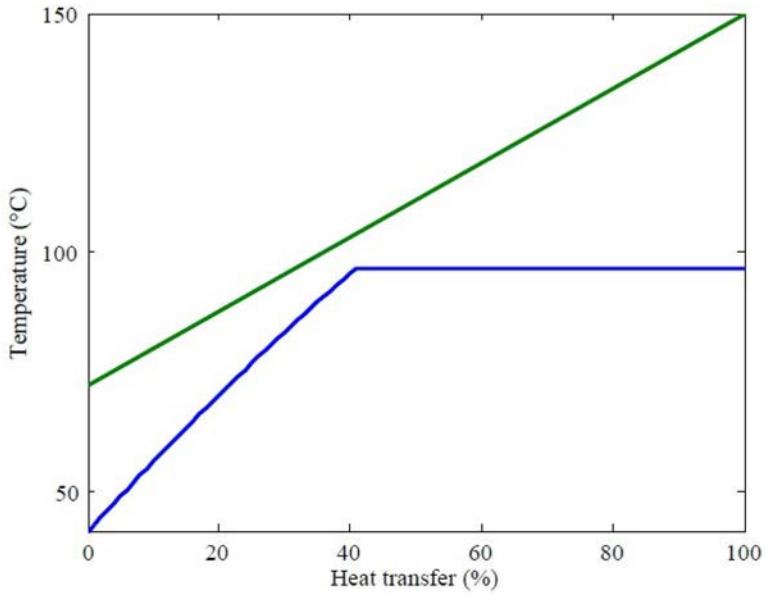

Figure 3.6: Saturated configuration: boiler temperature profile for the isobutane optimised configuration

3.4.3 Mixtures results

As a second step in the analysis of the low temperature heat source the genetic algorithm was run with 3 optimization parameters: maximum cycle pressure, turbine

inlet temperature and mixture composition. In order not to increase to much the computational time the various working fluids were fixed for every analysis. The same values described in section 3.4.2 were considered as lower and upper bounds for the maximum pressure and temperature, while the mixture composition was analysed by mean of the mass fraction of the first component (x_1), that was left free to vary from 0 to 1. The results of the optimization are depicted in table 3.6: the electrical output increase was calculated with respect to the best pure fluid among the two considered in the mixture.

Table 3.6: Low temperature mixtures results

Fluid 1	Fluid 2	High pressure $[bar]$	TIT $[^oC]$	x_1	W_{el} $[kW]$	$\%increase$
R1234yf	R1234ze	38,08	112,27	0,17	366,77	0,43
isobutane	pentane	15,42	94,87	0,89	320,87	2,89
ipentane	isobutane	14,61	91,79	0,13	320,83	2,88
ihexane	isobutane	16,65	96,83	0,06	320,37	2,73
cyclopentane	isobutane	16,95	98,45	0,07	318,72	2,20
hexane	isobutane	15,52	95,54	0,06	316,61	1,52
butane	ipentane	11,31	95,41	0,74	314,31	4,80
butane	pentane	10,76	90,41	0,86	312,90	4,33
butane	cyclopentane	12,09	94,18	0,92	311,22	3,77
butane	ihexane	11,99	97,91	0,88	310,72	3,60
butane	hexane	12,28	96,99	0,94	309,94	3,34
ihexane	pentane	3,31	88,80	0,51	308,69	6,99
butane	cyclohexane	11,83	93,85	0,97	307,88	2,65
hexane	pentane	5,40	95,01	0,14	306,93	6,58
ihexane	ipentane	2,64	90,52	0,90	306,01	4,18
hexane	ipentane	4,66	93,35	0,22	305,92	4,15
cyclohexane	ipentane	5,37	94,01	0,08	305,49	4,00
cyclohexane	pentane	3,94	93,84	0,17	304,24	6,48
cyclopentane	ipentane	5,05	93,41	0,35	300,87	2,42
cyclohexane	ihexane	1,66	89,26	0,54	298,42	3,43
cyclohexane	cyclopentane	1,63	92,64	0,82	297,95	6,73
cyclopentane	hexane	2,63	93,00	0,43	296,91	3,11
ipentane	pentane	5,91	92,00	0,89	293,99	0,09
hexane	ihexane	2,16	90,70	0,66	292,52	1,39
cyclopentane	pentane	4,31	90,73	0,31	291,83	2,13
cyclopentane	ihexane	2,66	89,55	0,29	291,87	1,16
cyclohexane	hexane	1,79	91,53	0,25	288,22	0,09

From the results of the analysis it appears that the use of mixtures can lead to an overall improvement of the plant performance. A net electrical output of 366.77 kW was achieved using a mixture 0.17/0.83 of R1234yf and R1234ze (0.43% more than pure R1234ze, the best pure fluid in the previous analysis). Looking at the results it appears that this performance increment is low if compared to other mixtures: this is probably related to the fact that the HFOs were characterised by

supercritical configurations with a good matching between the heat source and the working fluid in the boiler and therefore the introduction of the second component leads to a decrement of the irreversibility only in the condenser (see Figure 3.7 and 3.8).

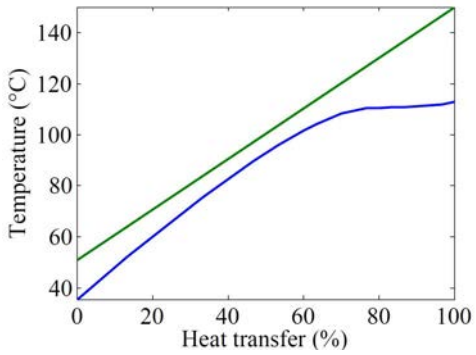

(a) Optimised R1234ze configuration

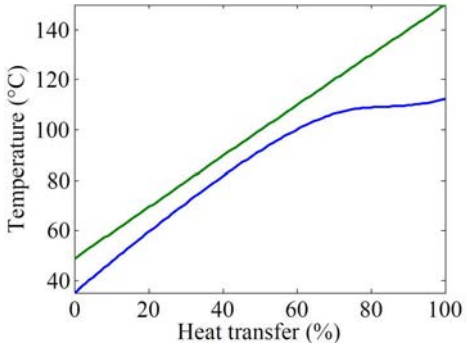

(b) Optimised R1234yf/R1234ze mixture

Figure 3.7: Boiler temperatures profile for: (a) R1234ze (b) R1234yf/R1234ze mixture

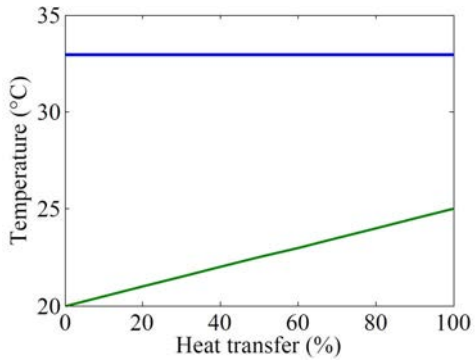

(a) Optimised R1234ze configuration

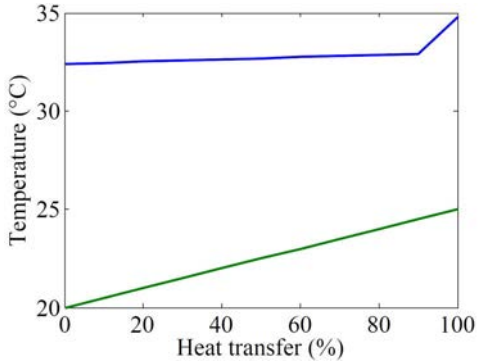

(b) Optimised R1234yf/R1234ze mixture

Figure 3.8: Condenser temperatures profile for: (a) R1234ze (b) R1234yf/R1234ze mixture

From the other results it clearly appears that for subcritical configurations the performance improvement is much greater than the one achieved with the two HFOs. In particular several mixtures using isobutane lead to electrical outputs above 320 kW (isobutane/pentane, isobutane/ipentane, isobutane/ihexane) which is about 12.5% lower than the maximum achieved electrical output. The best electrical input improvements are reached with the following mixtures:

- a mixture of ihexane and pentane (0.51/0.49) enables to produce 6.99 % more electricity than pure ihexane;
- a mixture of cyclohexane and cyclopentane (0.82/0.18) enables to produce 6.73 % more electricity than pure cyclohexane;

- a mixture of hexane and pentane (0.14/0.86) enables to produce 6.58 % more electricity than pure hexane;

The reasons behind the greater performance increment for these fluids can be found in their cycle configuration and in the temperature glide: since the pure fluid optimisation leads to a saturated cycle, the introduction of the non isothermal evaporation results in two advantages (see Figure 3.9):

1. the evaporation at variable temperature enables to decrease the irreversibility in the heat exchange process due to a better matching between the heat source and the working fluid;
2. the turbine inlet temperature increases and thus the cycle is more efficient;

The temperature glide is relevant even in the condensing process and enable to have lower pressures in the condenser (see Figure 3.10).

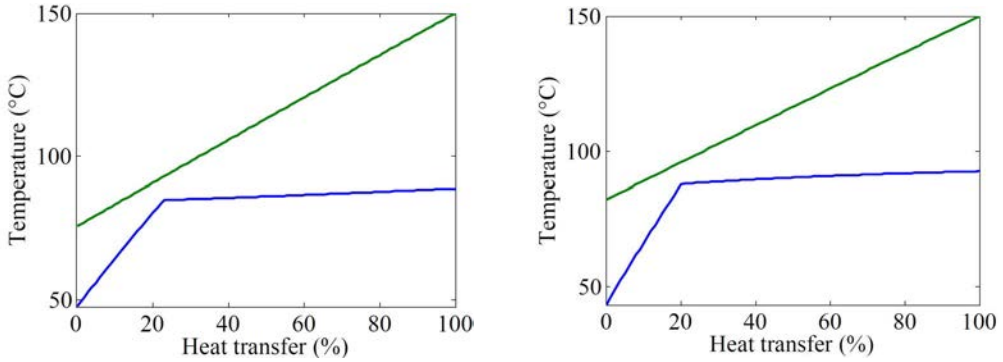

(a) ihexane/pentane **(b)** cyclohexane/cyclopentane

Figure 3.9: Boiler temperatures profile for mixtures: (a) ihexane/pentane (b) cyclohexane/cyclopentane

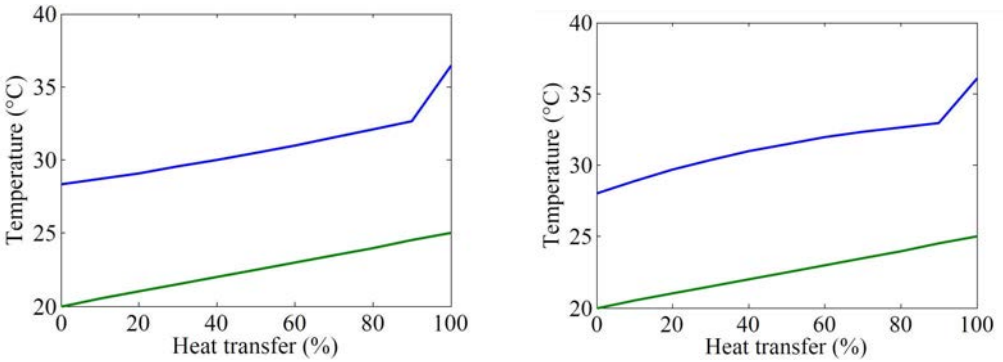

(a) ihexane/pentane **(b)** cyclohexane/cyclopentane

Figure 3.10: Condenser temperatures profile for mixtures: (a) ihexane/pentane (b) cyclohexane/cyclopentane

3.5 Moderate temperature heat source

As a second study case of this analysis a 310^oC heat source is analysed. The fixed parameters for the optimisation process are similar to the ones considered for the previous case and are listed in Table 3.7.

Table 3.7: Moderate temperature assumptions

Property	Value	Unit
Thermal oil mass flow rate	10	kg/s
Thermal oil inlet temperature	310	^oC
Cooling water inlet temperature	20	^oC
ΔT_{ap}	10	^oC
$\Delta T_{pp,evap}$	8	^oC
$\Delta T_{pp,rec}$	8	^oC
$\Delta T_{cooling-water}$	5	^oC
$\Delta T_{pp,cond}$	8	^oC
$\eta_{is,pump}$	0,70	
$\eta_{is,turbine}$	0,70	

3.5.1 Moderate temperature fluids

As the temperature level of the heat source increases it is important to investigate whether the selected working fluid are chemically stable at cycle maximum temperature. If most of the organic compound have no stability issues at 150^oC, the same cannot be taken for granted when the temperature reaches 300^oC. Since the aim of this analysis is to evaluate the potential performance of feasible power plants, thermal stability is one of the fundamental parameters that have to be considered during the working fluid selection.

The considered candidates (see Table 3.8) belong to two different categories:

- **Siloxanes**: these compounds have desirable thermodynamic characteristics like low toxicity and flammability, low foul formation over the heat transfer surfaces, good material compatibility and good thermal stability [47]. The maximum allowed working temperature for linear Siloxanes (MM, MDM, MD2M, MD3M) is about 300^oC [48, 49, 50]. Cyclic Siloxanes (like D4) are more stable: Angelino and Invernizzi [51] suggested a thermal limit near to 400^oC, ensuring 340^oC by means of an experimental test in presence of oxygen and humidity;

- **Hydrocarbons**: they are commonly used in biomass power plants and are characterised by desirable thermodynamic properties, but they can lead to safety hazards due to their flammability issues [9]. The typical values for maximum cycle temperature for existing ORC biomass power plants are around

300^oC and thus the maximum process temperature for Toluene and Ethylbenzene could be set to 327^oC [52]. According to N.A. Lai et al. [45] a maximum temperature of 300^oC an be considered for the remaining selected hydrocarbons;

Although the temperature limit for some refrigerants makes them suitable for the selected heat source level (according to [53] R227ea, R236fa and R23 can be stable up to 400^oC, while for R125 and R134a the temperature limit is about 368^oC), these compounds have not been considered since they are characterised by low values of the critical temperature and high GWP.

Table 3.8: Moderate temperature fluid list

Fluid	Category	T_c $[^oC]$	P_c $[bar]$	T auto ignition $[^oC]$	T stability $[^oC]$
Cyclohexane	Hydrocarbons	280	407	245	300
Decane	Hydrocarbons	321	22,7	210	300
Ethylbenzene	Hydrocarbons	344	36,1	432	327
m-Xylene	Hydrocarbons	343,9	35,41	527	300
o-Xylene	Hydrocarbons	603,18	31,72	463	300
p-Xylene	Hydrocarbons	589,08	35,11	528	300
n-Pentane	Hydrocarbons	196,7	33,6	260	n.a.
Toluene	Hydrocarbons	319	41,3	480	327
MM	Siloxanes	245	19,1	340	300
MDM	Siloxanes	291	14,4	350	300
MD2M	Siloxanes	326	12,2	n.a.	300
MD3M	Siloxanes	354	9,3	403	300
D4	Siloxanes	312	13,1	400	340

3.5.2 Pure fluids results

As for the low temperature case the best configuration for every working fluid has been calculated through an optimization process. In this case the maximum pressure limit has been set to 50 bar, while the turbine inlet temperature has been left free to vary between 150 and 300 ^oC . In order to avoid flammability issues, the maximum allowed temperature have been decreased respectively to 225, 190 and 240^oC for Cyclohexane, Decane and n-Pentane.

The results obtained through the optimisation process are the shown in Table 3.9. First of all it appears that using a higher temperature heat source leads to a consisten increment of the generated power: given the same mass flow rate for the thermal carrier the net power output increases from about 300 kW to roughly 1 MW. This is mostly related to the higher thermal efficiency that can be reached as the temperature level increases (the values of the thermal efficiency are almost double the values of the previous case).

As a second important consideration it appears that the higher temperature level leads to a more complex analysis of the potential configurations. Many of the output values are in fact characterised by values of the cycle parameters that are not feasible, lead to highly expensive installation costs, or are related to safety hazards:

1. The most performing fluid (Cyclohexane) has a turbine inlet temperature that is only 35^oC lower than its auto-ignition temperature and therefore a very accurate control system would be required in order to avoid undesired safety hazards during part load operation;

2. Looking at the condensing pressures it appears clearly that in most of the cases the calculated values are below the feasibility limit (0.03-0.05 bar) and therefore all these solutions have to be discarded;

3. Not even a solution considers an atmospheric condenser: the configuration with n-Pentane has a relatively high condensing pressure, but the other feasible configurations (the ones with Cyclohexane, MM and Toluene) would require high investment costs for the condenser.

Table 3.9: Moderate temperature fluid results

Fluid	High pressure $[bar]$	TIT $[^oC]$	P cond $[bar]$	η_{el}	T_c $[^oC]$	$\dot{W}_{el}$ $[kW]$	ΔW [%]
Cyclohexane	15,82	210,45	0,1835	0,22	108,35	938,18	0,00
Toluene	6,24	189,88	0,0564	0,21	98,74	909,26	-3,08
Ethylbenzene	2,64	175,81	0,0198	0,20	90,07	900,64	-4,00
P-xylene	2,42	174,27	0,0183	0,20	89,82	895,91	-4,50
M-xylene	2,71	185,84	0,0140	0,21	103,81	895,31	-4,57
Mxylene	2,60	178,11	0,0174	0,20	95,52	894,11	-4,70
n-Pentane	50,00	236,41	0,9034	0,21	111,70	867,52	-7,53
Decane	1,35	185,77	0,0031	0,21	117,81	855,62	-8,80
MM	21,12	245,57	0,0807	0,22	125,53	849,41	-9,46
D4	2,53	215,22	0,0023	0,23	146,81	812,38	-13,41
MDM	3,47	207,02	0,0081	0,23	144,32	796,35	-15,12
MD3M	1,03	230,71	0,0001	0,26	168,37	794,96	-15,27
MD2M	1,61	214,25	0,0010	0,24	154,85	784,86	-16,34

In order to make a comparison between feasible configurations a fixed condensing pressure level was set for the working fluids whose condensing pressure was not acceptable. Since increasing the condensing pressure will lead to a significant decrement of the power output two pressure levels have been chosen:

1. A sub-atmospheric level (P_{cond} = 0.05 bar) that will investigate the performance of feasible power plants;

2. An atmospheric pressure (P_{cond} = 1.05 bar) that will investigate the performance of plants with less expensive condensers;

In addition, as the condensing pressure is strictly related to the cold source temperature, the required water inlet temperature was recalculated for all the configurations (with the assumption of $\Delta pp_{cond} = 8^oC$ and $\Delta T_{cooling-water} = 5^oC$).

Condensing pressure = 0.05 bar

As a first case study the condensing pressure was set equal to 0.05 bar for all fluids with not feasible condensing pressure. After the recalculation, the results obtained are the following (Table 3.10):

Table 3.10: Moderate temperature fluid results with a minimum condensing pressure of 0.05 bar

Fluid	High pressure [bar]	TIT [^oC]	P cond [bar]	η_{el}	T_c [^oC]	W_{el} [kW]	$T_{water,in}$ [^oC]
MM	21,12	245,57	0,08	0,22	125,53	849,41	25,00
MDM	5,18	228,38	0,05	0,20	173,91	578,67	50,99
MD2M	2,38	232,60	0,05	0,16	195,44	397,28	86,42
MD3M	1,94	260,37	0,05	0,14	230,26	258,06	116,45
D4	3,07	224,71	0,05	0,17	178,62	479,80	71,79
Cyclohexane	15,82	210,45	0,18	0,22	108,35	938,18	25,00
Toluene	6,24	189,88	0,06	0,21	98,74	909,26	25,00
Ethylbenzene	3,89	194,65	0,05	0,19	122,47	756,08	35,52
M-xylene	3,28	189,03	0,05	0,18	120,93	728,93	38,07
O-xylene	2,70	185,72	0,05	0,18	120,53	695,69	42,27
P-xylene	2,62	177,87	0,05	0,17	107,92	730,85	37,16
n-Pentane	50,00	236,41	0,90	0,21	111,70	867,52	25,00
Decane	1,49	190,00	0,05	0,14	148,33	496,37	68,86

The greatest power output is still reached with cyclohexane (its configuration has not changed), but a significant performance decrement can be seen for other fluids. In particular for decane the estimated power outputs decreases by about 42% (from 855 kW to 496 kW). Siloxanes (except for MM) are also greatly affected by the condensing pressure constrain (see Table 3.11). Even if the condensing pressure is very low, the estimated cooling water inlet temperature for this category of compounds ranges between 51^oC and 116^oC and thus they seem more suitable for cogenerative solutions rather than for conventional power plants.

Fluid	$W_{el,max}$ [kW]	W_{el} (P_{cond} = 0.05 bar) [kW]	ΔW [%]
MDM	796,35	578,67	-27,34
MD2M	794,96	397,28	-50,02
MD3M	784,86	258,06	-67,12
D4	812,38	479,80	-40,94

Table 3.11: Siloxanes performance drop with a minimum condensing pressure of 0.05 bar

Other compounds like Ethylbenzene, m-xylene, p-xylene and o-xylene show acceptable electrical outputs (about 10-15 % lower than the cyclohexane configuration) and a fairly low condensing temperature.

Condensing pressure = 1.05 bar

As a second case study a condensing pressure of 1.05 bar was chosen in order to analyse the performance of power plants with atmospheric condensers. The use of this kind of technology for the condenser greatly simplifies the plant configurations since there is no need to prevent air infiltration from the environment and thus enables to have relevant reduction of invesment costs. The results of this second case can be found in Table 3.12.

Table 3.12: Moderate temperature fluid results with a minimum condensing pressure of 1.05 bar

Fluid	High pressure $[bar]$	TIT $[^oC]$	P cond $[bar]$	η_{el}	T_c $[^oC]$	W_{el} $[kW]$	$T_{water,in}$ $[^oC]$
MM	22,23	253,86	1,05	0,14	171,07	428,48	86,07
MDM	18,27	291,00	1,05	0,11	221,54	221,23	138,94
MD2M	4,63	267,51	1,05	0,08	251,84	99,51	180,60
MD3M	1,97	261,10	1,05	0,03	255,26	39,63	216,38
D4	6,02	261,85	1,05	0,09	234,59	152,89	161,45
Cyclohexane	17,61	217,58	1,05	0,17	144,63	580,64	66,18
Toluene	11,08	223,06	1,05	0,14	177,67	390,39	96,09
Ethylbenzene	7,42	230,12	1,05	0,11	201,09	272,56	121,78
M-xylene	7,92	236,53	1,05	0,12	209,67	258,24	124,67
O-xylene	6,56	232,13	1,05	0,11	207,84	239,84	130,00
P-xylene	7,17	230,28	1,05	0,11	202,21	264,06	123,93
n-Pentane	49,23	235,66	1,05	0,20	114,68	831,86	21,49
Decane	1,49	190,00	1,05	0,02	185,85	53,26	160,00

The use of an atmospheric condensing pressure leads to great changes in the results. First of all it appears a clear reduction of the maximum achievable power output: the only working fluid that shows power outputs similar to the previous cases is n-Pentane, while for all the other configurations the net electrical output is lower than 600 kW. This performance drop is strictly related to the super imposed condensing pressure: by decreasing the lower pressure of the cycle the pressure ratio across the turbine decreases and this leads to lower power productions. As a consequence the fluids that are penalised the most are those who had the lowest condensing pressures in the first analysis (MD2M, MD3M and decane), while the less penalised is n-pentane that had a condensing pressure of 0.9 bar.

Secondly it is clear that in this case most of the hydrocarbons and the siloxanes would be suitable for cogenerative applications: the inlet temperature of the cooling water ranges from 66^oC for cyclohexane to 216^oC for MD3M and therefore it would be a waste not to recover the heat released in the condenser. For the cyclohexane the use of an air condenser unit could be investigated, but it would be preferable

to couple the plant with a process requiring low temperature heat (a drying system for example).

Analysing the results as in section 3.4.2 it appears that, as for the low temperature case, there is a strong relationship between the thermal oil outlet temperature and the net power output (Figure 3.11). However if for the low temperature case a higher value for the turbine inlet temperature was associated with a higher power output, this is not always true for the moderate temperature case; instead there seems to be a connection between the cycle high pressure and the net power output (since the condensing pressure is fixed the increment of the cycle maximum pressure leads to an increment of the pressure ratio across the turbine and thus to higher power outputs).

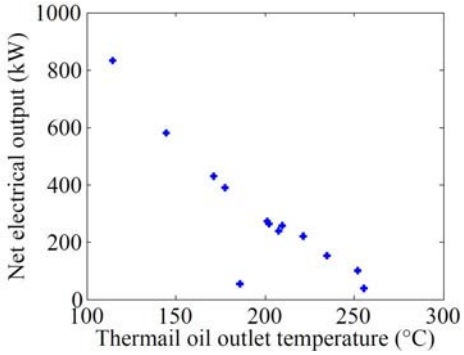

(a) Influence of thermal oil outlet temperature on W_{el}

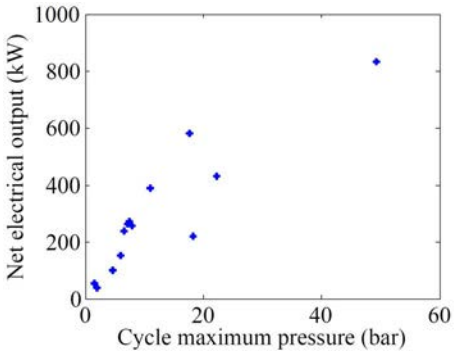

(b) Influence of cycle maximum pressure on W_{el}

Figure 3.11: Influence of different parameters on the net electrical output: (a) thermal oil outlet temperature (b) cycle maximum pressure

Pure fluids discussion

As it emerges from the previous sections, many parameters have to be taken into account in order to define which pure fluid is the most suitable for a moderate temperature heat source. First of all, a minimum value for the condensing pressure should be fixed: sub-atmospheric pressures enable to effectively produce power with several working fluids (in this case good results are achieved with cyclohexane and MM), while the choice of an atmospheric condenser leads to a more simple design of this component and thus to lower investment costs.

The most suitable candidate for power only plants with an atmospheric condenser is n-pentane and in fact this fluid was selected as working fluid for the 1 MW_{el} Saguaro Concentrated solar plant [60].

Hydrocarbons seems to be more promising when used in cogenerative plants: as the condensing pressure increases they release heat at higher temperature levels and so they could be couple with different kind of industrial processes. If a sub-atmospheric condenser is considered m-oxylene, p-xylene and o-xylene could be

used in connection with an air condenser and still produce a relevant power output (about 700 kW). The same goes for a cyclohexane configuration coupled with an atmospheric condenser (in this case the net electrical output decreases to 580 kW).

Siloxanes are greatly affected by the condensing pressure: ideally, they are potential fluids, but as the condensing pressure increases their power output drops drastically. The most interesting fluid among this category is MM either in atmospheric (cogenerative or coupled with air condenser) or sub-atmospheric (cogenerative only) configurations. All the other compounds are characterised by high condensing temperatures and so their use would be reasonable only in cogenerative applications.

3.5.3 Mixtures results

As stated at the beginning of Chapter 2 few references are available for moderate temperature applications using zeotropic mixtures. The following analysis is therefore carried out investigating the performance of possible mixtures composed by the pure fluids described in section 3.5.1. The metodology is the same explained for the low temperature case: the performance of every mixture is analysed by means of an optimization process that considers turbine inlet temperature, maximum cycle pressure and mixture mass fraction as optimization parameters.

In order to avoid problems related to the composition itself, only mixtures made of two compounds from the same category have been investigated. For the condensing pressure two different approaches have been considered:

1. For mixtures composed by toluene, cyclohexane and n-pentane the pressure level is left free to vary accordingly to the pinch point criteria: since the pure fluids had technically feasible values for the condensing pressure, their mixture will most probably behave similarly;

2. For the other mixtures the condensing pressure has been set as a fixed parameter in the optimisation process: the selected pressure levels are 1.05 and 0.05 bar (like for the pure fluids case). This way it will be possible to find out whether the selected pressure level has any relevance on the mixture performance.

Free condensing pressure

As shown in Table 3.13 the introduction of mixtures for this temperature range leads to more performing configurations: using a combination of cyclohexane and toluene improves the net electrical output by 2.77 %, while the increment is equal to 1.53% with n-pentane and cyclohexane. Nonetheless no performance gain is reached with a mixture of toluene and n-pentane.

Analysing the temperature profiles of the cyclohexane/toluene mixture both for the boiler (Figure 3.12) and the condenser (Figure 3.13) it clearly appears a better match between the working fluid and the two heat sources. Anyway, looking at

the results it is easy to understand that the performance gain is mainly related to the higher turbine inlet temperature (that reaches about 222 ^oC) and the lower condensing pressure (0.13 bar instead of 0.18). While the lower condensing pressure is still in the feasibility range, the increased maximum temperature might lead to safety hazards considering the auto ignition temperature of 245 ^oC for cyclohexane.

Table 3.13: Moderate temperature mixtures results

Fluid 1	Fluid 2	High pressure $[bar]$	TIT $[^oC]$	x_1	W_{cl} $[kW]$	$\%increase$
Cyclohexane	Toluene	17,19	222,26	0,83	964,12	2,77
Cyclohexane	n-pentane	19,29	220,74	0,95	952,56	1,53

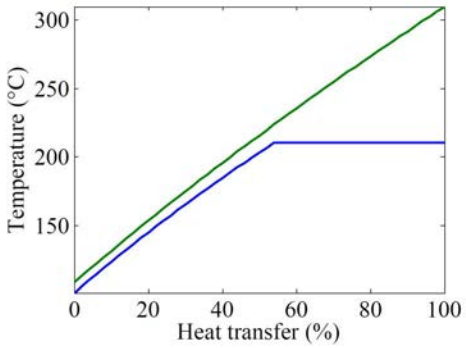

(a) Optimised Cyclohexane configuration

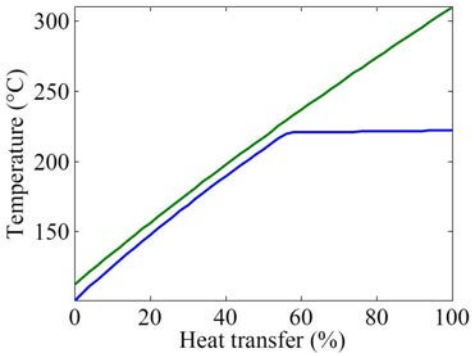

(b) Optimised Cyclohexane/Toluene mixture

Figure 3.12: Boiler temperatures profile for: (a) Cyclohexane (b) Cyclohexane/Toluene mixture

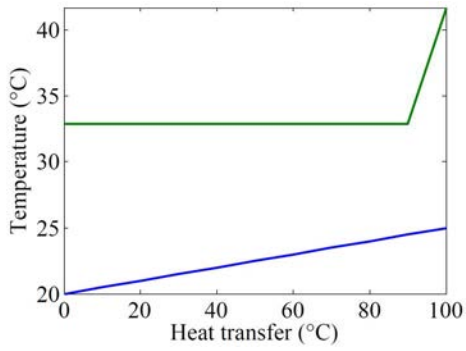

(a) Optimised Cyclohexane configuration

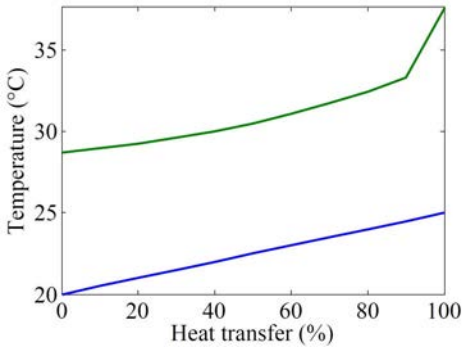

(b) Optimised Cyclohexane/Toluene mixture

Figure 3.13: Condenser temperatures profile for: (a) Cyclohexane (b) Cyclohexane/Toluene mixture

Fixed condensing pressure

The optimization of the other possible mixtures shows little or no power output improvement within the selected thermal level. The only slight gains are obtained using ethylbenzene/m-xylene and p-xylene/m-xylene mixtures (see Table 3.14).

Looking at the results from the optimized configuration for p-xylene/m-xylene it seems that changing the condensing pressure has little relevance in the performance of the mixtures: the performance gain with both the selected pressures is really similar and occurs with the almost the same mixture composition.

Table 3.14: Moderate temperature mixtures results

Fluid 1	Fluid 2	High pressure [bar]	TIT [bar]	P cond [^oC]	x_1	W_{el} [kW]	$\%increase$
Ethylbenzene	p-xylene	3,51	188,96	0,05	0,71	759,01	0,39
p-xylene	m-xylene	2,93	181,71	0,05	0,63	741,59	1,47
p-xylene	m-xylene	6,76	225,26	1,05	0,57	268,35	1,62

The estimated power output increment is anyway not enough to make such mixtures particularly interesting for the considered heat source level:

- if an atmospheric condenser is chosen MM and Cyclohexane show better performances for power productions, while for cogenerative solutions Ethylbenzene seems to be a more suitable candidate (it enables to produce slightly more electrical output and it releases heat at the same temperature level);
- if sub-atmospheric condenser is chosen the considered mixture could lead to good results when coupled to a air cooling unit, but a performance increment lower than 2% might not enough to justify the use of the mixture rather than the corresponding pure fluids;

3.6 Discussion

In this chapter the performance of different power cycle configurations was analysed. The fixed parameters in the optimization process were the cooling water inlet temperature, the heat source mass flow rate and maximum temperature, while cycle maximum pressure and temperature were chosen as the optimization parameters. No constrain was defined for the outlet temperature of the heat source and therefore the aim of this first study was to define which configurations were capable of producing the greatest amount of electrical power out of a given heat source. Moreover, since both pure fluids and binary mixtures were considered as possible candidates, the results enabled to understand whether the use of zeotropic mixtures could allow relevant performance improvement for the two selected heat source levels.

In the first case study a 150^oC heat source was analysed. The optimization process showed that the most performing fluids among the the selected candidates

are the HFOs R1234ze and R1234yf in supercritical configuration. For the hydrocarbons, the optimization process leads to a saturated cycle configuration and the most performing fluid of this category is isobutane, whose power production is 14.6% lower than R1234ze. Primary indicators of the effectiveness of a power cycle configuration are the heat source outlet temperature (the power production increases for those configurations that are able to effectively extract heat from the heat transfer fluid) and the turbine inlet temperature.

As the use of mixtures was introduced into the power cycle analysis two different results emerged. The configurations using a mixture of R1234yz and R1234ze as working fluid show a very little power output increment (lower than 0.5 %). This might be related to their supercritical configuration: in this case the introduction of the temperature glide during the evaporation and condensation process has a lower incidence since the evaporation process is not isothermal even in the pure fluid case.

On the other hand when the analysis considered mixtures of different hydrocarbons a relevant performance increment appeared. The configurations that show the best performance improvement are ihexane-pentane (0.51/0.49), cyclohexane-cyclopentane (0.82/0.18) and hexane-pentane (0.14/0.86) that enable to produce respectively 6.99, 6,73 and 6.58 % more power than the best pure fluid in the considered mixture. All of these mixtures show the best results in a saturated cycle configuration: in this case the introduction of the temperature glide enables to increase the turbine inlet temperature and to decrease the irreversibility both in the boiler and in the condenser.

In the second case study a 310^oC heat source was analysed. As the temperature level of the heat source increases, stability and flammability issues might appear for some working fluid and therefore the analysis considered only fluids whose stability have been proved up to 300^oC. Additional constrains for the cycle maximum temperature have been considered for fluids with flammability issues.

A primary optimization process showed that, given the considered cooling water inlet temperature, most of the selected working fluids configuration were characterised by not feasible condensing pressures (the only feasible configurations are those with Cyclohexane, Toluene, n-Pentane and MM). As a consequence, in order to compare the performance of the other candidates two fixed condensing pressure were considered: a sub-atmospheric level (P_{cond} = 0.05 bar) and an atmospheric level (P_{cond} = 1.05 bar).

The optimization of the pure fluid configurations shows that the greatest electrical outputs are achievable with Cyclohexane and Toluene (both these fluids have feasible condensing pressures). As the condensing pressure increases the power output decreases and at the same time the required temperature for the condensing water increases. In particular, for Siloxanes the performance drops by 50% even with a condensing pressure of 0.05 bar and the required water temperature ranges between 51 and 116^oC.

When an atmospheric condenser is considered the only fluid that reaches a power output comparable to the previous cases is n-Pentane, while for the other configurations the net electrical output drops at least by 40 %. In this case most of the fluids release heat at high temperature ($> 100^oC$) and thus it is clear that those configurations would be more suitable for cogenerative applications.

The use of mixtures seems less profitable for this temperature level: a mixture of Cyclohexane and Toluene (0.83/0.17) shows a performance improvement of 2.77% but this is mostly related to a lower condensing pressure and to and increased turbine inlet temperature. The increased value for the turbine inlet temperature is also related to safety issues: cyclohexane is characterised by a low value for the auto-ignition temperature and thus by increasing the cycle maximum temperature safety hazards might appear. A mixture of cyclohexane and n-Pentane (0.95/0.05) shows a performance improvement of 1.53%, but the increased value for turbine inlet temperature leads to the same considerations of the previous case.

Considering the behaviour of mixtures for configurations with a fixed value for the condensing pressure a performance increment is possible using a mixture of p-xylene and m-xylene: the power output increases by 1.47% with $P_{cond} = 0.05$ bar and by 1.62% with $P_{cond} = 1.05$ bar. From this result it appears that the effectiveness of mixtures is not strictly related to the considered condensing pressure. Nonetheless it should be considered that fixing the condensing pressure instead of the cooling water inlet temperature might not be a fair way to compare pure fluids and mixtures: by fixing the condensing pressure the analysis neglects the benefits of the temperature glide in the condensing process. Furthermore it is not a common practice to fix the condensing pressure: usually the design study takes into account the cooling water availability and the condensing pressure is chosen so that to fulfil the cooling requirements.

The moderate temperature case seems more complex and less promising for mixtures: detailed plant specification (range of acceptable condensing pressures, purpose of the plant, possibility to recover the released heat in a bottoming process) and tests on the working fluids (thermal stability should be ensured and the limits to avoid flammability issues should be defined) are required in order to pick the most suitable configuration. As a consequence, after the first analysis carried out in this chapter, it has been decided to keep analysing the performance of power cycles tailored to low temperature heat sources.

Chapter 4

Concentrated solar power technology

In order to investigate the behaviour of mixtures in organic rankine cycles tailored for solar applications a model for the solar field has to be built. In the previous chapter it has been shown that the use of mixtures allows to produce more power out of a hot source, but the behaviour of an overall solar power system is more complex.

When the purpose is to produce the maximum power, like for example in geothermal power plants, the optimal solution is the one that better exploits the available heat source by decreasing its temperature as much as possible (a minimum allowed re injection temperature is usually defined), but this is not necessarily true for solar-driven power plants. In a concentrated solar plant the heat transfer fluids operates in a closed loop so that the outlet of the boiler is the inlet of the solar field: solutions with very low boiler outlet temperatures for the heat carrier will require bigger collecting surfaces and thus will be characterised by higher losses of the solar field. On the other hand solutions with small temperature drops in the boiler might enable to have lower losses in the solar field but might be penalised by higher values of the heat transfer fluid mass flow rate.

In order to find out a trade off between costs and power production a thermoeconomic optimization is usually performed for this kind of plants: the purpose is thus to define which configuration will enable to have the lower levelised cost of electricity.

In this chapter a brief overview of this technology will be presented and then the considered solar field model will be described.

4.1 Technology overview

The increasing awareness on the environmental problems related to the traditional fuel based power plants forces us to investigate and exploit more sustainable sources of energy. Among the different renewable sources of energy, the solar power could play a primary role in the development of a new and more sustainable electricity generation system. A schematic view of solar conversion technologies can be seen

in Figure 4.1.

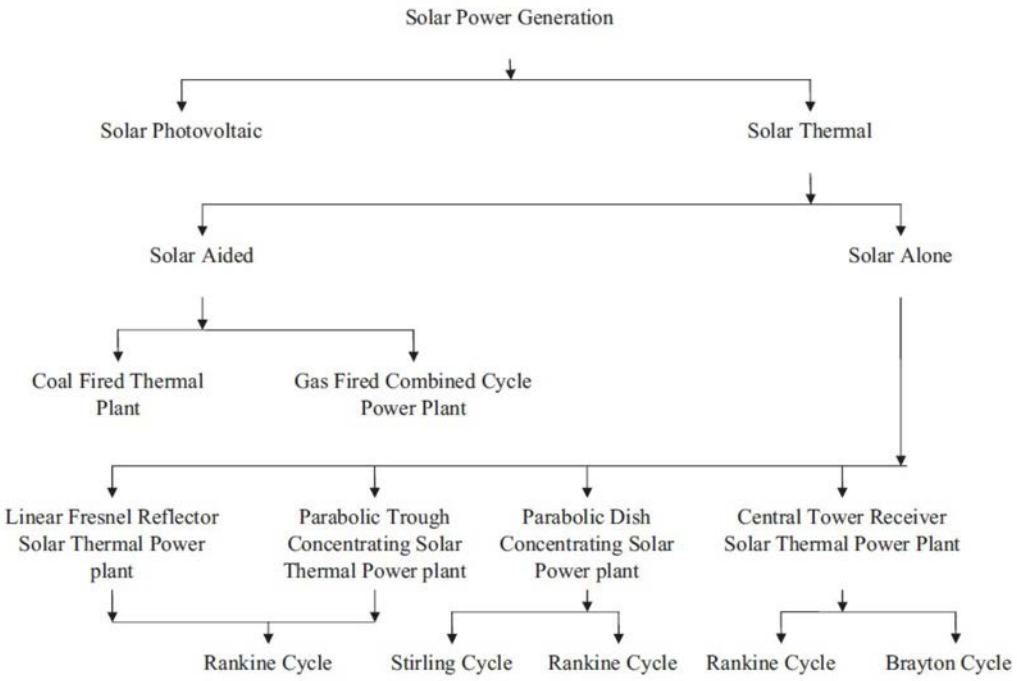

Figure 4.1: Schematic representation of solar conversion technologies [56]

In a concentrated solar power plants the solar irradiation is concentrated into a small area: this enables to heat the heat transfer fluid up to 1000 ^oC and thus to increase the efficiency of the conversion system. In order to be able to provide electricity as it is needed, most of these plants are equipped with a thermal storage system or a backup system: both of these technologies enable to extend the power production period and to shift the electricity production from the source availability to the peak demand hours [56].

Another possibility is to couple a solar driven power system with a traditional power generation plant: in this way it is possible to perform a more effective conversion of sun energy into electricity and to obtain a more constant power production. As already mentioned in Chapter 2 both solar aided coal-fired [4] and solar gas-turbine [5] power plants have been proposed.

Although Concentrated power plants have already been proved to be a economically feasible, their installation is only possible in those locations characterised by high values of direct normal irradiation. At present four technologies are available:

4.1.1 Solar power towers

In this application a field of distributed mirrors (heliostats) concentrates the sun radiation into a central receiver usually placed at the top of a fixed tower (see Figure 4.2). The heliostats follows the sun thanks to a two-axis tracking system and since the sun radiation is concentrated up to 600-1000 times the selected heat

transfer fluid can reach temperatures of 800-1000^oC [57]. The operating plants are usually linked to a steam Rankine cycle and different heating transfer media can be considered: air, molten salts (both as heat transfer and storage media) and steam (also in direct steam generation applications). Given the high temperature that can be achieved, solar tower power plants can be also used to drive gas turbines or combined cycles: a volumetric receiver developed within the European SOLGATE project have already been successfully used to operate a 250 kW gas turbine over 800 ^oC [57].

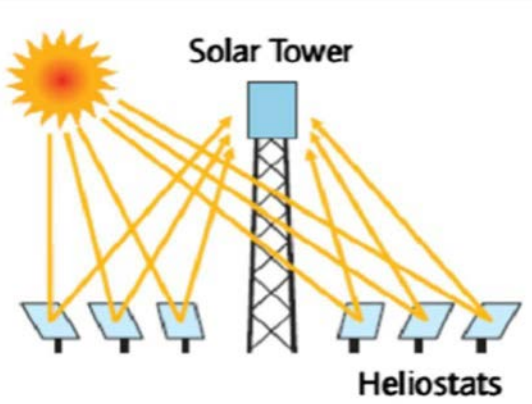

Figure 4.2: Solar tower [56]

4.1.2 Parabolic dish systems

A second application that enables to reach very high temperatures is the parabolic dish system. In this case a parabolic dish collector continuously tracks the sun and concentrates the solar irradiation in its focal point (see Figure 4.3). The conversion of the heat into power is usually performed with a stirling engine or a small gas turbine. As all the system tracks the sun, only small capacity units are feasible (the typical size is 10 kW or smaller) and thus hundreds of dishes would be required in order to reach significant power outputs. Nonetheless this technology enables to reach the highest conversion efficiency among all the CSP systems and mass production might allow to substantially decrease the investment costs [58].

4.1.3 Parabolic trough collectors

Parabolic trough are the most common CSP technology: the solar energy is collected by curved mirrors and reflected onto a linear shaped receiver (see Figure 4.5). As the concentrating ratio is lower than in previous applications, the heat transfer fluid (usually pressurized water, thermal oils or molten salts) can be heated up to temperatures around 350-550 ^oC and can supply either a steam or an organic Rankine cycle. Parabolic trough are generally installed along a one-axis tracking system: both east-west and north-south configurations are possible. The biggest parabolic trough application is the Solar Electric Generation System (SEGS) located in southern California and has an overall capacity of 354 MW_e [59]. As reported by Quoilin et al [60] few systems operate with an organic rankine cycle: a 1 MW_e power plant

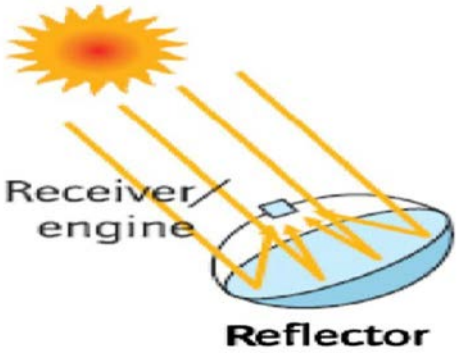

Figure 4.3: Parabolic dish system [56]

using n-pentane is located in Arizona, a 100 kW_e was commissioned in Hawaii and some kW-size prototypes are under study for remote off-grid applications. Even though the control of two-phase steam water flow inside horizontal absorber tubes is a major engineering challenge, direct steam generation have already been demonstrated by CIEMAT and DLR in a 500 m test loop with an aperture of 5.78 m [57].

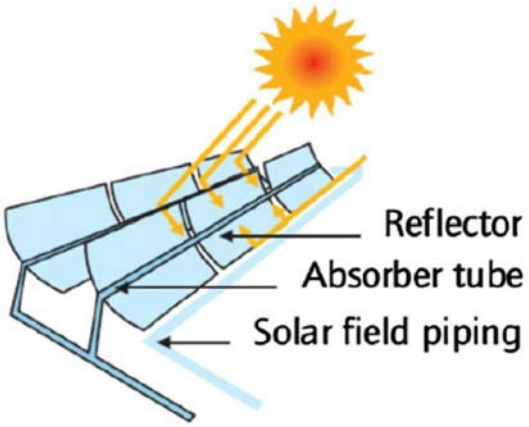

Figure 4.4: Parabolic trough system [56]

4.1.4 Linear Fresnel reflectors

Linear Fresnel are based on the same principle of the parabolic trough collectors: the sunlight is collected by mirrors and then reflected into a linear receiver. However in this case a set of flat mirrors emulate the presence of a parabolic receiver: this allows to install the receiver on a separate unit and thus to have a cheaper and more effective tracking system [58]. The downside of this system lies in the shading that can occur between adjacent mirrors: in order to reduce this shading effects it would be necessary either to increase the spacing between to consecutive rows (and thus to increase the land usage) or to increase the height of the receiver with the related increment of the investment costs.

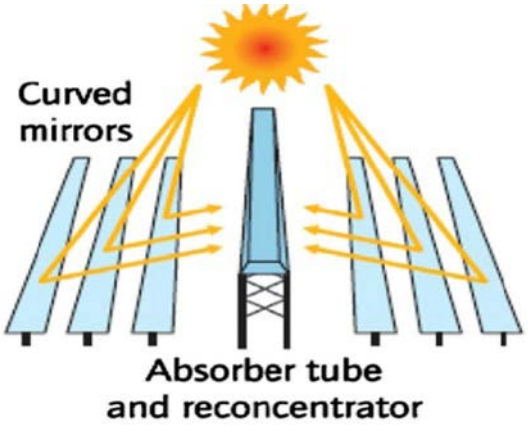

Figure 4.5: Linear Fresnel reflectors [56]

4.2 Calculation of collected solar energy

This thesis considers a parabolic trough solar system as this is a very well known technology and it enables to reach the required temperature (150 ^oC) for the heat transfer fluid.

In order to perform an annual simulation of the considered power system it is necessary to define solar energy impinging on the solar collectors in every moment of the day. The energy that is received and reflected into the receiver depends on various factors, some of them are:

- the day and the hour of the day;
- the location of the power plant;
- the considered collector technology;
- the tracking system;

As reported by Burkeholder et al. [61], the solar irradiation absorbed per unit of collector length, expressed in W/m can be calculated in the following way:

$$Q_{SolAbs} = DNI \cos(\theta) A_p \eta_{opt} IAM \tag{4.1}$$

where:

DNI is direct normal irradiation in W/m^2;

Θ is the incidence angle: the angle between the direction of the sunlight and the direction normal to the surface (see Figure 4.6);

A_p is the collector aperture (m);

η_{opt} is the optical efficiency at normal incidence: it includes the reflectance of the reflector, the glass envelope transmittance and effects of dirt, geometry and shading;

IAM is the incidence angle modifier and it's a function of the incidence angle and the optical qualities of the collectors. According to Dudley et al. [63], it can be estimated as:

$$IAM = min\left\{1; \frac{\cos(\theta) + 0.000884\,\theta - 0.0000537\,\theta^2}{\cos(\theta)}\right\} \tag{4.2}$$

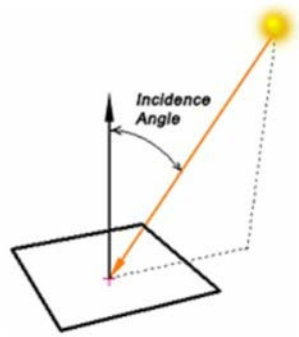

Figure 4.6: Incidence angle: the angle between the direction of the sunlight and the normal to the surface

The parabolic trough system is continuously adjusted in order to maximize the collected solar energy but a perfect tracking is possible only by using a 2-axis system. According to Duffie et al [64] the incidence angle for an horizontal plane continuously rotated about an east-west axis in order to maximize the collected energy is given by:

$$cos(\theta) = \sqrt{1 - cos^2(\delta)sin^2(\omega)} \tag{4.3}$$

If instead the considered surface rotates about a north-south axis, the incidence angle can be calculated as:

$$cos(\theta) = \sqrt{cos^2(\theta_z) - cos^2(\delta)sin^2(\omega)} \tag{4.4}$$

In order to evaluate the value of the incident angle, three new parameters have to be defined:

1. The declination angle (δ) that is the angular position of the sun at solar noon with respect to the plane of the equator, north positive;

2. The zenit angle (θ_z) that is the angle between the vertical and the line to the sun;

3. The hour angle (ω) that is the angular displacement of the sun east or west of the local meridian due to the rotation of the earth on its axis at 15^o per hour;

The declination angle is function of the number of the day n (1 for the 1st of January, 365 for 31st of December) and can be evaluated using the approximated equation of Cooper [64]:

$$\delta = 23.45\ sin\left(360\ \frac{284+n}{365}\right) \tag{4.5}$$

The zenit angle is related to the latitude (ϕ) and is given by:

$$cos(\theta_z) = cos(\phi)cos(\delta)cos(\omega) + sin(\phi)sin(\delta) \tag{4.6}$$

The hour angle is zero at noon, positive after noon and negative in the morning, it can be calculate as:

$$\omega = 15^o\ (Local\ solar\ time - 12^o) \tag{4.7}$$

The local solar time can be calculated from the standard time:

$$Solar\ time = Local\ time + 4(L_{st} - L_{loc}) + E \tag{4.8}$$

where:

L_{st} is the standard meridian for the local time zone;

L_{loc} is the longitude of the selected location;

E is the equation of time (see Figure 4.8) and is given by the following equation from Spencer (1971) [64]:

$$\begin{aligned} E = 229.2(&0.000075 + 0.001868cos(B) - 0.032077sin(B) \\ &- 0.014615cos(2B) - 0.04089sin(2B)) \end{aligned} \tag{4.9}$$

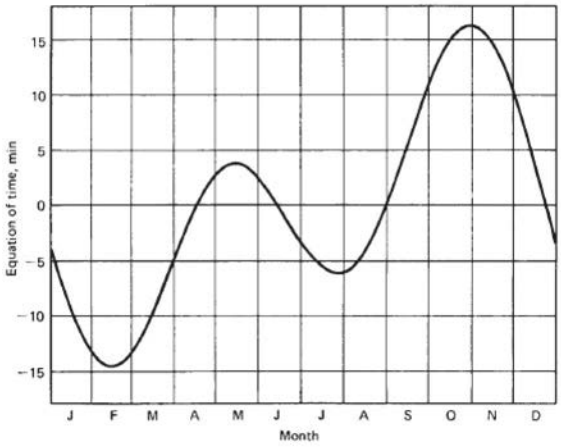

Figure 4.7: Equation of time as a function of time of the year [65]

B is given by:

$$B = (n-1)\left(\frac{360}{365}\right) \tag{4.10}$$

4.3 Solar field model

Once calculated the energy that can be collected at a given hour of a given day it is still necessary to evaluate how much of this energy can be effectively absorbed by the heat transfer fluid and how much is instead rejected back to the environment as a heat loss.

In order to evaluate the usefull collected energy the collector and receiver technology have to be defined. In this study it has been decided to consider a LS-3 parabolic trough collector and a 2008 PTR70 receiver (see Table 4.1). These collectors and receiver have been usually considered for large scale power plants due to their high performance, but they can be also considered for smaller plants in order to have high efficiencies for the solar field. A power plant using this kind of technology will surely require higher investment cost, but at the same time it will enable to decrease the land use of the overall system, which is one of the primary goals for concentrated solar power plants.

Table 4.1: 2008 PTR70 receiver design specifications [61]

Parameter	Value
Conductivity of the glass (k_{gl})	1.1 $W/m\ K$
Conductivity of the absorber (k_{abs})	14.8+0.0153T_{abs} $W/m\ K$
Emissivity of the glass (ϵ_{gl})	0.89
Emissivity of the absorber (ϵ_{abs})	0.062+(2.00E-7)T_{abs}^2
Inner radius of the absorber ($r_{abs,i}$)	0.033 m
Outer radius of the absorber ($r_{abs,o}$)	0.035 m
Inner radius of the glazing element ($r_{gl,i}$)	0.057 m
Outer radius of the glazing element ($r_{gl,o}$)	0.060 m
Pressure in anulus	$< 10^{-3}$ $mbar$

The developed heat transfer model is based on the EES Forristall model [65].

As it is possible to see in Figure 4.7 the original model considers 8 heat fluxes:

1. $\dot{q}_{12,conv}$: convective heat flux between the heat transfer fluid and the inner surface of the absorber;

2. $\dot{q}_{23,cond}$: conductive heat flux between the inner and the outer surface of the absorber;

3. $\dot{q}_{34,conv}$: convective heat flux between the outer surface of the absorber and the inner surface of the protective glass;
4. $\dot{q}_{34,rad}$: radiative heat flux between the outer surface of the absorber and the inner surface of the protective glass;
5. $\dot{q}_{cond,bracket}$: conductive losses trough the support brackets;
6. $\dot{q}_{45,cond}$: conductive heat flux between the inner and the outer surface of the protective glass;
7. $\dot{q}_{56,conv}$: convective heat flux between the outer surface of the protective glass and the environment;
8. $\dot{q}_{57,rad}$: radiative heat flux between the outer surface of the protective glass and the environment;

The solar irradiation is modelled as two additional heat fluxes:

1. $\dot{q}_{3,SolAbs}$: solar irradiation absorbed by the outer surface of the absorber;
2. $\dot{q}_{5,SolAbs}$: solar irradiation absorbed by the outer surface of the protective glass;

Finally the calculation of the absorbed energy and of the heat losses is performed with 4 energy balances:

$$q_{12,conv} = q_{23,cond} \tag{4.11}$$

$$q_{3,SolAbs} = q_{34,conv} + q_{34,rad} + q_{23,cond} + q_{cond,bracket} \tag{4.12}$$

$$q_{34,conv} + q_{34,rad} = q_{45,cond} \tag{4.13}$$

$$q_{45,cond} + q_{5,SolAbs} = q_{56,conv} + q_{57,rad} \tag{4.14}$$

$$q_{heat,Loss} = q_{56,conv} + q_{57,rad} + q_{cond,bracket} \tag{4.15}$$

In the developed model some variations from the original model have been made. First of all the heat losses trough the support brackets have been neglected: those losses are really low compared to the other heat flux and they become even smaller since the considered temperature level (150 ^oC) is lower than the usual 400 ^oC of large scale parabolic trough systems.

As a second step, two additional heat fluxes ($q_{4,SolAbs}$ and $q_{Sol,Refl}$) have been introduced. The former considers the solar energy that is transmitted trough the protective glass, reflected back from the absorber element and absorbed into the inner surface of the glass; the latter takes into account the solar energy that is reflected back into the environment and thus does not participate to the overall energy balance.

The Forristal model did not take into consideration the reflected solar energy, nor considered the possibility that part of the energy transmitted trough the glazing element could have been reflected back from the absorber element (the absorber

element was characterised by an absorption coefficient lower than 1, but the the energy that was not absorbed was not considered into any energy balance).

The energy balances considered in the developed model are:

$$q_{12,conv} = q_{23,cond} \tag{4.16}$$

$$q_{3,SolAbs} = q_{34,conv} + q_{34,rad} + q_{23,cond} \tag{4.17}$$

$$q_{34,conv} + q_{34,rad} + q_{4,SolAbs} = q_{45,cond} \tag{4.18}$$

$$q_{45,cond} + q_{5,SolAbs} = q_{56,conv} + q_{57,rad} \tag{4.19}$$

$$q_{heat,Loss} = q_{56,conv} + q_{57,rad} + q_{Sol,Refl} \tag{4.20}$$

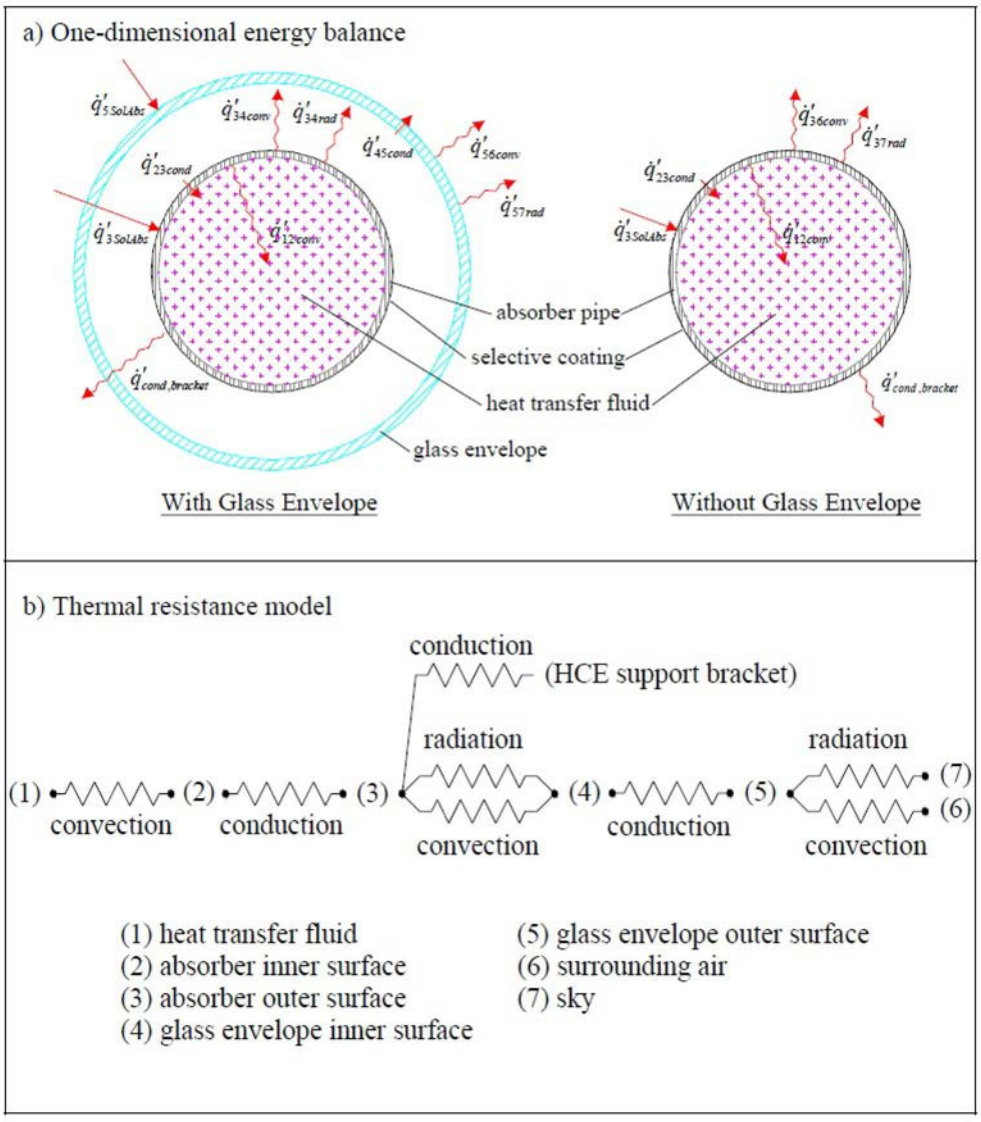

Figure 4.8: Forristall model: (a) One-dimensional steady state energy balance (b) Thermal resistance model for a cross section of a heat collector element [64]

The solar energy collected per meter of solar field is equal to:

$$q_{SolAbs} = DNI\ cos(\theta)\ A_p\ \eta_{opt}\ IAM \tag{4.21}$$

The optical efficiency takes into account collector geometry effects (shadowing, tracking, alignment), mirror and glass envelope transmittance effects (mirror reflectance and dirt) and is calculated as suggested by Forristall [65]:

$$\eta_{opt} = \epsilon'_1\ \epsilon'_2\ \epsilon'_3\ \epsilon'_4\ \epsilon'_5\ \epsilon'_6 \tag{4.22}$$

Table 4.2: Estimates of effective optical efficiency terms [65]

ϵ'_1 = HCE shadowing (bellows, shielding, supports)	0.974
ϵ'_2 = Tracking error	0.994
ϵ'_3 = Geometry error (mirror alignment)	0.98
ρ_{cl} = clean mirror reflectance	0.935
reflectivity	0.90
ϵ'_4 = Dirt on mirrors	reflectivity/ρ_{cl}
ϵ'_5 = Dirt on HCEs	(1 + ϵ'_4)/2
ϵ'_6 = Unaccounted	0.96

The solar energy absorbed by the outer surface of the glazing element (W/m) is given by:

$$q_{5,SolAbs} = q_{SolAbs}\ \alpha_{gl} \tag{4.23}$$

The energy that is transmitted trough the protective glazing is subjected to multiple reflections between the outer surface of the absorber and the inner surface of the glazing element (see Figure 4.9) and therefore, in order to evaluate the absorbed and reflected energy, it is necessary to define the transmittance, reflectivity and absorptance both of the glazing and of the absorber.

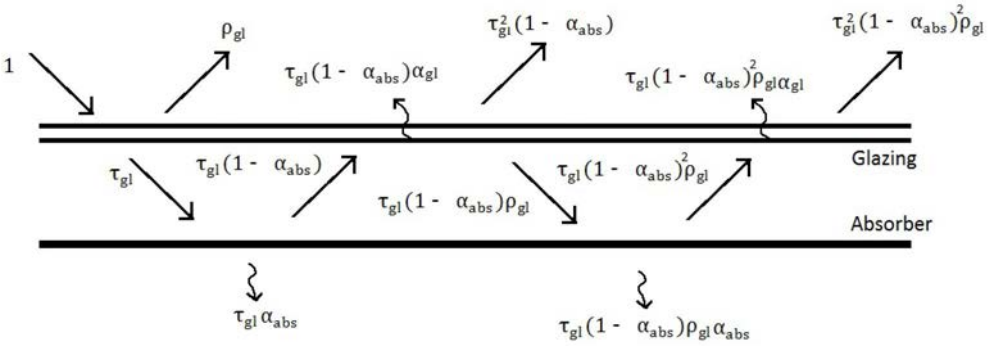

Figure 4.9: Scheme of the multiple reflections between the outer surface of the absorber and the inner surface of the glazing element

Table 4.3: Estimates of transmittance, reflectivity and absorptance for the glazing element and the absorber [65]

τ_{gl} = Transmittance of the protective glazing	0.963
ρ_{gl} = Reflectivity of the protective glazing	0.017
α_{gl} = Absorptance of the protective glazing	0.02
τ_{abs} = Transmittance of the absorber	0
ρ_{abs} = Reflectivity of the absorber	0.04
α_{abs} = Absorptance of the absorber	0.96

The solar energy absorbed by the absorber element is equal to:

$$q_{3,SolAbs} = q_{SolAbs}\ \tau_{gl}\ \alpha_{abs} \sum_{i=0}^{\infty} (1-\alpha_{abs})^i\ \rho_{gl}^i \tag{4.24}$$

$$= q_{SolAbs}\ \frac{\tau_{gl}\ \alpha_{abs}}{1-\rho_{gl}\,(1-\alpha_{abs})} \tag{4.25}$$

The energy absorbed by the inner surface of the protective glass is equal to:

$$q_{4,SolAbs} = q_{SolAbs}\ \tau_{gl}\ \alpha_{gl}\,(1-\alpha_{abs}) \sum_{i=0}^{\infty} (1-\alpha_{abs})^i\ \rho_{gl}^i \tag{4.26}$$

$$= q_{SolAbs}\ \frac{\tau_{gl}\ \alpha_{gl}\ (1-\alpha_{abs})}{1-\rho_{gl}\ (1-\alpha_{abs})} \tag{4.27}$$

The solar energy that is reflected back to the sky is equal to:

$$q_{Sol,Refl} = q_{SolAbs}\ \left[\rho_{gl} + \tau_{gl}^2\ (1-\alpha_{abs}) \sum_{i=0}^{\infty} (1-\alpha_{abs})^i\ \rho_{gl}^i\right] \tag{4.28}$$

$$= q_{SolAbs}\ \left[\rho_{gl} + \frac{\tau_{gl}^2\ (1-\alpha_{abs})}{1-\rho_{gl}\ (1-\alpha_{abs})}\right] \tag{4.29}$$

Once that all the solar fluxes have been evaluated it is possible to solve all the energy balances and to calculate the useful heat absorbed by the heat transfer fluid ($\dot{q}_{12,conv}$). The inclusion of the detailed calculation of the absorption, reflection and transmission coefficients for the solar light does not lead to substantial differences in the results, but it makes possible to verify the overall energy balance of the solar energy:

$$q_{Sol,abs} = q_{12,conv} + q_{heat,Loss} \tag{4.30}$$

The Forristall model doesn't consider the multiple reflections between the inner surface of the glazing and the outer surface of the absorber and does not include the reflected sunlight into the heat losses and therefore if it is directly used in order

to calculate the heat transfer fluid heat gain by calculating the absorbed energy ($q_{Sol,Abs}$) and the heat loss ($q_{heat,Loss}$) it leads to an overestimation of the useful collected energy. The heat transfer correlations that have been used in order to calculate the various heat fluxes in the model are the ones proposed in the Forristal model [65] and are listed in Table 4.4.

Table 4.4: Adopted heat transfer correlations

$q_{12,conv}$	Gnielinksy's correlation
$q_{23,cond}$	Fourier's law of conduction
$q_{34,conv}$	Free molecular convection, Ratzel et al. [66]
$q_{34,rad}$	Radiation heat transfer, Incropera et al. [67]
$q_{45,cond}$	Fourier's law of conduction
$q_{56,conv}$	Churchill and Chu / Zhukauskas's correlation
$q_{57,rad}$	Radiation heat transfer, Incropera et al. [67]

4.4 Solar model validation

The equations required in order to evaluate the declination angle, the zenit angle, the hour angle, and the conversion from the local time to the solar time have been validated using the example available in Duffie et al. [64].

The value of the incident angle modifier as a function of the incident angle has been plotted and it matches with the curves available in Dudley et al. [63] (see Figure 4.10).

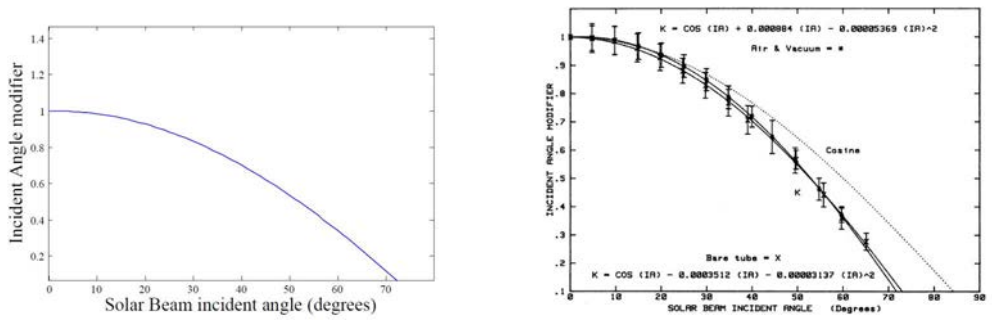

(a) **(b)**

Figure 4.10: IAM as a function of incident angle: (a) Calculated (b) from Dudley et al. [63]

The heat collector element model has been validated using the examples available in the appendix of Burkholder et al. [61]. In order to confront the developed model with the available results some of the equations and assumptions have been changed to the ones considered in the reference paper:

1. The heat transfer fluid has been changed to Therminol VP-1;

2. The convective heat exchanged between the inner surface of the glazing and the outer surface of the absorber has been neglected;

3. Simplified heat transfer correlations have been included to estimate the various heat fluxes;

4. The calculated heat loss is the conductive heat transfer between the inner and the outer surface of the protective glazing;

As it emerges from Table 4.5 the different values calculated in the model are very close to the ones obtained by Burkholder, the only slight differences are probably due to the not clear definition of some optical properties of the glazing element.

Table 4.5: Solar field model validation

	Case 1		Case 2		Case 3	
	Reference	Model	Reference	Model	Reference	Model
q_{SolAbs}	3834	3834	3229	3229	0	0
$q_{12,conv}$	3690	3690	3085	3086	-138	-137,9
$q_{23,cond}$	3690	3690	3085	3086	-138	-137,9
$q_{34,rad}$	144	144	144	143	138	137,9
$q_{45,cond}$	144	144	144	143	138	137,9
$q_{5,SolAbs}$	82	82.95	69	69.85	0	0
$q_{57,rad}$	76	76.14	72	71.82	50	49.6
$q_{56,conv}$	150	150.8	141	141.1	88	88.29

4.5 Solar field regression model

In order to reduce the computational time and to easily implement the solar field model, it has decided to fit it with a regression curve. Many studies have already proved that regression methods can be successfully applied to the solar models.

Patnode [68] developed a regression curve for the calculation of the heat losses of a parabolic trough solar field. The considered parameters are the heat transfer fluid temperature and the available direct normal irradiation:

$$HeatLoss = a_0 + a_1\, T + a_2\, T^2 + a_3\, T^3 + \ DNI(b_0 + \ b_1 T^2)) \tag{4.31}$$

Burkholder [61] developed a different regression model: in this case the input parameters to calculate the heat losses are the heat tranfer temperature, the ambient temperature, the wind speed and the collected energy:

$$HeatLoss = a_0 + a_1(T_{htf} - T_{amb}) + a_2 T_{htf}^2 + a_3 T_{htf}^3 + a_4 DNI\ IAM\ cos(\theta)\ T_{htf}^2 + \sqrt{V_w}(a_5 + a_6(T_{htf} - T_{amb}) \quad (4.32)$$

It can be easily noticed that both the previous correlations neglect the effect of the heat transfer fluid mass flow rate on the overall heat losses. This parameter has a low influence on the losses but it is not totally irrelevant: as the mass flow rate increases, the convective heat transfer coefficients of fluid increases (it depends on the Reynolds number, that is function of the fluid speed and thus to its mass flow rate) and therefore the heat losses should decrease.

In this study, since the solar field model is used both for design and off-design evaluations, it has been decided to include the mass flow rate as one of the parameters to be considered for the calculation of the heat losses. In order to define a proper regression curve, the model has been run 432 times changing the different values shown in Table 4.6.

Table 4.6: Considered parameters for the heat loss regression curve

Parameter	Value
T_{htf}	80, 110, 150 ^oC
T_{amb}	20, 35 ^oC
V_w	0, 2, 4, 8 m/s
$\dot{m}_{htf}$	4, 8, 12 kg/s
DNI	500 800 1000 W/m^2
θ	0, 20 ^{o}

The regression curve, estimated using DataFit 9.0 ($R^2 = 99.99\%$), is given by:

$$HeatLoss = a_0 + a_1 x_1 + a_2 x_2 + a_3 x_3 + a_4 x_4 + a_5 x_5 \quad (4.33)$$

As expected the increment of the heat transfer fluid mass flow rate has a positive impact on the losses (even though its value is very little), while, on the other hand, the increment of any of the other input values has as a consequence an increment of the losses: increasing the fluid temperature, the wind speed and the over-temperature with respect to the ambient temperature has in fact a positive effect on the heat transfer coefficients between the solar field and the surroundings.

What might appear strange is the linear relationship between the heat losses and the heat transfer fluid temperature: in all the other available regression models this dependence was exponential. The difference between the other available models and the one just developed can easily been justified: while the other works considered a temperature range between 50 and 400 ^oC, in this case the temperature range is much smaller (80-150^oC) and thus a linear dependence is enough to have a good fitting of the calculated points (see Figure 4.11).

Table 4.7: Regression parameters

Parameter	Value
x_1	$T_{htf} - T_{amb}$
x_2	T_{htf}
x_3	$A_p DNI\ IAM cos(\theta)$
x_4	V_w
x_5	$\dot{m}_{htf}$
a_0	-8.66861922262613
a_1	9.00163160366928E-02
a_2	0.110866312681543
a_3	6.31820732077251E-02
a_4	0.146451064512209
a_5	-1.06361666309851E-02

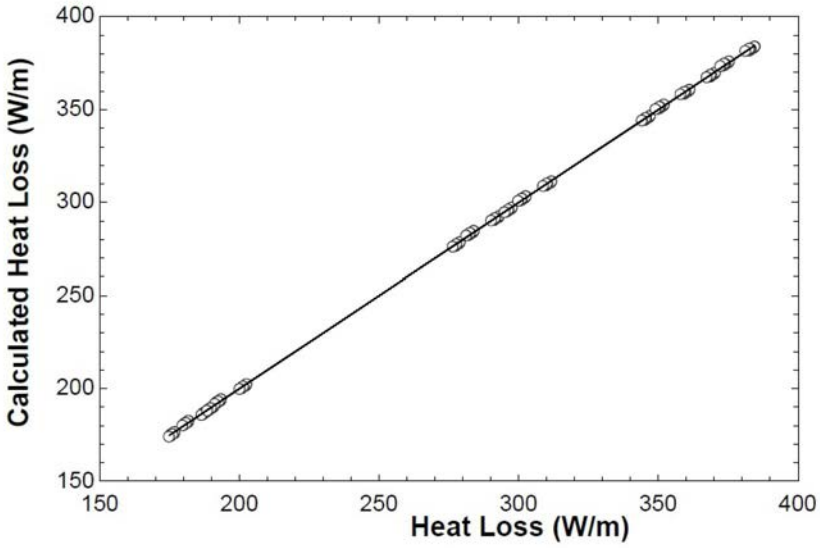

Figure 4.11: Goodness of the fit for the heat loss correlation

Chapter 5

Overall System Analysis

In this chapter the overall system that includes both the solar field and the power cycle is optimized and analysed. Looking at the literature it appears that when designing a solar power plant it is a common assumption to fix both the inlet and outlet temperature of the solar field and then to optimize the net power production. The defined values for the inlet and outlet temperature for the heat carrier are usually derived from previous thermoeconomic studies or assumed in order to have a desired temperature drop in the boiler.

Nonetheless, in this study it has been decided not to fix the outlet temperature of the pressurized water: the aim is to understand which configuration is the best from a thermodynamic point of view.

Given the relatively low level of the heat source temperature (150^oC) the target power output cannot be high otherwise the required land would be too big. As already mentioned in section 4.1.3 some kW-size prototypes are under study for remote off-grid applications: in this case even low temperature solar power plants could be an interesting solution due to their simpler configuration.

Here the electrical output is fixed to 100 kW so that the plant could be suitable to supply a group of houses in a remote area.

The considered optimization parameter is the overall solar to electrical efficiency, defined as:

$$\eta_{overall} = \frac{W_{el} - W_{piping}}{DNI\ S_{solarfield}} \tag{5.1}$$

The optimization of this parameter will lead both to the most efficient power plant and to the one that requires the smaller solar field area. The steps considered in the optimization process are the following:

1. A pure fluid or mixture is selected as working fluid;

2. The cycle maximum pressure and turbine inlet temperature are chosen;

3. The Organic rankine cycle model is solved and the calculated output are the heat transfer fluid mass flow rate and temperature at the outlet of the boiler (which is equal to the solar field inlet temperature);

4. The solar field model uses the power cycle outputs to calculate the required land area, the power absorbed by the pipings and the overall solar to electrical efficiency;

5. The genetic algorithm stores the result and repeats the scheme until the best solution is found.

In order to calculate the solar field area the regression model developed in chapter 4 is used in an energy balance between the solar irradiation and the heat transfer fluid [70]:

$$T_{htf,out} = T_{htf,i} + \frac{q_{12,conv}\ \Delta x}{(\dot{m}_{htf}\ cp)_{htf}} \tag{5.2}$$

$$q_{12,conv} = q_{SolAbs} - HeatLoss \tag{5.3}$$

In the design case the temperature difference between the inlet and the outlet of the solar field is discretized in 100 steps and for each of them the required absorber length (Δx) is calculated. Finally the required solar field surface is calculated by multiplying the absorber length for the collector aperture area. The solar field model sensitivity to the number of discretization steps is shown in Figure 5.1 (the inlet and outlet temperatures considered for the sensitivity analysis are 100 and 150^o C).

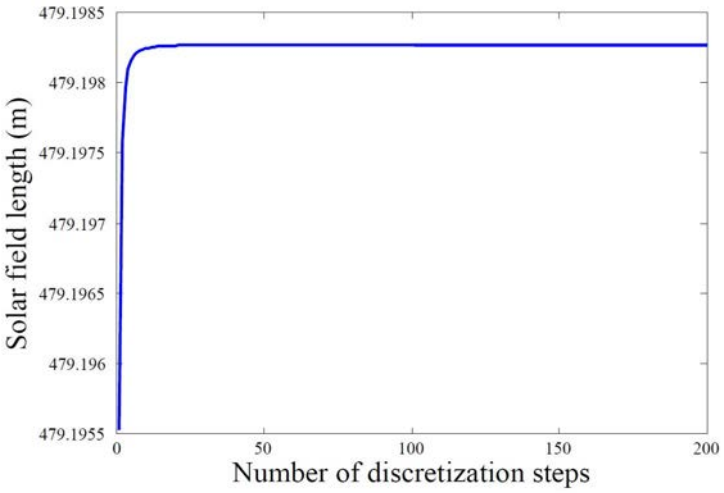

Figure 5.1: Solar field model sensitivity analysis

Furthermore, for every discretization step of the solar field the corresponding pressures loss (Pa) is calculated with the following relationship[18]:

$$\Delta p_i = f \frac{\Delta x \; G_{htf}^2}{2 \; D_{abs,i} \; \rho_{htf}} \tag{5.4}$$

$$G_{htf} = \frac{\dot{m}_{htf}}{S_{abs}} \tag{5.5}$$

$$S_{abs} = \pi \frac{D_{abs,i}^2}{4} \tag{5.6}$$

The friction factor f is estimated with the following equation from Incropera et al. [67]:

$$f = [0.790 ln(Re_D) \; - 1.64]^{-2} \tag{5.7}$$

$$Re_D = \frac{4 \dot{m}_{htf}}{\pi \; D_{abs,i} \; \mu} \tag{5.8}$$

Finally the pumping power requirement is estimated as:

$$W_{piping} = \frac{\dot{m}_{htf} \; \Delta p_{tot}}{\rho_{htf}} \tag{5.9}$$

where Δp_{tot} is the pressure loss of the overall solar field pipings:

$$\Delta p_{tot} = \sum_{i=0}^{n} \Delta p_i \tag{5.10}$$

The genetic algorithm is ran for 200 generations with a population size of 200 individuals in order to be sure to reach the real maximum point. The maximum and minimum allowed values for the optimization parameters are:

Table 5.1: Optimization parameters boundaries

Parameter	Min	Max
Cycle high pressure	1	40 $[bar]$
Turbine inlet temperature	60	140 $[^oC]$
Mass fraction	0	1

The fixed parameters in the optimization process are listed in Table 5.2.

Table 5.2: Fixed parameters in the optimization process

Heat transfer fluid:	Pressurized Water (8 bar)
Absorber type:	2008 PTR70
Solar collector:	LS-3
Incident angle modifier:	1
Incident angle:	0^o
Optical efficiency:	0.8448
Design DNI:	800 W/m^2K
Design ambient temperature:	25 ^oC
Design wind speed:	2 m/s
Cooling water inlet temperature:	20^oC
Cooling water temperature increase :	5^oC
ΔT_{pp} :	8^oC
$\eta_{is,t}$	0.70
$\eta_{is,p}$	0.70

5.1 Pure fluids results

As a first step only pure fluids are considered in the optimization process. The obtained results are enlightened in Table 5.3.

Table 5.3: Pure fluid results for the overall system optimization

Fluid	High pressure [bar]	TIT [^oC]	Super-heating [^oC]	ΔT_{rec} [^oC]	P_{cond} [bar]	$\eta_{overall}$	η_{el}
Butane	24,85	140,00	13,39	28,37	3,08	0,1053	0,1360
Cyclohexane	3,80	140,00	7,87	35,95	0,18	0,1193	0,1562
Cyclopentane	8,26	140,00	8,35	27,09	0,57	0,1159	0,1515
Hexane	5,25	140,00	7,68	43,01	0,28	0,1187	0,1544
Ihexane	6,38	140,00	7,67	44,38	0,39	0,1182	0,1546
Ipentane	13,53	140,00	8,34	37,90	1,20	0,1140	0,1483
Isobutane	29,07	140,00	18,56	30,11	4,37	0,1007	0,1297
Pentane	11,43	140,00	8,17	37,19	0,91	0,1149	0,1483
R1234yf	40,00	140,00	Supercritical	32,46	8,40	0,0882	0,1133
R1234ze	36,99	140,00	Supercritical	26,81	6,25	0,0917	0,1178

As a first result it appears that all the optimised configurations include a recuperator (ΔT_{rec} is the temperature increase of the cold fluid): this is the proof that this component enables to increase the effectiveness of the solar to electricity conversion. Secondly, looking at the turbine inlet temperatures it clearly emerges

that in all the cases its value is 140 ^oC. In the case analysed in chapter 3 the purpose was to extract the maximum amount of power from a hot stream and thus the fluids that had the best performance were those who were capable of effectively decrease the temperature of the source so that to absorb as much heat as possible. Here the purpose is to effectively convert the solar energy into electricity and thus the temperature at which the heat is absorbed by the working fluid is of primary importance: the highest the average temperature at which the heat is absorbed, the highest will be the power cycle efficiency.

The fact that all the optimized configurations are characterised by the maximum allowed turbine inlet temperature clearly shows that configurations where the heat is absorbed at a higher temperature outperform configurations where the heat absorption occurs at lower levels.

Looking at the optimized configurations it appears that when the selected working fluid is an hydrocarbon, the optimization leads to a super-heated cycle (super heating temperature ranges between 7 and 18^oC): on the other hand, when HFOs are considered the optimized cycle is supercritical (this is related to the lower critical temperature of these fluids, see Table 3.3).

All the calculated condensing pressures are in the feasibility range and in some cases the condensing pressure is above the atmospheric pressure (Butane, Ipentane, Isobutane, R1234yf and R2134ze).

From a thermodynamic point of view the most performing fluid is Cyclohexane with an overall efficiency of 11.93%, but also configurations with other fluids (Cyclopentane, Hexane and Ihexane) reach an effectiveness higher than 11.5%. Another interesting configuration is obtained with Ipentane: in this case the effectiveness is 11.4%, but the condensing pressure level (1.2 bar) would enable to install a cheaper condenser (the systems to prevent air leakages are in this case not required). When HFOs are considered the overall efficiency is lower (around 9%) and this is mainly related to the lower electrical efficiency of their configurations.

In table 5.4 the solar field parameters of the various configurations are depicted. The solar field efficiency is defined as:

$$\eta_{solar,field} = \frac{\dot{m}_{htf}\ (h_a - h_c)}{DNI\ S_{tot}} \tag{5.11}$$

A new parameter, the specific power production, is also introduced:

$$W_{spec} = \frac{W_{Net}}{S_{tot}} \tag{5.12}$$

Where:

$$W_{Net} = W_{el} - W_{piping} \tag{5.13}$$

All the configurations are characterised by the same electrical output (100 kW), but due to different values of the power required by the solar field piping their net

output is different. The specific power production is so an interesting parameter that enables to understand how much energy is produced in design condition by a square meter of solar field.

Table 5.4: Pure fluid results for the Solar field

Fluid	T_c $[°C]$	$\dot{m}_w$ $[kg/s]$	η_{solar}	S_{tot} $[m^2]$	W_{piping} $[kW]$	W_{spec} $[W/m^2]$
Butane	122,00	6,14	0,78	1181,37	0,45	84,27
Cyclohexane	135,94	10,61	0,78	1028,71	1,85	95,41
Cyclopentane	134,70	10,06	0,78	1060,57	1,64	92,74
Hexane	135,46	10,33	0,78	1035,27	1,73	94,92
Ihexane	135,22	10,21	0,78	1039,45	1,68	94,59
Ipentane	132,81	9,15	0,78	1082,75	1,28	91,18
Isobutane	111,73	4,72	0,78	1238,11	0,22	80,59
Pentane	133,55	9,46	0,78	1072,45	1,39	91,94
R1234yf	83,63	3,13	0,78	1415,77	0,08	70,58
R1234ze	89,20	3,29	0,78	1362,25	0,09	73,34

Looking at the results of table 5.4 it appears that the solar field efficiency is almost the same for every considered configuration. Since the overall solar to electrical efficiency is given by the solar field efficiency multiplied for the power cycle electrical efficiency, it easily follows that the primary factor that distinguishes the effectiveness of the various configurations is the power cycle efficiency, which is strictly related to the pressurized water boiler outlet temperature (T_c): as this temperature increases the power cycle efficiency increases (see Figure 5.2: every point represents a working fluid in its optimized configuration).

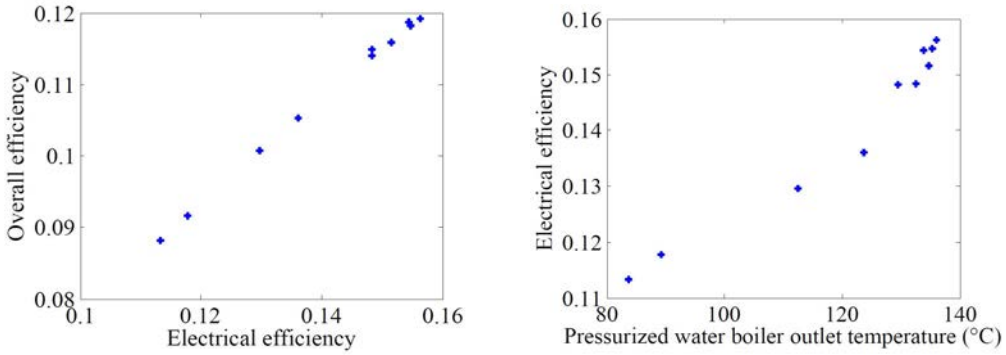

(a) Influence of the electrical efficiency on the overall efficiency

(b) Influence of the pressurized water boiler outlet temperature on the electrical efficiency

Figure 5.2: Relationship between various parameters: (a) Dependence of the overall efficiency on the electrical efficiency (b) Dependence of the electrical efficiency on the pressurized water boiler outlet temperature

Moreover the pressurized water boiler outlet temperature is connected to the mass flow required in the solar field. The heat released by the heat transfer fluid in the boiler is given by:

$$q_{released} = \dot{m}_{htf}\ c_p\ \Delta T \tag{5.14}$$

As a consequence, the temperature glide of the HTF fluid in the boiler is related to two opposite phenomena and plays a fundamental role in the optimization process:

1. When the temperature glide decreases the heat absorption in the power cycle can occur at a higher temperature an this enables to increase the power cycle efficiency;

2. When the temperature glide increase the required water mass flow rate decreases and thus the power absorbed by the pipings decreases, leading to higher net power outputs;

Looking at the most performing configurations it can be noticed that the temperature glide of the pressurized water ranges between 14 and 17 ^oC: a similar value (15^oC) has been found in a similar analysis carried out by Quoilin et al. [62] for low temperature CSP ($<200^oC$).

Anyway it is important to point out that the introduction of the pressure losses for the various heat exchangers and the estimation of the required heat exchange area might lead to increased values for this temperature glide (given a maximum allowed value for the heat exchanger pressure losses, the required surface area increases with the mass flow rate).

Analysing the boiler heat transfer profiles for the various configurations (see Figure 5.3) it emerges the reason why the HFOs are characterised by lower electrical efficiencies: when the selected working fluid is an hydrocarbon the heat is mainly absorbed at high temperature during the evaporation process and this enables to have high values for the average temperature at which the heat is absorbed into the cycle. When instead the fluid is an HFO the heat absorption process occurs at a varying temperature and as a consequence the electrical efficiency is lower.

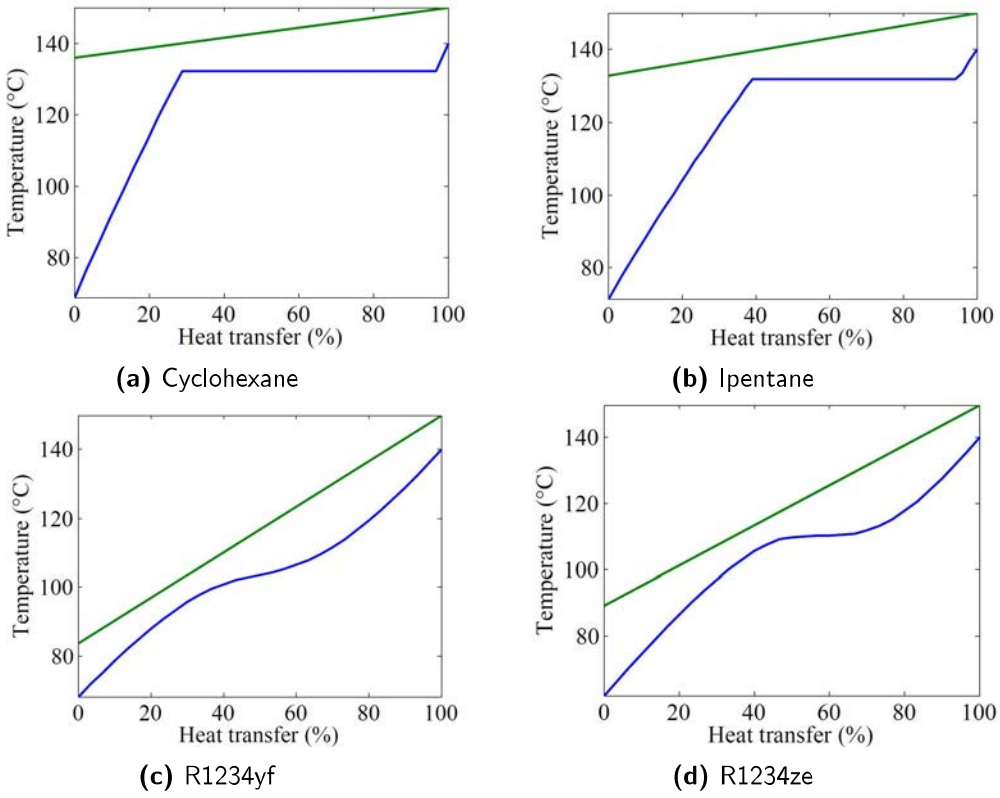

(a) Cyclohexane **(b)** Ipentane

(c) R1234yf **(d)** R1234ze

Figure 5.3: Boiler temperature profile for different optimized configurations: (a) Cyclohexane (b) Ipentane (c) R1234yf (d) R1234ze

5.2 Mixtures results

After the optimization of the pure fluids configuration, the focus has been shift on configurations with binary working fluids. All the fixed parameters in the optimization process and the genetic algorithm options are kept as defined in section 5.1. Similarly to section 3.4.3 the selected working fluids have been fixed for every analysis and the mixture composition is described by means of the mass fraction (x_1) of the first component.

The obtained results are depicted in Table 5.5: the overall efficiency increase have been calculated with respect to the best pure fluid among the two considered in the mixture.

Table 5.5: Mixture results for the overall system optimization

Fluid 1	Fluid 2	High pressure [bar]	TIT [^oC]	x_1	P_{cond} [bar]	$\eta_{overall}$	$\%increase$
Butane	Ipentane	16,24	140,00	0,20	1,42	0,1148	0,69
Cyclohexane	Cyclopentane	4,61	140,00	0,84	0,21	0,1220	2,27
Cyclohexane	Hexane	4,39	140,00	0,59	0,22	0,1203	0,81
Cyclohexane	Ihexane	5,01	140,00	0,55	0,25	0,1217	2,03
Cyclohexane	Ipentane	4,19	140,00	0,97	0,19	0,1212	1,55
Cyclohexane	Pentane	4,30	140,00	0,95	0,19	0,1216	1,89
Cyclopentane	Hexane	6,42	140,00	0,31	0,35	0,1201	1,22
Cyclopentane	Ipentane	10,56	140,00	0,58	0,75	0,1181	1,92
Cyclopentane	Pentane	9,53	140,00	0,65	0,67	0,1169	0,86
Hexane	Ihexane	5,71	140,00	0,76	0,31	0,1191	0,34
Hexane	Ipentane	5,92	140,00	0,93	0,30	0,1206	1,64
Hexane	Pentane	6,18	140,00	0,86	0,32	0,1209	1,89
Ihexane	Pentane	8,04	140,00	0,76	0,48	0,1205	1,90
Ihexane	Ipentane	7,35	140,00	0,90	0,43	0,1203	1,77

From the tables it emerges that the introduction of binary working fluids lead to an increment of the overall conversion efficiency between 0.34 and 2.27%. The best increment is reached with a mixture of cyclohexane and cyclopentane ($\eta_{overall}$ + 2.27%), but a similar result can also be achieved with cyclohexane and ihexane (+2.03%). The mixture of butane and ipentane ($\eta_{overall} = 11.48\%$) is characterised by a fairly high value for the condensing pressure (which is a positive parameter), but at the same time the performance increment with respect to the configuration using pure ipentane is not significant (+0.7%).

Comparing these results with the ones obtained in section 3.4.3 it appears that in this case the performance gain obtained with the mixtures is lower. This can be explained by several reasons. First of all the purpose of the optimization process in the two cases is different: in the first analysis the the optimal solution was the one that was able to extract as much power as possible from a defined heat source, while here the purpose is to have an effective conversion and so to decrease the irreversibility of the process.

Secondly, looking at the results of section 3.4.3 it is easy to understand that the performance increment due to the introduction of binary working fluid was mainly related to the better match between the working fluid and the heat source in the boiler which enabled either to reach higher values for the turbine inlet temperatures and thus to increase the efficiency of the power cycle, or to decrease the pressurized water boiler outlet temperature and thus to increase the amount of heat that the power cycle was able to absorb from the selected heat source.

In this case, since the purpose is to reach high efficiencies for the power cycle, the turbine inlet temperature reaches the maximum allowed value even with the pure fluid configurations and the decrement of the pressurized water boiler outlet temperature is not a positive factor (by decreasing this parameter the heat required to heat up the water to its maximum value increases and therefore the overall efficiency decreases).

As a consequence, since the turbine inlet is a fixed parameter and the temperature profile does not change significantly (as shown in table 5.6 the water outlet temperature for all the configurations using cyclohexane is around 135^oC which is the water outlet temperature of the pure cyclohexane optimized configuration) the only benefit related to the use of mixtures is the decrement of the irreversibility in the heat exchange process: as shown in Figure 5.4 and 5.5 the temperature difference through which the heat is exchanged is slightly decreased both in the boiler and in the condenser.

Table 5.6: Mixtures results for the Solar field

Fluid 1	Fluid 2	T_c $[^oC]$	$\dot{m}_w$ $[kg/s]$	η_{solar}	S_{tot} $[m^2]$	W_{piping} $[kW]$	W_{spec} $[W/m^2]$
Butane	Ipentane	130,85	8,19	0,7778	1078,88	0,93	91,83
Cyclohexane	Cyclopentane	135,52	10,10	0,7777	1008,68	1,58	97,57
Cyclohexane	Hexane	135,88	10,49	0,7777	1020,89	1,78	96,21
Cyclohexane	Ihexane	135,69	10,24	0,7777	1010,04	1,65	97,38
Cyclohexane	Ipentane	135,69	10,29	0,7777	1014,52	1,67	96,92
Cyclohexane	Pentane	135,78	10,32	0,7777	1011,05	1,68	97,24
Cyclopentane	Hexane	135,14	10,00	0,7777	1024,16	1,56	96,12
Cyclopentane	Ipentane	134,08	9,52	0,7778	1043,59	1,38	94,50
Cyclopentane	Pentane	134,37	9,78	0,7778	1053,19	1,50	93,52
Hexane	Ihexane	135,35	10,22	0,7777	1031,94	1,67	95,29
Hexane	Ipentane	135,18	9,99	0,7777	1020,08	1,55	96,51
Hexane	Pentane	135,00	9,85	0,7777	1018,21	1,48	96,75
Ihexane	Pentane	134,59	9,64	0,7778	1023,22	1,40	96,36
Ihexane	Ipentane	134,88	9,83	0,7777	1023,70	1,48	96,24

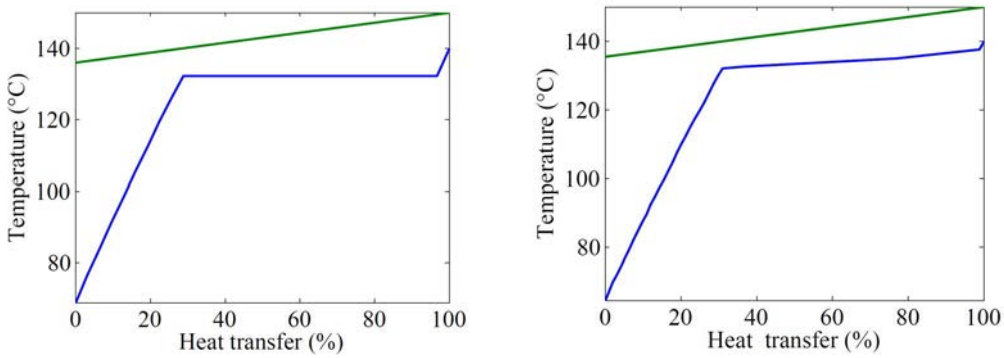

(a) Cyclohexane **(b)** Cyclohexane/Cyclopentane

Figure 5.4: Boiler temperature profile (a) Cyclohexane (b) Cyclohexane/Cyclopentane

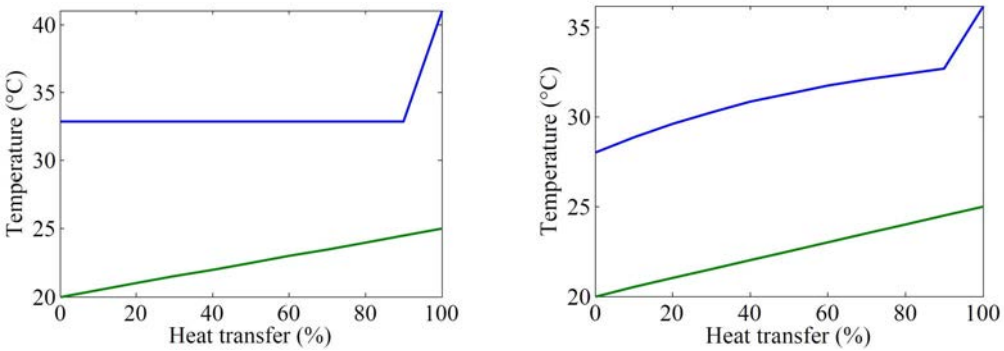

(a) Cyclohexane **(b)** Cyclohexane/Cyclopentane

Figure 5.5: Condenser temperature profile (a) Cyclohexane (b) Cyclohexane/Cyclopentane

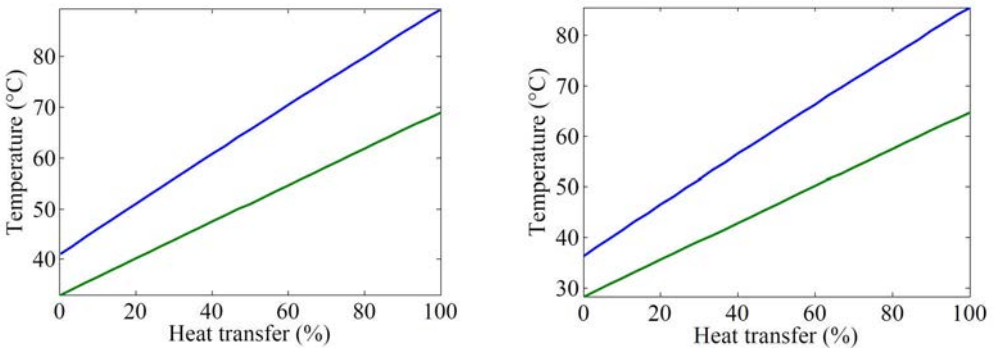

(a) Cyclohexane **(b)** Cyclohexane/Cyclopentane

Figure 5.6: Recuperator temperature profile (a) Cyclohexane (b) Cyclohexane/Cyclopentane

5.3 Pure Cyclohexane and Cyclohexane/Cyclopentane comparison

The optimization process showed that the use of a mixture Cyclohexane/Cyclopentane (0.84/0.16) leads to an overall efficiency 2.27% greater than with pure Cyclohexane. Nonetheless the overall efficiency is not the only parameter that should be taken into account to compare the two optimum configurations.

Table 5.7: Parameter comparison between the pure fluid and the mixture

Parameter	Unit	Cyclohexane	Cyclohexane/Cyclopentane	Δ%
m_{wf}	$[kg/s]$	1,35	1,30	-3,45
m_w	$[kg/s]$	10,61	10,10	-4,81
W_{piping}	$[kW]$	1,85	1,58	-14,75
P_{cond}	$[bar]$	0,18	0,21	15,41
S_{tot}	$[m^2]$	1028,71	1008,68	-1,95
W_{Net}	$[kW]$	98,15	98,42	0,28
$\eta_{overall}$		0,1193	0,1220	2,27
W_{spec}	$[W/m^2]$	95,41	97,57	2,27

Looking at table 5.7 it clearly appear that a primary factor that makes the mixture configuration more efficient is the decrement of the pressurized mass flow rate in the solar field (-4.81%) that enables to reduce the power absorbed by the solar field by almost 15%. As a consequence, when the mixture is selected as working fluid, both the net power production and the solar field surface decrease and so the power plant is able to produce slightly more power ($+0.28\%$) and with a lower surface area (1009 m^2 instead of 1029 m^2).

5.3.1 Economical considerations

A specific power production increment of 2% is not neglectable but at the same time an economical evaluation of both the power plants should be made in order to find out which one enables to have the lowest levelized cost of the electricity. Even though it is not the purpose of this work to make a thermo-economic analysis, still some comments can be made.

Since the investment costs for the power cycle pump and turbine will be very similar (the two cycle operate with almost the same pressure ratio and mass flow rate) and the same technology can be considered for the condenser (in both the cases suitable precautions should be taken in order to avoid air leakages) the parameter that has to be analysed is the investment cost for the heat exchangers.

The cost of the heat exchanger is usually function of the required surface area, but it is necessary to design every heat exchanger in order to define this parameter.

Nonetheless some conclusion can be drawn by looking at the UA requirements of the two configurations. The UA value of an heat exchanger can be calculate as:

$$UA = \frac{q}{\Delta T_{ml}} \tag{5.15}$$

Where q is the heat exchanged and ΔT_{ml} is the logarithm mean temperature, given by:

$$\Delta T_{ml} = \frac{(T_1 - t_2) - (T_2 - t_1)}{ln\left(\frac{T_1 - t_2}{T_2 - t_1}\right)} \tag{5.16}$$

Where:

- T_1 and T_2 are the inlet and outlet temperatures of the hot stream;
- t_1 and t_2 are the inlet and outlet temperatures of the cold stream.

The UA values and the other parameters of the various heat exchangers of the two considered configurations are listed in table 5.8.

Table 5.8: Heat exchanger parameters

	Cyclohexane			Cyclohexane/Cyclopentane		
	$\dot{q}$ $[kW]$	UA $[W/K]$	ΔT_{ml} $[K]$	$\dot{q}$ $[kW]$	UA $[W/K]$	ΔT_{ml} $[K]$
Preheater	190	6849	27,74	194	6748	28,79
Evaporator	430	35483	12,11	423	39629	10,67
Superheater	20	1526	13,37	10	875	11,84
Condenser	538	37334	14,41	526	55133	9,53
Recuperator	96	7293	13,19	93	6923	13,41

As it can be noted in the previous table, when the mixture is considered the UA requirement increases a lot for the evaporator and the Condenser (respectively +11 and +47%): this is related to the lower ΔT_{ml} trough which the heat is exchanged. A lower value for this temperature difference obviously results in a decrement of the irreversibility, but at the same time the increment of the required surface area should not be neglected.

The UA value is given by the multiplication between the surface area and the overall heat transfer coefficient (U). For a tubolar heat exchanger where the fouling effects and the conductive resistance between the inner and the outer surface of the heat exchanger are neglected, this parameter can be approximated to:

$$U = \frac{1}{\frac{1}{h_i} + \frac{1}{h_o}} \tag{5.17}$$

h_i = convective heat transfer coefficient of the fluid flowing inside the tube;

h_o = convective heat transfer coefficient of the fluid flowing outside the tube;

If the overall heat exchange coefficient can be considered as a fixed parameter an increase of the UA value results in an equivalent increase of the heat exchanger required area. Nonetheless several studies have shown that mixtures are characterised by lower values for the heat transfer coefficients [69] if compared to pure fluids and thus the increment of the surface area required by the various heat exchangers will probably be higher than the increment of the UA values.

Even though the investment costs for the heat exchangers will most probably be higher for the mixture it should not be forgotten that the pure fluid configuration is characterised by a higher extension of the solar field and by a lower power production in design condition. As a consequence from an economic point of view is still not clear which power plant would result more profitable; this could be assessed only by means of a thermo-economic analysis.

5.3.2 Sensitivity Analysis

Many parameters have been fixed during the optimization process. It is therefore interesting to find out how much they affect the overall efficiency and whether one of the two considered configurations is more sensitive to any of those parameters.

The following sensitivity analysis considers as variable parameters the efficiency of the turbomachinery (pump and turbine), the condensing water inlet temperature and the boiler pinch point. All of them have been varied from -20% to +20% their design value.

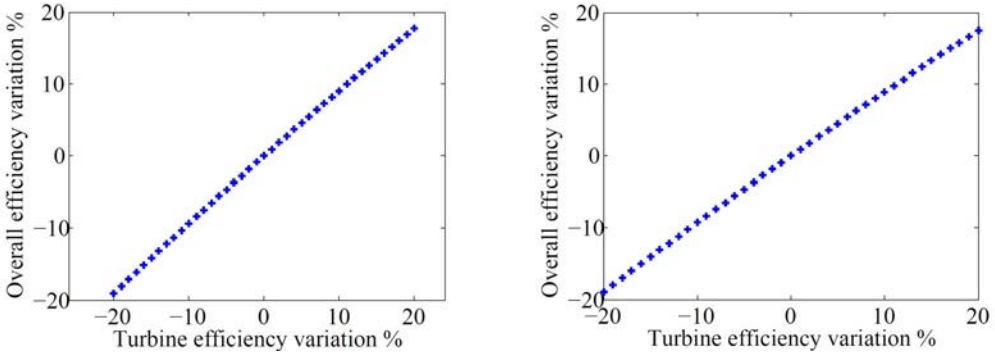

(a) Cyclohexane **(b)** Cyclohexane/Cyclopentane

Figure 5.7: Configuration sensitivity to the turbine efficiency (a) Cyclohexane (b) Cyclohexane/Cyclopentane

Looking at the results for the sensitivity analysis for the turbine efficiency (Figure 5.7) it appears that in both the cases the behaviour is similar: an increase of 20% in the turbine isentropic efficiency leads to an increase of almost 20% of the overall efficiency and an equal decrement takes place when the turbine efficiency is decreased.

The pump efficiency has a very low incidence on the results: the maximum variation is in fact within $\pm 0.2\%$. This can be explained by the different order of magnitude of the produced and absorbed power (the turbine output is slightly more than 100 kW, while the power absorption by the pump is roughly 1 kW). Similarly, the variation of the boiler pinch point lead to performance variations within 1% (see Figure 5.8).

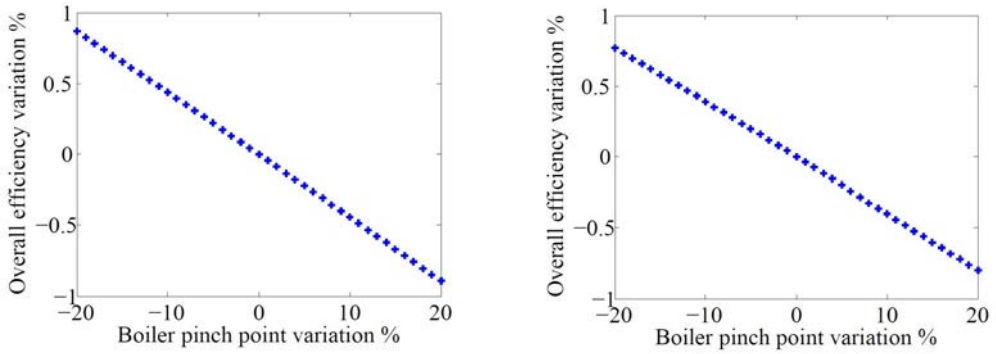

(a) Cyclohexane **(b)** Cyclohexane/Cyclopentane

Figure 5.8: Configuration sensitivity to boiler pinch point (a) Cyclohexane (b) Cyclohexane/Cyclopentane

Finally the influence of the cooling water inlet temperature has been investigated: from the following plots (Figure 5.9) it emerges that this parameter highly affects the plant performance. An increment of 20% of this parameters (cooling water inlet temperature 24^oC) leads to an overall efficiency reduction of almost 5%.

This result has to be taken into particular consideration: it is not always possible to have high availability of cooling water in those locations where the installation of solar power plants is profitable and as a consequence the efficiency of these technology is often affected by the requirement of having an higher value for the condensing temperature. Furthermore it should also be mentioned that the two configurations show very similar behaviours with respect to all the considered parameters.

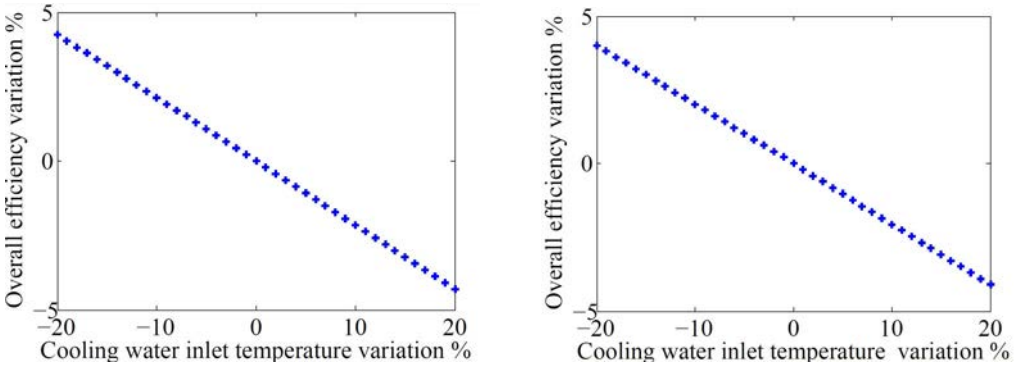

(a) Cyclohexane **(b)** Cyclohexane/Cyclopentane

Figure 5.9: Configuration sensitivity to the cooling water inlet temperature (a) Cyclohexane (b) Cyclohexane/Cyclopentane

5.4 Discussion

In this Chapter an overall solar power system composed of a parabolic trough solar field and an organic Rankine cycle has been optimized in order to find out which configuration enables to obtain the highest solar to electrical efficiency.

The target power output has been fixed to 100 kW and for the solar field an outlet temperature of 150^oC has been considered. All the cycle performance parameters (pump and turbine efficiencies, pinch point temperatures and cooling water inlet temperature) are the same considered for the low temperature case discussed in Chapter 2.

For every tentative configuration the water solar field inlet and outlet temperature have been calculated with the power cycle model and then the required collecting area has been estimated discretizing the water temperature increase into 100 steps and using the regression model shown in section 4.5. In addition the calculation of the pressure losses along the solar field enabled to estimate the power required by the circulating pump and thus to evaluate the overall system efficiency.

A primary analysis considered only pure fluids as possible candidates and showed that the all the most performing configurations are characterised by the maximum allowed value for the turbine inlet temperature and that the most important parameter to be optimized is the power cycle efficiency. The solar field efficiency, defined as the ratio between the heat released in the boiler by the heat transfer fluid and the incident solar energy is almost the same for every configuration: this is probably related to the highly insulation of the considered solar field receiver and to the relatively low temperature at which the pressurized water is heated up.

Another key parameter to be considered during the optimization process is the temperature glide of the heat transfer fluid: lower values of this parameter enable to release the heat at a higher temperature level and thus to increase the efficiency of the power cycle. At the same time, configurations characterised by too low values of the temperature glide require very high water mass flow rates and are therefore penalised by high power absorption by the solar field circulating pumps. The most performing systems show that a trade-off between this two phenomena is found with a temperature glide between 14 and 17^oC (similar values can be found in literature).

After the performance of the various pure fluid has been assessed, mixtures have been analysed as possible working fluids for the power cycle. In this case the optimization process was carried changing the mixture composition (mass fraction of the first component), turbine inlet temperature and cycle maximum pressure. The obtained results show that the use of mixtures can lead to efficiency increments between 0.3 and 2.27%. This performance increment is lower to the one obtained in chapter 2, but can be explained by several reasons. In the previous case the optimization aimed at extracting the maximum amount of power out of a given hot stream and thus the use of mixture was beneficial from two points of view: first it enabled to reach higher values for the turbine inlet temperature and so to

increase the power cycle effectiveness, and secondly it allowed to further decrease the heat source outlet temperature and so to increase the overall heat absorption. Here instead the turbine inlet temperature is always fixed to its maximum value and decreasing the heat source outlet temperature doesn't lead to performance gains. As a consequence the use of binary working fluids results only in a better thermal matching between heat source and power cycle and to reduced irreversibility in the condenser.

The comparison between the best configuration using a pure fluid (Cyclohexane $\eta_{overall}$ = 11.93%) and the best configuration using a mixture (Cyclohexane/Cylopentane 0.84/0.16 $\eta_{overall}$ = 12.20%) shows that the mixture leads to a greater net power output (+0.28%) with a lower solar field surface area (-1.95%). From an economical point of view similar costs are expected for the power cycle pump and turbine since both the configurations operate with similar mass flow rates and pressure ratios. On the other hand the configuration using the mixture is characterised by higher UA requirements for the heat exchangers, especially for the evaporator (+ 11%) and for the condenser (+47%) which will lead to higher investment costs.

Both the configurations are characterised by fairly high values for the overall solar to electricity efficiency, but this can be explained by two main reasons. First of all the considered solar field technology is usually adopted for high temperature solar plants and thus the heat losses are very low (with a less insulated absorber and a lower optical efficiency of the collectors the solar field efficiency can decrease a lot). Secondly, most of the existing CSP plant are equipped with an air condenser, which further decreases the overall efficiency by increasing the condensing temperature and absorbing a not neglectable amount of power due to the fans consumptions.

Here only thermodynamic parameters have been taken into account, but in order to find out which configurations is more profitable it would be necessary to carry out a thermo-economic optimization where for every possible configuration the investment costs and power production are evaluated so that to estimate the levelised cost of the electricity.

In the end it is useful to point out that this analysis neglected the effect of the pressure losses in the various heat exchangers. The introduction of this parameter in the optimization process would probably lead to configurations characterised by higher temperature drops for the pressurized water in the boiler and thus to higher performance gains for the mixtures.

Chapter 6

Annual Analysis

Once that the performance of the pure fluids and mixtures have been compared in the design case the focus is set on the overall power production that can be achieved with the different configurations. The final aim of a solar power plant is produce as much energy as possible out of the solar source and thus a power plant that is highly efficient when the solar irradiation is high, but whose efficiency drops very fast as the solar source decreases wouldn't be preferred over another power plant with a lower efficiency but less dependent on the solar irradiation.

Primary factors that affect the overall annual production of a power plant are the minimum acceptable load (the minimum amount of power that it is able to produce), the minimum required solar irradiation (power plants that are able to operate with lower values of solar irradiation are preferable since they have lower inactivity times) and the dependence of the plant efficiency on the solar irradiation (as mentioned before, a plant whose efficiency decreases slowly with the load is preferable).

Here the annual performance of the two most performing configurations compared in the previous chapter is analysed so that to find whether the use of a mixture in part load conditions leads to a different behaviour with respect to a pure fluid configuration.

6.1 Part Load model

In order to asses the power cycle performance as the available energy source decreases it is necessary to build a part load model. While in the design model the fixed parameters were the electrical output, the solar irradiation and the performance parameters of the various components of the power plant (the isentropic efficiency of the pump and turbine, the pinch point temperatures and the environmental conditions) in the part load case the fixed parameters are the size of the various components (solar field, turbine, pump, electric generator and heat exchangers).

The effectiveness of the various components is no longer constant but has to be estimated trough performance curves. The input values to the part load models will

be the environmental conditions (Direct normal irradiation, ambient temperature and wind speed) and the desired output will be the electrical output of the power plant.

6.1.1 Heat Exchangers

The heat exchangers are modelled in part load by means of UA values. The heat exchanged in design conditions can be calculated as:

$$\dot{q}_{des} = (UA)_{des} \Delta T_{ml} \tag{6.1}$$

Where ΔT_{ml} is the mean logarithm temperature difference already defined in section 5.3.1.

According to Patnode [68] the performance of a heat exchanger in part load condition can be estimated with the following equation:

$$\frac{UA}{(UA)_{des}} = \left(\frac{\dot{m}_c^{0.8} \, \dot{m}_h^{0.8}}{\dot{m}_{c,des}^{0.8} \, \dot{m}_{h,des}^{0.8}} \right) \left(\frac{\dot{m}_{c,des}^{0.8} + \dot{m}_{h,des}^{0.8}}{\dot{m}_c^{0.8} + \dot{m}_h^{0.8}} \right) \tag{6.2}$$

The heat exchanger performance is therefore a function of the mass flow rate of the two fluids ($\dot{m}_c$ and $\dot{m}_h$ are respectively the mass flow rate of the cold and hot fluids and the subscript *des* stands for design conditions). For the recuperator, where the mass flow ratio between the hot and the cold fluid remains constant, the previous relationship can be further simplified:

$$\frac{UA}{(UA)_{des}} = \left(\frac{\dot{m}_c}{\dot{m}_{c,des}} \right)^{0.8} \tag{6.3}$$

In part load conditions both the mass flow rates and the temperatures are accordingly changed so that to fulfil the following system of equations:

$$\begin{cases} \dot{q} = \dot{m}_c \, \Delta h_c \\ \dot{q} = -\dot{m}_h \, \Delta h_h \\ \dot{q} = UA \, \Delta T_{ml} \end{cases} \tag{6.4}$$

In order to have higher accuracy in the calculations the boiler is subdivided into 3 zones: pre-heater, evaporator and super-heater, a single zone is instead considered for the recuperator. In addition, with the purpose of obtaining a more precise analysis of the two phase zone (especially for the mixture case) the evaporator is further divided into 3 volumes .

6.1.2 Turbine

The turbine performance in off-design condition is modelled with the hypothesis that the flow is chocked at the nozzle outlet. In this case the turbine mass flow rate, inlet temperature and pressure ratio are related to each other by means of the constant of Stodola [71]:

$$C_T = \frac{\dot{m}\sqrt{T_{in}}}{\sqrt{P_{in}^2 - P_{out}^2}} \tag{6.5}$$

The mass flow rate trough the turbine in part load condition can be estimated as follows:

$$\dot{m} = \dot{m}_{des} \frac{\sqrt{T_{in,des}}}{\sqrt{T_{in}}} \frac{\sqrt{P_{in}^2 - P_{out}^2}}{\sqrt{P_{in,des}^2 - P_{out,des}^2}} \tag{6.6}$$

6.1.3 Pump

The part load efficiency of the pump is calculated with the following relationship [72]:

$$\eta_p = \eta_{p,des}(-0.168f^3 - 0.336f^2 + 0.6317f + 0.5669) \tag{6.7}$$

Where f is the ratio between the mass flow rate in off-design and design conditions.

6.1.4 Electric generator

The efficiency of the electric generator in part load is affected by the copper losses which are variable with the load. As a consequence the efficiency drop of the generator is calculated with the following correlation suggested by Fredrik and Elmegaard [73]:

$$\eta_{gen} = \frac{\eta_{gen,des}\ Load}{\eta_{gen,des}\ Load + (1 - \eta_{gen,des})[(1 - F_{Cu}) + F_{Cu}\ Load^2]} \tag{6.8}$$

Where $Load$ is the mechanical input in per unit and F_{Cu} the copper loss fraction in design condition (here assumed equal to 0.43).

6.1.5 Condenser

The condenser is modelled as a fixed pressure component: the idea is to have a suitable control in the cooling circuit so that the condensing pressures can be kept nearly constant.

6.1.6 Solar Field

In order to keep the overall system as high as possible during the part load operation it has been decided to keep the solar field outlet temperature fixed to 150 ^oC and as a consequence the solar field part load model is modelled in order to fulfil this requirement.

The solar field part load model is verified by mean of two steps process:

1. Given the environmental conditions (DNI, ambient temperature and wind speed) the organic Rankine cycle part load model is solved with a tentative value of the pressurized water mass flow rate and this enables to calculate the required solar field inlet temperature;

2. The absorber length is discretized into a finite number of elements and the outlet temperature is calculated using equation 5.2 for each element (the considered solar field mass flow rate and inlet temperature are the ones estimated at point 1);

The solar field part load model is considered solved when the calculated solar field outlet temperature is equal to $150^{o}C$.

The pumping power required for the solar field pipelines is estimated as in the design model (the hypothesis is to have an unitary efficiency for the pump).

6.2 Control Strategies

In order to solve the overall system part load model some control strategy has to be defined. As already mentioned in section 6.1.6 for the solar field it has been decided to keep the outlet temperature constant and to vary the pressurized water mass flow rate accordingly to the available solar irradiation.

For the power cycle 3 different control strategies have been investigated:

1. **Constant turbine inlet temperature**: this control strategy aims to keep the cycle maximum temperature at its highest values. The cycle efficiency is strictly related to the maximum temperature of the working fluid and therefore by keeping it at its design value the efficiency drop should be as low as possible;

2. **Constant super-heating temperature**: by using this control strategy the cycle configuration is kept as close as possible to the one optimized for the design case.

3. **Constant solar field inlet temperature**: in this case the solar field inlet and outlet temperature are kept constant and thus the control of the solar field mass flow rates is particularly easy.

6.3 Part Load results

As already mentioned the overall system performance are affected by several parameters: the available direct normal irradiation, the ambient temperature, the wind speed, the tracking system orientation, the day of the year (n) and the hour of the day (h). The purpose is therefore to find out an equation that correlates all these parameters to the power cycle net output:

$$W_{Net} = f\left(DNI,\ T_{amb},\ v_{wind},\ tracking,\ n,\ h\right) \tag{6.9}$$

Given the DNI, the tranking system, n and h, the collected solar energy per square meter of solar field can be calculated as:

$$\dot{q}_{collected} = DNI\ IAM\ cos(\theta) \tag{6.10}$$

and thus equation 6.9 can be simplified to:

$$W_{Net} = f\left(\dot{q}_{collected},\ T_{amb},\ v_{wind}\right) \tag{6.11}$$

As a first analysis the ambient temperature and wind speed are kept constant to their design values and the collected energy is progressively decreased. The Net power decrement is calculated with respect to the design value:

$$Load = \frac{W_{Net}}{(W_{net})_{des}} = \frac{W_{el} - W_{piping}}{(W_{net})_{des}} \tag{6.12}$$

The results, for the two considered configurations are shown in Figure 6.1 and 6.2.

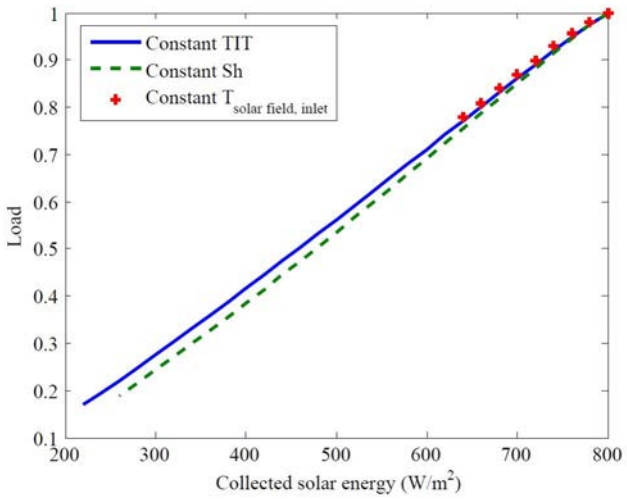

Figure 6.1: Part load performance of Cyclohexane optimized configuration

In both the cases the most performing control strategy is to keep a constant value for the turbine inlet temperature (different boiler temperature profiles for this control strategy are shown in Figure 6.5). The mixture configuration seems able to operate at lower loads: the minimum required collected energy for the mixture case is 140 W/m^2 (load = 8%), while this value increases to 220 W/m^2 (load = 17%) when pure cyclohexane is taken into account. This difference can be explained by the fact that in the mixture configuration, when the load is very low, the evaporation process starts in the recuperator where some heat is recovered even from the first stages of the condenser. On the other hand, the constant evaporation temperature of the pure fluid leads to the violation of the pinch point in the saturation point when the load is particularly low.

Looking at the other control strategies it emerges that keeping a constant value for the super-heating enables to operate in a wide range of collected energies, but

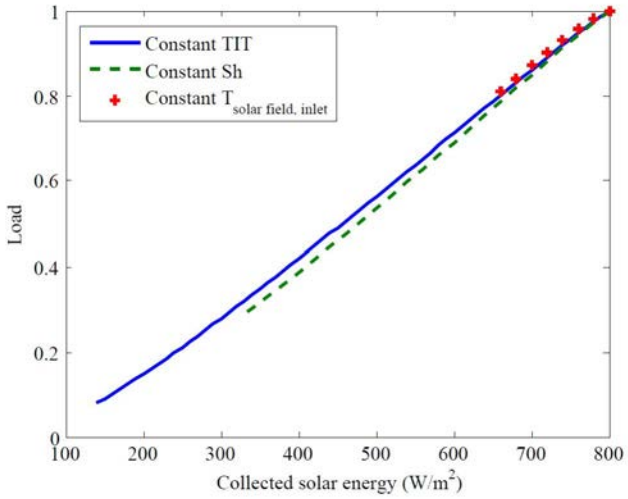

Figure 6.2: Part load performance of Cyclohexane/Cyclopentane optimized configuration

that the corresponding load is always lower if compared to strategy 1. In this case the mixture shows a greater value for the minimum required collected energy: this is related to the lower temperature difference between the hot and cold streams in the boiler that leads to faster decrement of the pinch point values.

The last considered control strategy (constant solar field outlet temperature) is the more restrictive: the minimum required collected energy in this case are respectively 640 and 680 W/m^2. On the other hand, as shown in Figures 6.3 and 6.4, this control strategy is characterised by higher efficiencies than the previous cases: the decrement of the pinch point values enables to keep the effectiveness of the power plant very close or even slightly higher than in the design case.

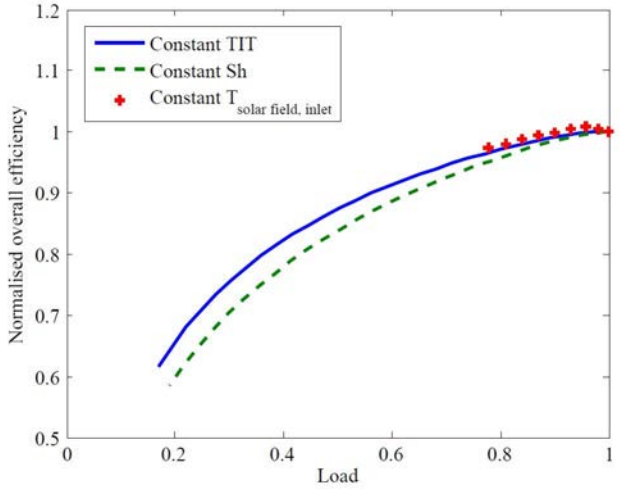

Figure 6.3: Part load efficiency of Cyclohexane optimized configuration

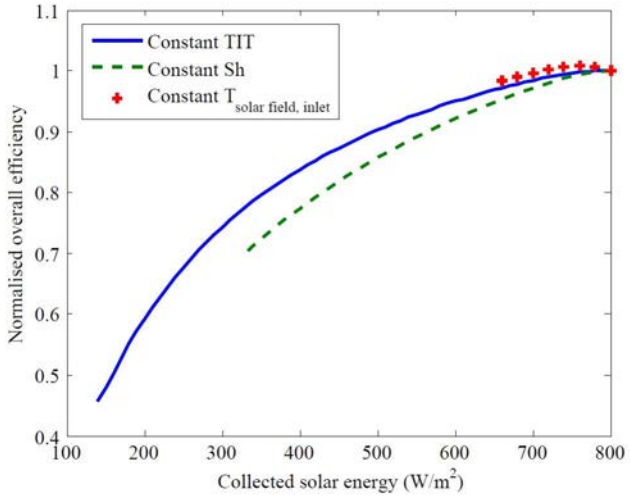

Figure 6.4: Part load efficiency of Cyclohexane/Cyclopentane optimized configuration

The power plant behaviour for values of the collected energy greater than the design one is here not taken into account since it is common practice in CSP power plants to limit the maximum power production at the design value by increasing the optical losses of the solar field during very high irradiation hours.

6.3.1 Influence of Ambient temperature

In order to estimate the influence of ambient temperature on the power cycle performance 2 simulations have been carried out. In both the cases the analysed configuration is the optimized cyclohexane solar system and the selected control strategy is to keep a constant value for the turbine inlet temperature. The considered values for the ambient temperature are 15 (case 1) and 35 ^oC (case 2). The obtained results, see Table 6.1, show that the influence of the ambient temperature on the overall performance is neglectable: when the collected energy is higher than 500 W/m^2 the difference between the two cases is lower than 0.1% and even at lower values of the collected energy the difference is always smaller than 0.3%.

6.3.2 Influence of Wind speed

As for the previous case, the influence of the wind speed on the overall performance has been investigated by mean of two simulations. The selected values for this parameters have been respectively 0 and 8 m/s. The results of Table 6.3 show than even this parameter has very little influence of the part load performance: the maximum difference is around 0.2%.

Table 6.1: Influence of the ambient temperature on the part load performance

Collected solar energy	Load		$\Delta\%$
	Case 1	Case 2	
$[W/m^2]$	15^oC	35^oC	
800	1,000	1,000	0,047
780	0,975	0,975	0,054
760	0,948	0,948	0,059
740	0,919	0,920	0,063
720	0,890	0,891	0,066
700	0,861	0,861	0,069
680	0,831	0,832	0,072
660	0,801	0,802	0,075
640	0,771	0,772	0,078
620	0,741	0,742	0,081
600	0,711	0,711	0,085
580	0,681	0,681	0,088
560	0,651	0,652	0,092
540	0,621	0,622	0,096
520	0,591	0,592	0,101
500	0,562	0,562	0,106
480	0,532	0,533	0,111
460	0,503	0,503	0,117
440	0,473	0,474	0,123
420	0,444	0,445	0,130
400	0,416	0,416	0,139
380	0,387	0,388	0,148
360	0,359	0,359	0,158
340	0,330	0,331	0,170
320	0,302	0,303	0,184
300	0,275	0,275	0,200
280	0,248	0,248	0,219
260	0,221	0,221	0,242
240	0,194	0,195	0,271
220	0,169	0,170	0,292

Table 6.2: Influence of the wind speed on the part load performance

Collected solar energy	Load		Δ%
	Case 1	Case 2	
$[W/m^2]$	0 m/s	8 m/s	
800	1,000	1,000	-0,030
780	0,975	0,975	-0,035
760	0,948	0,948	-0,038
740	0,920	0,919	-0,041
720	0,891	0,890	-0,043
700	0,861	0,861	-0,045
680	0,831	0,831	-0,047
660	0,801	0,801	-0,049
640	0,771	0,771	-0,051
620	0,741	0,741	-0,053
600	0,711	0,711	-0,055
580	0,681	0,681	-0,057
560	0,651	0,651	-0,060
540	0,621	0,621	-0,063
520	0,592	0,591	-0,066
500	0,562	0,562	-0,069
480	0,532	0,532	-0,072
460	0,503	0,503	-0,076
440	0,474	0,473	-0,080
420	0,445	0,444	-0,085
400	0,416	0,416	-0,090
380	0,387	0,387	-0,096
360	0,359	0,359	-0,103
340	0,331	0,330	-0,111
320	0,303	0,302	-0,120
300	0,275	0,275	-0,130
280	0,248	0,248	-0,142
260	0,221	0,221	-0,158
240	0,195	0,194	-0,176
220	0,170	0,169	-0,190

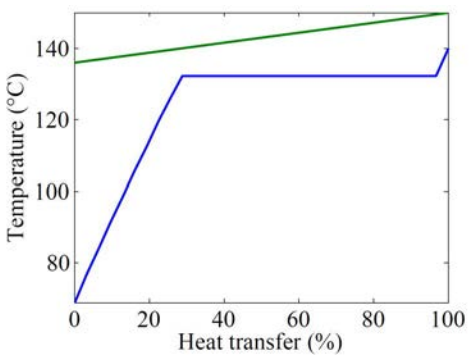

(a) Pure fluid, Load = 100%

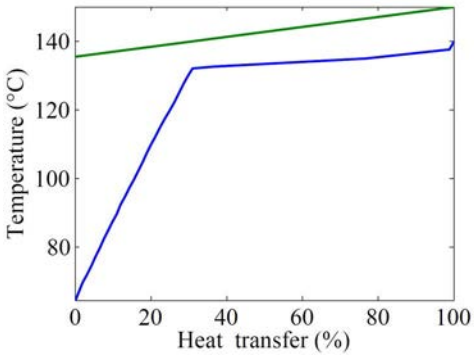

(b) Mixture, Load = 100%

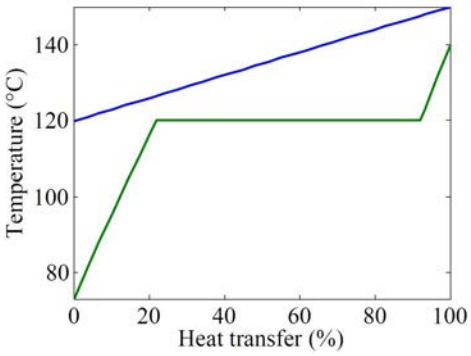

(c) Pure fluid, Load = 70%

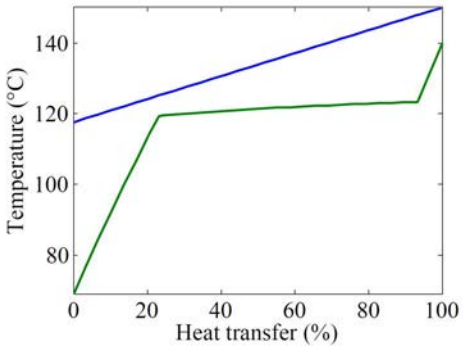

(d) Mixture, Load = 70%

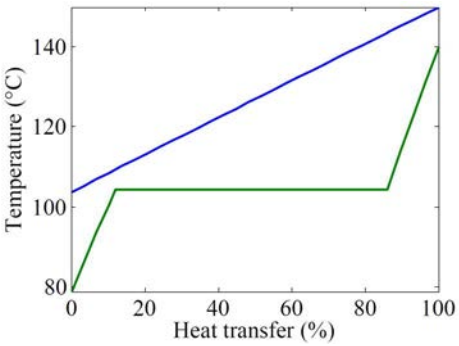

(e) Pure fluid, Load = 40%

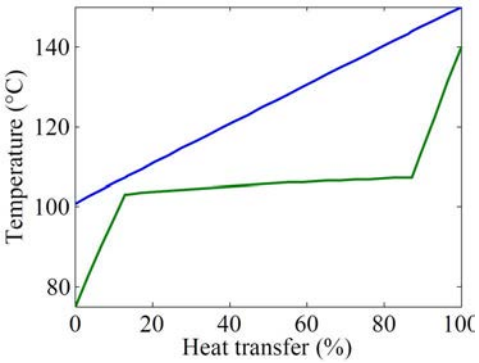

(f) Mixture, Load = 40%

Figure 6.5: Boiler temperature profiles at different loads using the first control strategy

6.3.3 Minimum acceptable load

In the part load model the overall system is solved with different values for the decision variables and the solution is considered acceptable when all the considered equations are verified and the pinch point temperatures are not negative (the pinch point is estimated for every calculation by subdividing the boiler into 30 steps plus the saturation points).

On the other hand the minimum load for a power cycle is usually defined by the minimum acceptable load of the various components, which is given by their performance curves. For example, in well known software for large scale parabolic trough power plants as SAM and Greenius the minimum allowed power output for the turbine is usually between 10 and 20%. A similar value could be expected for smaller scale turbines, like the one considered in this analysis. As shown in Figure 6.6 for the mixture case the turbine load goes below this limit (the minimum calculated turbine load is 8.7%). In order to take into account this parameter, it has been decided to fix the mixture turbine minimum load to 10% and 15% (160 and 200 W/m^2 of collected energy).

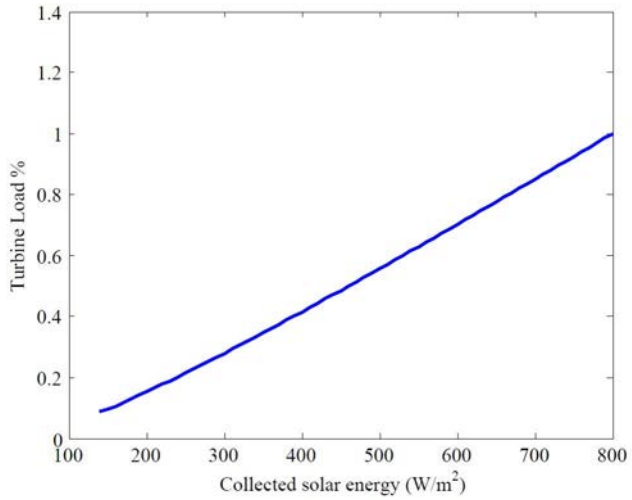

Figure 6.6: Variation of turbine load in part load conditions (Mixture)

Another important parameter to be considered is the solar field mass flow rate, its value decreases a lot during the part load operation and goes below 10% of the design case, which is the solar field mass flow rate during night operation for large scale solar power plants. Further analysis should be therefore carried out in order to ensure whether the overall system could operate with such low mass flow rates.

6.4 Regression model

In order to perform a faster calculation of the annual energy production the part load behaviour of the two power plants have been fitted with a regression curve obtained with Data Fit 9.0. Since the influence of the wind speed and of the

ambient temperature are neglectable, the only parameter that has been considered for this regression model is the solar collected energy. The resulting best fitting equation is a tenth order polinomial:

$$Load = ax^{10} + bx^9 + cx^8 + dx^7 + ex^6 + fx^5 + gx^4 + hx^3 + ix^2 + jx + k \quad (6.13)$$

Table 6.3: Parameters of the regression curve

Parameter	Configuration	
	Pure Fluid	Mixture
a	2,1719E-27	1,6449E-27
b	-1,2246E-23	-8,1702E-24
c	3,0330E-20	1,7715E-20
d	-4,3509E-17	-2,2063E-17
e	4,0064E-14	1,7461E-14
f	-2,4751E-11	-9,1699E-12
g	1,0392E-08	3,2370E-09
h	-2,9282E-06	-7,6077E-07
i	5,3057E-04	1,1521E-04
j	-5,4586E-02	-9,0653E-03
k	2,4817E+00	0,3171E+00

6.5 Annual Simulation

Given the regression model for the part load behaviour of the two power plants an annual simulation was performed using the weather data of Sevilla (Spain). The analysis considered the two optimized configurations and both a north-south and a east-west orientation for the solar field collectors. The results are shown in Table 6.4.

Looking at the results it emerges that the mixture configuration is characterised by higher values of the annual production, especially when the turbine minimum load is set to 10% and the solar field orientation is east-west (in this case the annual production is 2.47% higher than in the pure fluid configuration and both the annual efficiency and the specific production increase by 4.5%).

On the other hand when the north-south configuration is taken into account the the overall production increase is equal to 0.95% (minimum load = 15%) and 1.56% (minimum load = 10%). The overall efficiency and the specific production increase by 3% when the minimum turbine load is set to 15% and by 3.58% when it is set to 10%.

Analysing the results of the two different orientations of the solar field it can be concluded that the highest productions are obtained with a north-south orientation.

Table 6.4: Annual simulation results

Configuration	Annual Production $[MWh]$	Annual Efficiency	Annual Specific production $[kWh/m^2]$
North-South orientation			
Pure fluid	221,37	8,95	215,19
Mixture (min load = 15%)	223,46	9,22	221,54
Mixture (min load = 10%)	224,83	9,27	222,89
East-West orientation			
Pure fluid	174,81	7,07	169,93
Mixture (min load = 15%)	176,93	7,3	175,40
Mixture (min load = 10%)	179,13	7,39	177,59

As shown in Figure 6.7 this configuration enables to maximize the production during the summer period when the irradiation is usually higher, but drops its effectiveness during the winter month when the solar hight is lower and therefore the cosine of the incident angle decreases. The resulting power production is therefore very unbalanced and varies between 30 MWh in the most productive months (June, July and August) and 5-10 MWh in November, December, January and February.

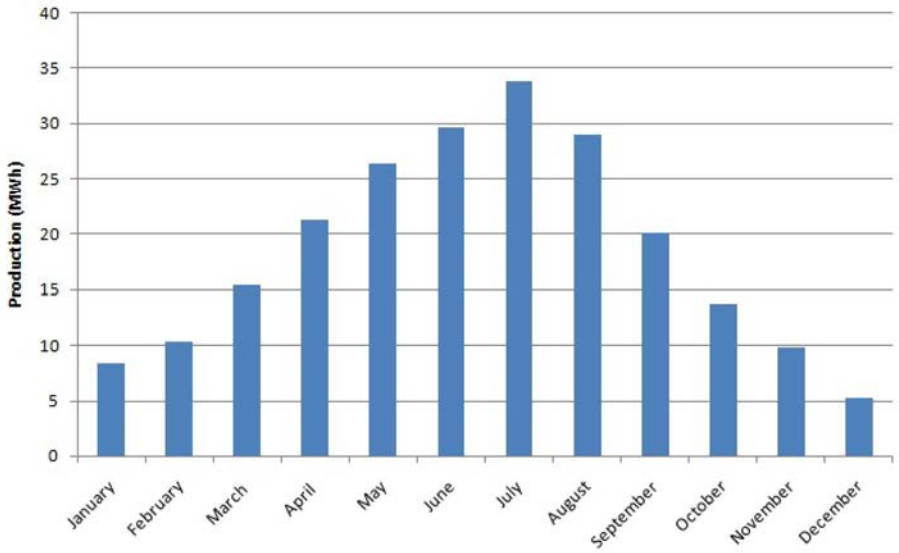

Figure 6.7: Monthly production with a north-south orientation of the solar field (Cyclohexane/Cyclopentane optimized configuration with minimum turbine load = 15%)

On the other hand the east-west configuration is characterised by a more balanced power production profile and the monthly production never drops below 10 MWh (see Figure 6.7). Nonetheless in this case the overall production is 20% lower

and the productivity of the summer months decreases from almost 35 to $20 MWh$.

Moreover, looking at the load duration curve of the two configurations (Figure 6.9) it emerges that with the north-south orientation the plant is operative for about 3480 hours every year, while with the second option the operative time drops to about 2700. This can be easily explained: with the east-west configuration the production is concentrated around the solar noon (from 11.00 to 15.00), while this range is highly increased with the north-south configuration (in summer the power production takes place from 9.00 to 18.00). Evidence of this fact can be seen in Figures 6.10 and 6.11 where Q_{Sol} is the solar energy theoretically available ($= DNI\ S_{tot}$) and $Q_{Sol,eff}$ is the solar energy that participates to the energy balance in the absorber ($= DNI\ IAM\ cos(\theta)\ \eta_{opt}\ S_{tot}$).

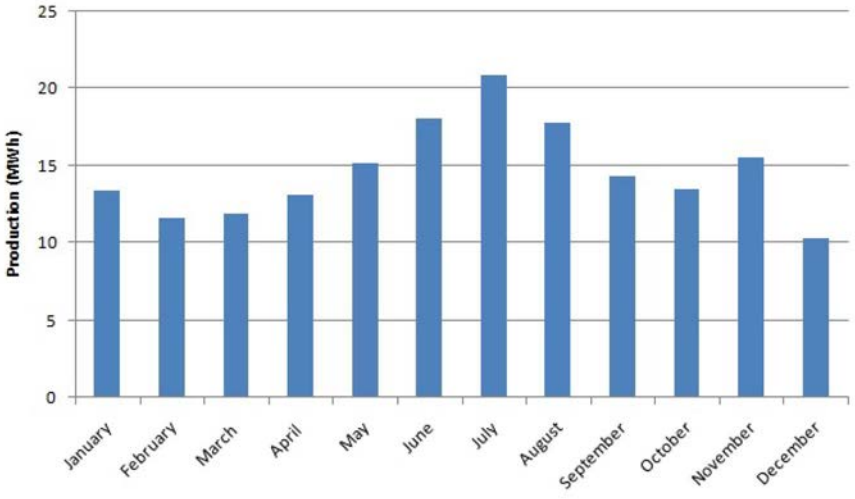

Figure 6.8: Monthly production with a east-west orientation of the solar field (Cyclohexane/Cyclopentane optimized configuration, min load = 15%)

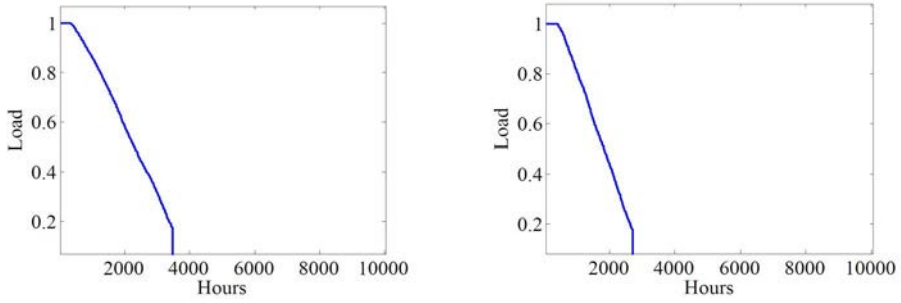

Figure 6.9: Load duration curve for Cyclohexane/Cyclopentane configuration with minimum turbine load = 15% (a) North-South solar field orientation (b) East-West solar field orientation

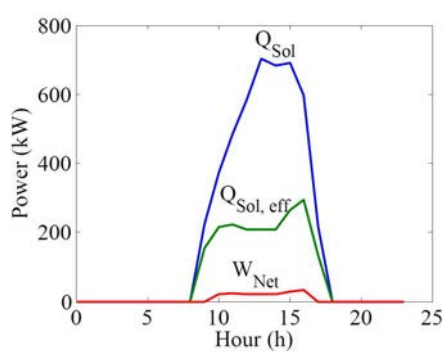

(a) 21 December, N-S orientation

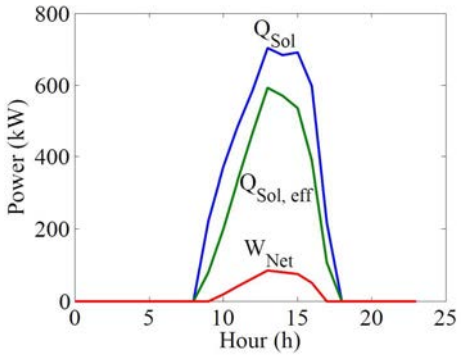

(b) 21 December, E-W orientation

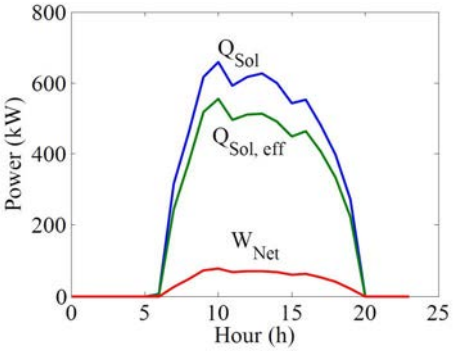

(c) 21 June, N-S orientation

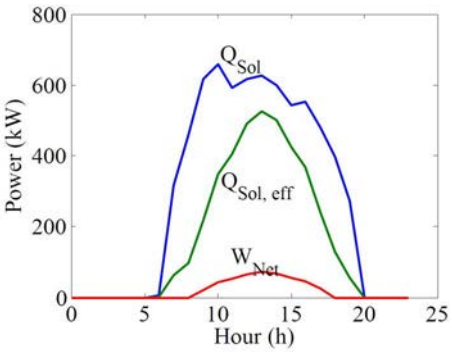

(d) 21 June, E-W orientation

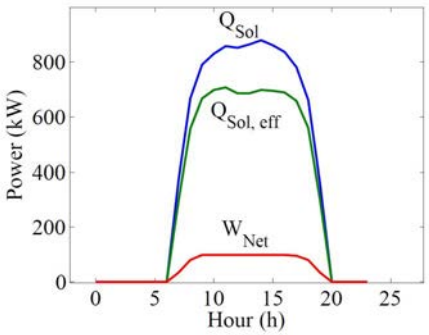

(e) 2 August, N-S orientation

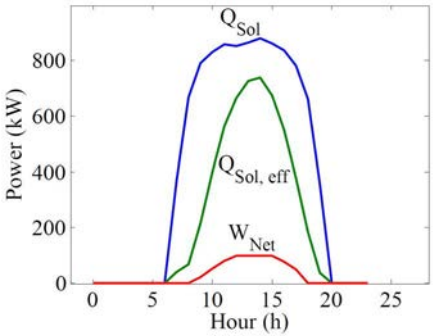

(f) 2 August, E-W orientation

Figure 6.10: Energy balances for three representative days for the mixture configuration (minimum turbine load = 15%)

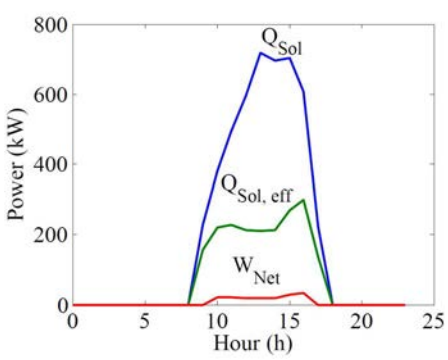

(a) 21 December, N-S orientation

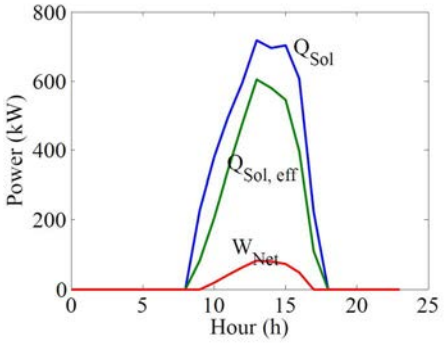

(b) 21 December, E-W orientation

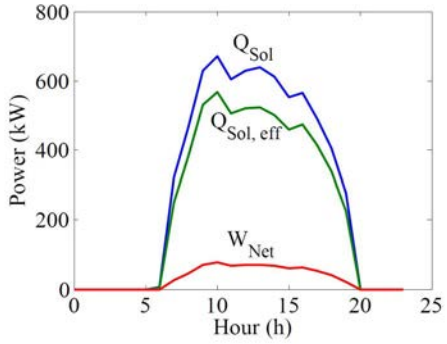

(c) 21 June, N-S orientation

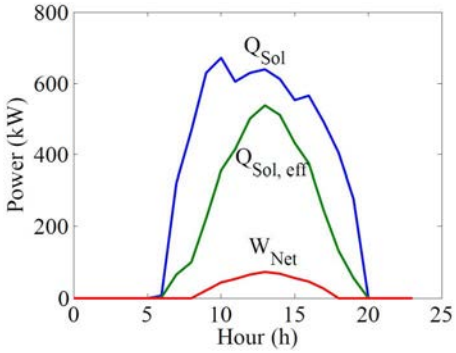

(d) 21 June, E-W orientation

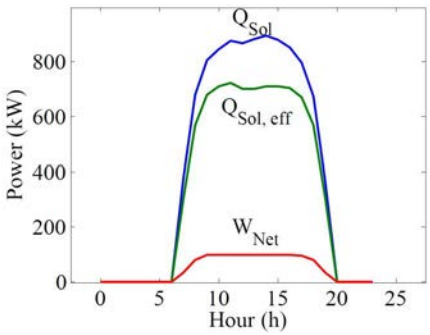

(e) 2 August, N-S orientation

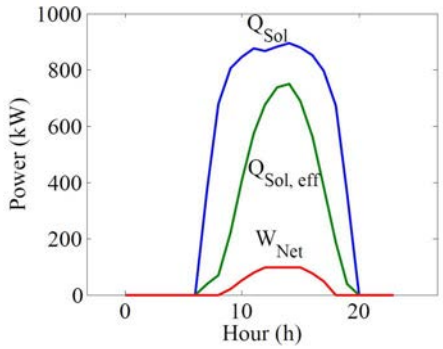

(f) 2 August, E-W orientation

Figure 6.11: Energy balances for three representative days for the pure fluid configuration

6.5.1 Influence of Design DNI

In all the previous calculation a design value of 800 W/m^2 was considered for the direct normal irradiation. This value is one of the most commonly used in CSP literature. Nonetheless it should be considered that the value of this parameter greatly affects the overall productivity of the solar system and as a consequence more detailed analysis would be required to estimate its optimum value.

As the DNI design value increases the plant becomes more efficient during those hours characterised by high values of solar irradiation, but at the same time the effectiveness during low irradiation periods decreases. At the same time power plants with higher values for the design DNI require lower surface area for the solar field and as a consequence the investment costs decrease. A trade off between a higher and more constant productivity (low design DNI value) and lower surfaces of the solar field and high efficiency during pick hours (high design DNI value) should be therefore found.

In order to investigate the influence of this parameter on the developed model a parametric analysis was carried out: the optimized configuration using cyclohexane as working fluid was considered as case study and the analysed value for the design DNI have been: 750, 775, 800, 825, 850, 875 and 900 W/m^2. As depicted in Figure 6.12 varying from the lower value to the higher the annual productivity decreases from 228 MWh to 190 MWh and a similar trend appears for the solar field surface area (the maximum value is 1098 m^2 and the lowest 914 m^2).

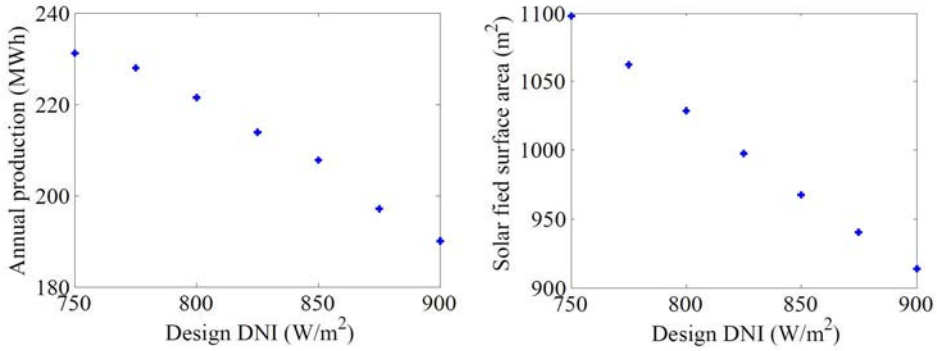

Figure 6.12: Influence of the design DNI on: (a) Annual production (b) Solar field surface area

From a thermodynamic point of view the best solutions are those characterised by the highest overall efficiency and with the highest specific productivity of the solar field (annual production divided by the overall solar field surface area). Figure 6.13 shows that both this parameters reach their maximum for a DNI value that is probably very close to the one considered in this analysis.

In the end it should be considered that the most performing power plant from a thermodynamic point of view does not necessarily coincide with the most profitable

one and thus even in this case a thermo-economic analysis would be required to define which design value for the DNI would lead to the lowest value for the levelized cost of the electricity.

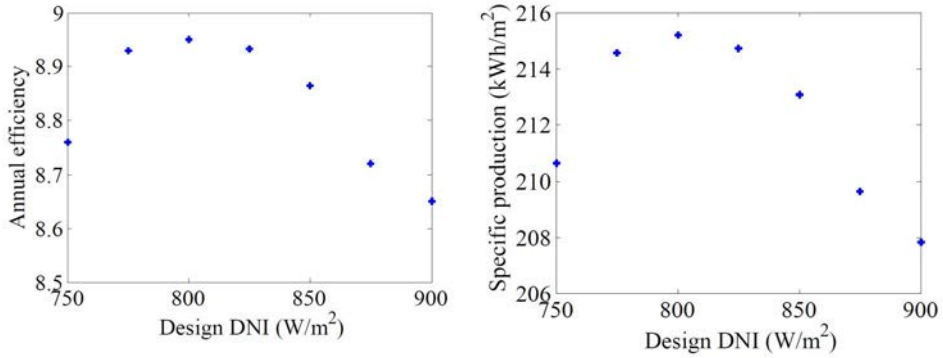

(a) **(b)**

Figure 6.13: Influence of the design DNI on: (a) Annual efficiency (b) Specific production

6.6 Discussion

In this chapter the part load behaviour of the two optimized configurations described in the previous chapter is analysed so that to estimate whether the use of binary working fluids may lead to better annual performance.

In order to estimate the off-design performance of the two solar systems a part load model is at first developed and then a regression curve is obtained so that to reduce the computational time required to perform an annual simulation.

For the solar field it has been decided to keep its outlet temperature at the design value and to vary accordingly the heat transfer fluid mass flow rate, for the power cycle three possible control strategies are instead investigated. The first considers a constant value for the turbine inlet temperature, the second a constant super-heating temperature and the latter a constant value for the solar field inlet temperature. The part load behaviour was analysed only for values of the irradiation lower than the design one, since it is common practice in CSP power plants to limit the power production at the design value by decreasing the optical losses of the solar field during very high irradiation hours.

As a first step the behaviour of the two power plants was analysed with a varying value for the solar collected energy per square meter of solar field ($\dot{q}_{collected} = DNI\ IAM\ cos(\theta)$). The results show that using the first control strategy the mixture configuration is able to operate with lower values of the solar collected energy ($140\ W/m^2$ against $220\ W/m^2$), but when the irradiation is very low the turbine operates under its minimum acceptable load (here two possible values have been taken into account: 10 and 15%). On the other hand, when the other control strategies

are analysed it emerges that the configuration that uses a mixture as working fluid requires higher values for the minimum required solar collected energy and thus is less effective than the pure fluid configuration. This is mainly related to a faster decrement of the pinch point temperature that does not allow to reach low values for the minimum load.

Secondly the effects of the ambient temperature and the wind speed have been taken into account by means of a parametric analysis. The simulations showed that variation of the ambient temperature from 15^oC to 35^oC influenced the power system load less than 0.3%. Similarly the variation of the wind speed from 0 to 8 m/s lead to a load difference lower than 0.2% and as a consequence it has been decided to neglect the effect of these two parameters in the annual simulation (the very low influence of these two parameters is probably related to the high insulation level of the considered absorber technology).

The annual simulation was carried out using the weather data of Sevilla (Spain) and showed an overall annual production of 221.37 MWh for the pure fluid configuration and of $223.44MWh$ for the mixture (for both the configurations a north-south orientation of the solar field is considered and for the mixture the minimum turbine load is set to 15%). This result amplifies the differences obtained in design case: as already mentioned the mixture configuration is able to produce 0.28% more power in design conditions and this value increases to 0.95% for the annual production. Similarly the overall efficiency and specific production of the mixture increases from the +2.27% (design case) to +3% (annual value).

The mixture configuration performance further increases when the minimum turbine load is set to 10%: in this case the annual production reaches $224.83MWh$ (+1.56%) and the overall efficiency increases by 3.58% with respect to the pure fluid system. These results show that with the selected control strategy (constant turbine inlet temperature) mixtures lead to performance improvement even during the part load behaviour and that the relative percentage increment in the annual parameters is strictly related to the minimum load accepted in the turbine.

At the same time it should not be forgotten that this result is strongly related to the selected control strategy for the annual simulation. If any of the two other control strategies is selected then the overall performance of the mixture configuration would decrease due to the higher values of the minimum required collected solar energy.

Lastly a parametric analysis for power plant design DNI was performed: the results show that the considered value of 800 W/m^2 enables to reach high values of the overall efficiency and specific production if compared to lower and higher values of this parameter. Nonetheless a thermo-economic analysis is suggested in order to find out which value would lead to the highest net present value for the overall system.

Chapter 7

Conclusions

The purpose of this work was to better understand the behaviour of solar driven power plants using mixtures as working fluids and to understand whether the introduction of binary working fluids might lead to performance gains with respect to the well known pure fluid configurations.

The primary screening performed in chapter 2 showed that the use of mixture is more profitable in low temperature applications: when the heat source level increase the benefits are lower and flammability/stability issues have to be taken into account. If a 150^oC heat source is considered the use of binary working fluid enables to increase the power cycle net output by almost 7% with respect to the best performing fluid among the two considered in the mixture. Given this result it has been decided to investigate the use of mixture in 100 kW parabolic trough solar system suitable to supply electricity to a group of houses in a remote area.

From the optimization of the overall solar system it emerged that a primary factor in the definition of the system effectiveness is the temperature glide of the heat transfer fluid in the boiler: in all the best performing configuration this parameter ranges between 14 and 17^oC. Configurations characterised by lower values of this parameter are penalised by high power absorption for the circulating pump, while the power cycle efficiency decreases when the temperature glide increases (the temperature level at which the heat is absorbed in the cycle decreases and this leads to lower efficiencies).

The introduction of binary working fluids in the overall system optimization shows that the obtainable performance gain is lower if compared to the waste heat recovery case. This is mainly related to the different purpose of the two technologies: in the waste heat recovery case the most performing plant is the one that is able to extract as much heat as possible from the selected heat source and to convert it effectively into power, for the solar system, instead, the purpose is to perform an efficient conversion of heat into power without decreasing too much the heat source temperature. In this context the use of mixture leads to reduced irreversibility both in the boiler and in the condenser, but is penalised by the lower temperature glide of the heat source.

The best performance is reached with a mixture of Cyclohexane and Cyclopentane (0.84/0.16) which enables to increase the overall system efficiency by 2.27% with respect to the pure Cyclohexane configuration. The comparison between the two optimized solar systems shows that the use of this mixture leads to an increased design power (+0.28%) and to lower surface of the solar field (-1.95%). From an economical point of view the main difference between the two configurations lies in the surface area required for the heat exchangers: a primary analysis shows increased UA requirements for the mixture, especially for the condenser (+47%) and for the boiler (+11%). Since the heat transfer coefficient for the mixtures are lower than for the pure fluids even higher increment in the required heat transfer areas are expected.

In order to assess the mixture behaviour in part load conditions an annual simulation of the two optimized power plant was performed using the solar irradiation data of Sevilla (Spain). The obtained results show that the two configurations behave similarly, with the mixture system slightly improving its gains with respect to the pure fluid due to lower values for the minimum required solar collected energy. When the minimum acceptable turbine load is fixed to 15% the use of mixtures leads an increment of the annual production of 0.95% and of the annual efficiency of 3%, greater performance increment are possible with lower values of the turbine minimum load. Anyway, a similar behaviour of mixtures and pure fluids configurations has not to be taken for granted: as shown in chapter 6 the performance of the mixture configuration is highly dependent on the selected control strategy and thus every case should be analysed on its own.

From a parametric analysis on the design value for the DNI emerges that the considered value of 800 W/m^2 enables to reach satisfactory values for the annual efficiency. With lower values of this parameter the annual production increases but at the expense of an increased solar field surface area, conversely lower surface area are required when the design value of the DNI increases but this lead to lower annual productions.

It should not be neglected that all the results presented in this thesis are subjected to some inaccuracies: first of all the pressure losses of the various heat exchangers have been neglected (their introduction might penalize those configurations characterised by higher values for the pressurized water mass flow rate and thus increase the optimum value for the heat source temperature glide), secondly the calculation of the pinch point location has been performed with a discretization process which is associated with possible errors and lastly the genetic algorithm itself does not guarantee that the real maximum is reached during the optimization process.

In the end it is worth to mention that in this thesis all the configurations have been analysed only from a thermodynamic point of view: a thermo-economic approach would most likely lead to different configurations and thus to different performance gains for the mixtures.

7.1 Recommendations for further work

This work represents only a fist step in the analysis of a solar power system using mixtures as working fluids. Here some suggestion on how to carry out more detailed analysis are listed:

1. The model should be improved with suitable models for the heat exchangers so that to estimate the resulting pressure losses and the required heat transfer area;

2. An air condenser model should be included in order to make the overall system suitable even for those locations where the water availability is not guaranteed. The performance of this new component should be analysed even in part load conditions with the aim of understanding how much the variation of the ambient temperature affects the overall system efficiency;

3. A screening of the possible heat transfer fluid should be done so that to understand which one is the most suitable for this application. In this thesis it has been decided to consider pressurized water as heat transfer fluid due to its high availability and low price, but it should not be forgotten that safety hazard may occur in case of leakages in the pipelines. A possible candidate could be Propylene glycol;

4. Different technologies for the absorber and the collectors should be considered and their influence on the overall performances should be evaluated;

5. Mixtures with more than two components should also be considered as possible candidates so that to understand if their introduction could enable to achieve noticeable gains;

6. New control strategies could be considered: for example it would be interesting to set a minimum value for the heat transfer fluid mass flow rate and operate with a variable solar field outlet temperature once this minimum value is reached;

7. Some dynamic analysis could be carried out in order to asses how to overall system responds to fast variations in the available direct normal irradiation;

8. Finally a thermo-economic optimization is suggested, so that to understand which configurations would be the most profitable from an economic point of view. It would be of great interest to compare the results of the thermodynamic optimization with the ones of the thermo-economic approach.The optimization might also include a thermal storage and consider different values for the solar multiple.

Bibliography

[1] G. Lozza *Turbine a gas e cicli combinati* 2006 2nd Edition: Esculapio, Bologna.

[2] Modi Anish, Fredrik Haglind *Performance analysis of a Kalina cycle for a central receiver solar thermal power plant with direct steam generation* Applied Thermal Engineering 2014; 65:201-208.

[3] Truscello, Vincent C. *Parabolic dish collectors: a solar option* Sunworld 1981; 5:80-86.

[4] Shou Peng, Hui Hong, Yanjuang Wang, Zhaoguo Wang, Hongguang Jin *Off-design thermodynamic performances on typical days of a 330 MW solar aided coal-fired power plant in China* Applied Energy 2014; 130:500-509.

[5] James D. Spelling Doctoral thesis *Hybrid solar gas-turbine power plants, a thermoeconomic analysis* Stockholm, 2013.

[6] Bahram Saadatfar, Reza Fakhrai and Torsten Fransson *Waste heat recovery Organic Rankine cycles in sustainable energy coversion: A state-of-the-art review* The Journal of Macro Trends in Energy and Sustainability, Vol 1 issue 2003.

[7] Tchanche BF, Lambrinos G, Frangoukakis A, Papadakis G *Low grade heat conversion into power using organic Rankine cycles - A review of various applications* Renewable and Sustainable Energy Reviews 2011; 15(8):3963-79.

[8] Wali E. *Optimum working fluids for solar powered Rankine cycle cooling of buildings*Solar Energy 1980;25:235–41.

[9] Junjiang Bao, Li Zhao *A review of working fluids and expander selections for organic Rankine cycle* Renewable and Sustainable Energy Reviews 24 (2013) 325-342.

[10] Rachel Anne Victor, Jin-Kuk Kim, Robin Smith *Composition optimisation of working fluids for organic Rankine cycles and Kalina cycles* Energy 55 (2013) 114-126.

[11] Hung TC, Shai TY, Way SK *A review of thermodynamic cycles ad working fluids for the conversion of low-grade waste heat* Energy (1997); 22(7): 661-7.

[12] Maizza V, Maizza A *Uncoventional working fluids in Organic-Rankine cycle for waste heat recovery systems* Applied Thermal Energineering 2007; 21(3):381-90.

[13] Larjola J *Electricity from industrial waste heat using high-speed organic Rankine cycle (ORC)* International Journal of Production Economics 1995;41(1-3):227-35.

[14] Chen H, Goswami DY, Stefanokos EK *A review of thermodynamic cycles and working fluids for the coversion of low-grade heat into power* Renewable and Sustainable Energy Reviews 2010; 14(9): 3059-67.

[15] Borsukiewicz-Godzur A *Pumping work in the organic Rankine cycle* Applied Thermal Engineering 2013; 51(1-2):781-6.

[16] Quolin S, Lemort V *Technological and Economical Survey of Organic Rankine Cycle Systems* n.d.

[17] Bruno JC, López-Villada J, Letelier E, Romera S, Coronas A *Modelling and optimisation of solar organic Rankine cycle engines for reverse osmosis desalination* Applied Thermal Engineering 2008; 28(17-18):2212-26.

[18] Quolin S *Sustainable energy conversion through the use of organic Rankine cycles for waste heat recovery and solar applications* PhD thesis. University of Liège, Belgium; 2011.

[19] Mago PJ, Chamra LM, Srinivasan K, Somayaji C *An examination of regenerative organic Rankine cycles using dry fluids* Applied Thermal Engineering 2008:(8-9):998-1007.

[20] Saleh B, Koglbauer G, Wendland M, Fisher J *Working fluids for low-temperature organic Rankine cycles* Energy 2007;32(7):1210-21.

[21] Aljundi IH *Effect of dry hydrocarbons and critical point temperature on he efficiencies of oganic Rankine cycle* Renewable Energy 2011;36(4):1196-202.

[22] Stijepovic MZ, Linke P, Papadopoulos AI, Grujic AS *On the role of working fluid properties in organic Rankine cycle performance* Applied Thermal Enginnergin 2001;36:406-13.

[23] Huijuan Chen, D. Yogi Goswami, MUhammad M. Rahman, Elias K. Stefanos *A supercritical Rankine cycle using zeotropic mixture working fluids for the conversion of low grade heat into power* Energy 36 (2011); 549-555;

[24] Jovana Radulovic, Nadia I. Beleno Castaneda *On the potential of zeotropic mixtures in supercritical ORC powered by geothermal energy source* Energy conversion and Management 88 (2014):365-371.

[25] J.G. Andreasen, U. Larsen, T. Knudsen, L. Pierobon, F. Haglind *Selection and optimization of pure and mixed working fluids for low grade heat utilization using organic Rankine cycles* Energy 73 (2014): 204-213.

[26] J.G. Andreasen MSc thesis *Optimization of organic Rankine cycles for power production from low temperature heat source using binary working fluids* Copenhagen, 2013.

[27] J.L. Wang, L. Zhao, X.D. Wang *A comparative study of pure and zeotropic mixtures in low-temperature solar rankine cycle* Energy 87 (2010): 3366-3373.

[28] Gianfranco Angelino, Piero Colonna di Paliano *Multicomponent Working fluids for organic Rankine cycles (ORCs)* Energy 23 (1998): 449-163.

[29] Floran Heberle, Markus Preißinger, Dieter Brüggemann *Zeotropic mixtures as working fluids in organic Rankine cycles for low-enthalpy geothermal resources* Energy 37 (2012): 364-370.

[30] M. Chys, M. van Broek, B. Vanslambrouck, M. de Paepe *Potential of zeotropic mixtures as working fluids in organic Rankine cycles* Energy 44 (2012): 623-632.

[31] Young-Jin Baik, Minsung Kim, Ki-Chang Chang, Young-Soo Lee, Hyung-Kee Yoon *Power enhancement potential of a mixture transcritical cycle for a low-temperature geothermal power generation* Energy 47 (2012): 70-76.

[32] Pardeep Garg, Pramod Kumar, Kandadai Srinivasan, Pradip Dutta *Evaluation of isopentane,R-245fa and their mixtures as working fluids for organic Rankine cycles* Energy 51 (2013): 292-300.

[33] L. Barbazza MSc thesis *Design and optimization of heat exchangers for Organic Rankine cycles* Copenhagen 2013 .

[34] *HFCs, the Montreal Protocol and the UNFCCC* Bangkok climate change conference, August-September 2012.

[35] Theresa Weith, Florian Heberle, Markus Preißinger, Dieter Brüggemann *Performance of Siloxanes Mixtures in High-Temperature Organic Rankine cycle considering the The heat transfer characteristics during evaporation* Energies 7 (2014): 5548-5565.

[36] Bensi Dong, Guoqiang Xu, Yi Cai, Haiwang Li *Analysis of zeotropic mixtures used in High-temperature organic Rankine cycle* Energy Conversion and Management 84 (2014): 253-260.

[37] Yongping Yang, Qin Yan, Rongrong Zhai, Abbas Kouzani, Eric Hu *An efficient way to use medium-or-low temperature solar heat for power generation - integration into conventional power plant* Applied Thermal Engineering 31 (2011): 157-162.

[38] Antti Uusitalo, Teemu Turunen-Saaresti, Juha Honkatukia, Piero Colonna, Jaako Larjola *Siloxanes as working fluids for Mini-ORC systems based on High-Speed turbogenerator Technology* Journal of Engineering for Gas Turbines and Power 135 (2013): 042305-1.

[39] Jiangfeng Wang, Zhequan Yan, Pan Zhao, Yiping Dai *Off-design performance analysis of a solar-powered organic Rankine cycle* Energy Conversion and Management 80 (2014): 150-157.

[40] E. H. Wang, H.G. Zhang, B.Y. Fan, M.G. Ouyang, Y. Zhao, Q.H. Mu *Study of working fluid selection of organic Rankine cycle (ORC) for engine waste heat recovery* Energy 36 (2011):3406-18.

[41] Bertrand Frankam Tchanche, George Papadakis, Gregory Lambrinos, Antonios rangoudakis *Fluid selection for a low-temperature solar organic Rankine cycle*Applied Thermal Engineering 29 (2009): 2468-76.

[42] J Nouman *Comparative studies and analyses of working fluids for Organic Rankine Cycles-ORC* Master of Science Thesis, KTH school of Industrial Engineering and Management (2012).

[43] Isam H. Aljundi *Effect of dry hydrocarbons and critical point temperature on the efficiencies of organic Rankine cycle* Renewable Energy 36 (2011):1196-1202.

[44] Guoquan Qiu *Selection of working fluids for micro-CHP systems with ORC* Renewable Energy 48 (2012):565-570.

[45] Ngoc Anh Lai, Martin Wendland, Johann Fischer *Working fluids for high-temperature organic Rankine cycles* Energy 36 (2011):199-211.

[46] S. Lecompte, B. Ameel, D. Ziviani, M. van der Broek, M. De Paepe *Exergy analysis of zeotropic mixtures as working fluids in Organic Rankine cycles* Energy Conversion and Management 85 (2014): 727-739.

[47] F.J. Fernández, M.M. Prieto, I. Suárez *Thermodynamic analysis of high-temperature regenerative organic Rankine cycles using siloxanes as working fluids* Energy 36 (2011): 5239-5249.

[48] Deshpande Girish, Rezac E Mary *Kinetic aspects of the thermal degradation of poly(dimethyl siloxane) and poly(dimethyl diphenyl siloxane* Polymer Degradation and Stability 76 (2002): 17-24.

[49] N. Grassie, I.G. Macfarlane *The thermal degradation of polysiloxanes—I. Poly(dimethylsiloxane)* European Polymer Journal 14 (1978): 875-884.

[50] F. Heberle, M. Preißinger, T Weith, D. Brüggemann *Experimental Investigation of Heat Transfer Characteristics and Thermal Stability of Siloxanes* 2nd International Seminar on ORC Power Systems, Rotterdam (Netherlands).

[51] G. Angelino, C. Invernizzi *Cyclic methylsiloxanes as working fluids for space power cycles* Journal of Solar Energy Engineering 115(3): 130-137 (1993).

[52] Ulli Drescher , Dieter Bruggemann *Fluid selection for the Organic Rankine Cycle (ORC) in biomass power and heat plants* Applied Thermal Engineering 27 (2007): 223-228;

[53] L. Calderazzi, P. Colonna *Thermal stability of R-134a, R-141b, R-13I1, R-7146, R-125 associated with stainless steel as a containing material* International Journal of Refrigeration, 20 (1997), 381–389.

[54] A. Hemidi, Y. Bartosiewicz, J.M. Seynhaeve *Ejector air-conditioning system: cycle modeling, and two-phase aspects* HEAT 2008, Fifth International Conference on Transport Phenomena In Multiphase Systems June 30 - July 3, 2008, Bialystok, Poland.

[55] L. Barbazza, L. Pierobon, A. Mirandola, F. Haglind *Optimal design of compact organic Rankine cycle units for domestic solar applications* Thermal Science, 18 (2014): 811-822.

[56] H.L. Zhang, J. Baeyens, J. Degrève, G.Cacères *Concentrated solar power plants: Review and design methodology* Renewable and Sustainable Energy Reviews, 22 (2013): 466-481.

[57] Hans Müller-Steinhagen, Freng and Franz Trie *Concentrating solar power: a review of the technology* Energy.

[58] David Barlev, Ruxandra Vidu, Pieter Stroeve *Innovation in concentrated solar power* Solar Energy Materials & Solar Cells, 95 (2011): 2703-2725.

[59] Kearney DW, Price HW *Solar thermal plants - LUZ concept (current status of the SEGS plants* Proceeding of the second renewable energy congress, UK, 1992; vol 2: p 582-588.

[60] S. Quoilin, M van der Broek, S. Declaye , P. Dellawef, V. Lemort *Techno-economic survey of organic Rankine cycle (ORC) systems* Renewable and Sustainable Energy reviews (2013), 22: 168-186.

[61] F. Burkholder, C. Kutscher *Heat loss testing of Scott's PTR70 Parabolic trough receiver* National Renewable Energy Laboratory, Technical Report NREL/TP-550-45633 May 2009.

[62] S. Quoilin, M. Orosz, H. Hemond, V. Lemort *Performance and design optimization of a low-cost organic Rankine cycle for remote power generation* Solar Energy 85 (2011): 995-996.

[63] Dudley, V., G. Kolb, A. R. Mahoney, T. Mancini, C. Matthews, M. Sloan, D. Kearney *Test Results SEGS LS-2 Solar Collector* SAND94-1884, December 1994.

[64] J. A. Duffie, W. A. Beckham *Solar engineering of thermal processes, forth edition* New York, NY: John Wiley and sons.

[65] R. Forristall *EES heat transfer model for solar receiver performance* Proceedings of ISEC, Solar 2004, Portland, Oregon, July 11-14, 2004

[66] A. Ratzel, C. Hickox, D. Gartling (February 1979) *Techniques for reducing thermal conduction and natural convection heat losses in annular receiver geometries* Journal of heat transfer (101:1); pp: 108 - 113.

[67] F. Incropera, D. DeWitt *Fundamentals of heat and mass transfer, third edition* New York, NY: John Wiley and sons.

[68] Angela M. Patnode Doctoral thesis *Simulation and Performance Evaluation of Parabolic Trough Solar Power Plants* University of Wisconsin-Madison (2006).

[69] Radermacher Reinhard, Yunho Hwang *Vapor Compression Heat Pumps with Refrigerant Mixtures* Taylor and Francis, 2005.

[70] M. K. Ireland Msc Thesis *Dynamic modelling and control strategies for Micro-CSP plant with thermal storage powered by the organic rankine cycle*Massachusetts Institute of Technology, February 2014

[71] D. H. Cooke *On prediction of Off-Design Multistage Turbine Pressures by Stodola's Ellispse* Journal of Engineering for Gas Turbines and Power, July 1985, Vol. 107/597.

[72] E. Scolari MSc Thesis *Design and Control of Steam Rankine Bottoming cycles for Offshore Applications* Copenhagen 2013.

[73] F. Haglind, B.Elmegaard *Methodologies for predicting the part-load performance of aero-derivative gas turbines* Energy 34, 1484-1492.